JUL 15 1996 20

ENGINEERING DATA TRANSMITTAL

Page 1 of 1

1. EDT № 614678

2. To: (Receiving Organization)	3. From: (Originating Organization)	4. Related EDT No.:
Distribution	Process Engineering Analysis	N/A
5. Proj./Prog./Dept./Div.: W74A50	6. Cog. Engr.: K. Sathyanarayana KS 6/8/96	7. Purchase Order No.: N/A
8. Originator Remarks: Approval/Release		9. Equip./Component No.: N/A
		10. System/Bldg./Facility: N/A
11. Receiver Remarks:		12. Major Assm. Dwg. No.: N/A
		13. Permit/Permit Application No.: N/A
		14. Required Response Date:

15. DATA TRANSMITTED

(A) Item No.	(B) Document/Drawing No.	(C) Sheet No.	(D) Rev. No.	(E) Title or Description of Data Transmitted	(F) Approval Designator	(G) Reason for Transmittal	(H) Originator Disposition	(I) Receiver Disposition
1	WHC-SD-WM-CN-022		0	Evaluation of Potential and Consequences of Steam Bump in High Heat Waste Tanks and Assessment and Validation of GOTH Computer Code	S	1	1	

16. KEY

Approval Designator (F)	Reason for Transmittal (G)	Disposition (H) & (I)
E, S, Q, D or N/A (see WHC-CM-3-5, Sec.12.7)	1. Approval 2. Release 3. Information 4. Review 5. Post-Review 6. Dist. (Receipt Acknow. Required)	1. Approved 2. Approved w/comment 3. Disapproved w/comment 4. Reviewed no/comment 5. Reviewed w/comment 6. Receipt acknowledged

17. SIGNATURE/DISTRIBUTION (See Approval Designator for required signatures)

(G) Reason	(H) Disp.	(J) Name	(K) Signature	(L) Date	(M) MSIN	(J) Name	(K) Signature	(L) Date	(M) MSIN	(G) Reason	(H) Disp.
1	1	Cog.Eng. K. Sathyanarayana		6/8/96	H0-34						
1	1	Cog. Mgr. D. M. Ogden		6/24/96	H0-34						
		QA									
1	1	Safety ~~B. D. Board~~ MN Islam	for Standing Signature	6/7/96	R3-08						
		Env.									
4	1	G. T. MacLean		6/7/96	H5-61						
1	1	M. J. Thurgood		6/9/96	H0-34						

18. K. Sathyanarayana 6/8/96
Signature of EDT Originator — Date

19. BD Board for MN Islam 6/7/96
Authorized Representative for Receiving Organization — Date

20. D. M. Ogden 6/24/96
Cognizant Manager — Date

21. DOE APPROVAL (if required) Ctrl. No.
[ ] Approved
[ ] Approved w/comments
[ ] Disapproved w/comments

BD-7400-172-2 (04/94) GEF097

Evaluation of Potential and Consequences of Steam Bump in High Heat Waste Tanks and Assessment and Validation of GOTH Computer Code

K. Sathyanarayana
Westinghouse Hanford Company, Richland, WA 99352
U.S. Department of Energy Contract DE-AC06-87RL10930

EDT/ECN: 614677 UC: 2020
Org Code: 74A50 Charge Code: N1FC3
B&R Code: EW3135040 Total Pages: 220

Key Words: Steam Bumps, Aging Waste Tanks, Waste Consolidation, High Heat Tanks, GOTH Computer Code

Abstract: This report describes the thermal hydraulic analysis performed using the GOTH[1] computer code to evaluate the potential and consequences of steam bumps in high heat waste tanks. The analysis was performed for three different sludge volumes that correspond to the current sludge volume in tank AZ-101, combined sludge volumes of tank AZ-101 and tank AZ-102 and the projected consolidated sludge volume of tank C-106 and tank AY-102. For each case, the steam bump potential was evaluated starting the simulation with a realistic best estimate initial temperature distribution as well as with a conservative potentially possible axial temperature distribution in the sludge. To include further conservatism in estimating the consequent release of radioactive material, steam bump analyses were also performed suppressing steam condensation with subcooled liquid in waste. In addition, calculations were performed with inleakage flow paths corresponding to open risers and pump and sluice pit cover blocks as well as with normal inleakage flow paths due to drain pipes and infiltration paths. Therefore, the report presents the steam bump evaluations encompassing from an extremely conservative case of initiating a steam bump with local saturation temperature throughout the sludge with condensation suppressed and open risers to a realistic potential case with loss of cooling of initiating a steam bump with only the bottom layer with local saturation temperature with condensation included considering only the normal inleakage flow paths. The results show that in all cases the consequences from an energetic bump may not be acceptable, and the safe operation should include keeping peak sludge temperatures below local saturation values.

The report also includes a brief description of the capability and validation of models used in the GOTH computer code.

[1] GOTH is a trademark of JMI, which is derived from GOTHIC--a registered trademark of the EPRI Corp. of California.

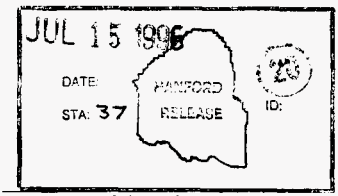

Release Approval Date

Release Stamp

Approved for Public Release

Evaluation of Potential and Consequences of Steam Bump in High Heat Waste Tanks and Assessment and Validation of GOTH Computer Code

K. Sathyanarayana
Westinghouse Hanford Company
Richland, Washington

Brent C. Fryer
John Marvin, Inc.
Richland, Washington

June 1996

Issued by
Westinghouse Hanford Company
for the

U.S. DEPARTMENT OF ENERGY
RICHLAND OPERATIONS OFFICE
RICHLAND, WASHINGTON

TABLE OF CONTENTS

LIST OF FIGURES

LIST OF TABLES

1.0 INTRODUCTION

The occurrence of tank bumps have been reported in the mid-1950's in aging waste storage tanks. Some of these incidents have led to undesirable releases of radioactive contaminants in the immediate surrounding areas. The recorded history of tank bumps suggests that increasing heat loads have caused bumps with increasing intensity and duration. The current heat load and the operation of active ventilation systems have virtually eliminated the possibility of a bump. However, the consolidation and processing of waste will increase both the heat loads and sludge levels thus providing conditions conducive for steam bumps, especially during accident conditions such as ventilation outages and/or pumps operation.

The loss of primary cooling with increased sludge levels and high heat loads will increase the sludge temperatures in the lower elevations of the tank. Sludge temperatures may approach the local saturation temperature of the liquid that is trapped in the sludge. As the sludge reaches local saturation temperatures, steam will form leading to the possibility for a steam bump to occur. A steam bump can occur if the steam trapped in the sludge is released in sufficient quantity from the surface of the waste to cause a pressurization of the tank dome space. Such an event may have unacceptable consequences if the magnitude of the over pressurization is sufficiently large to cause entrainment of aerosols from the tank and failure of HEPA filters on the inlet and/or outlet sides of the ventilation system.

Steam release to the dome can only occur if the steam released from the sludge is not condensed in the supernatant layer. If the steam is released as individual steam bubbles and the supernatant is subcooled, complete condensation of the steam will almost certainly occur. Under normal operating conditions (i.e., all active cooling systems are functioning), the tank supernatant liquid above the sludge is well below its local saturation temperature. However, if steam is released from the sludge in a rollover event (i.e., an event in which a layer of sludge which contains sufficient steam voids to become neutrally buoyant with respect to the supernatant layer rises to the surface), the steam may be surrounded by saturated sludge as it rises. This plume of saturated liquid, particles and steam bubbles may isolate the steam from the subcooled supernatant, drastically reducing the rate at which the steam can condense. Also, as the hot liquid within the plume rises to higher elevations in the tank, it will flash into more steam due to decreased hydrostatic pressure. The two competing processes of heat transfer from the plume to the subcooled supernatant and flashing of the rising hot liquid will determine the severity of the steam bump.

The heat loss from the plume to the subcooled supernatant is comprised of both conduction heat transfer and turbulent mixing of the plume with the supernatant. The mixing process is likely to be the most dominant plume heat loss mechanism. The ability of the subcooled supernatant to penetrate the plume is determined by the balance between the density gradients driving the supernatant into the plume and the volumetric expansion forcing flow outward from the plume core due to rapid formation of steam as the plume rises. These processes will ultimately act to break up the sludge plume and release the steam. The concern is whether the steam will reach the surface in sufficient volume to cause pressurization of the tank dome and release of aerosols to the

environment or will the steam released before it reaches the waste surface and condensed in the supernatant. Condensation is less likely to occur if the heat load is sufficiently high and the ventilation flow sufficiently low to allow the supernatant to reach the saturation temperature.

The potential of steam bumps and their consequences for tank AZ-101 with its current 18 inches, tank AZ-101 with an increased 4 ft sludge level corresponding to the combined sludge volumes of tank AZ-101 and tank AZ-102, and for tank AY-102 with the proposed consolidation of waste from tank C-106 with an estimated sludge level of 11 feet are evaluated and bounding estimates are made for the vapor, liquid and particle flows through the leakage and ventilation flow paths.

2.0 SUMMARY

This report presents the results of the analyses performed to evaluate the potential for and consequences of steam bumps in the high heat tanks due to the presence of settled sludge layers on the bottom of the tank. Steam bumps have historically occurred in aging waste tanks having heat loads in excess of 10^6 Btu/h. The current tank heat loads, sludge thicknesses and supernatant volumes are such that, under normal ventilation system operation, the peak sludge temperatures are well below the local saturation temperature of the liquid so it is unlikely that such an event will occur. However, accident conditions, such as the loss of ventilation flow, combined with increased sludge thicknesses and heat loadings due to mixing pump operation, may lead to conditions that are conducive to bump formation. Transient conditions which may lead to local waste temperatures reaching the local saturation temperature in three sludge thicknesses, 18 inches and 48 inches in tank AZ-101 and 11 feet of consolidated sludge in tank AY-102, have been considered in the analysis. The radioactive material release resulting from bumps that develop from these conditions have been estimated.

The sludge temperatures can increase to the local saturation temperature due to the loss, or degradation, of the tank ventilation system. The transient vertical temperature profile in the waste that exists at the time when the first point in the sludge reaches the saturation temperature is referred to as the best estimate temperature distribution. Sludge at or higher than the local saturation temperature will generate steam. The steam, if trapped by the sludge, will accumulate until the steam laden sludge becomes neutrally buoyant with the supernatant. Depending on the yield strength of the sludge, the hydrodynamic instability caused by the presence of the steam will result in the development of a sludge plume that may travel through the supernatant and release solid and liquid particles and steam to the tank dome space.

The best estimate temperature distribution will exist prior to the first plume release only. Once a plume is released, hot sludge mixes with cooler sludge and this changes the axial temperature distribution in the sludge. Heat continues to accumulate in the sludge subsequent to the first plume release since ventilation is not available. Repetitive releases of sludge plumes are likely, and the combined effects of heat accumulation and mixing

caused by plume releases may eventually lead to a condition in which most of the sludge is near the local saturation temperature over its entire height. It is possible for this condition to be reached as long as ventilation has not been restored to the tank. Once bumps begin, they are likely to continue until ventilation is restored, growing in severity as the sludge temperature profile approaches saturation over its entire length. It is not practical to simulate this entire bump history so the saturation temperature at each elevation in the waste has been chosen as the bounding temperature distribution for the maximum possible steam bump for a given sludge thickness. This temperature distribution is referred to as the conservative temperature distribution.

Steam bump simulations corresponding to both the best estimate and conservative initial sludge temperature distributions have been performed and the results are discussed in this report.

Other conditions, in addition to the axial temperature distribution in the sludge, that have a significant impact on the magnitude of a steam bump are the subcooling of the tank supernatant, the degree of mixing between the hot sludge plume and the supernatant and the resistance to flow offered by the leakage and ventilation flow paths leading from the tank dome. The full range of these conditions has been investigated to determine the sensitivity of bump size and release rates to these parameters. This has been done by performing simulations that permit lower bound estimates on supernatant temperatures, best estimate mixing between the plume and supernatant and best estimate steam condensation rates on the one extreme and simulations that do not allow steam condensation to occur in the supernatant no matter how much mixing or subcooling is calculated to exist. Calculations have also been performed in which the size of the flow paths from the tank dome have been assumed to be as large as an open 42 inch riser to as small as that offered by the filtered inlets and normal ventilation system.

Therefore, the steam bump evaluations presented in this report encompass the full range of conditions from that of a tank that has been without ventilation sufficiently long that the supernatant has reached saturation so little or no condensation can occur, the sludge is saturated throughout its thickness, and the large 42 inch riser with the accompanying pit covers has been opened up to the atmosphere so the maximum flow from the tank can be achieved; to that of the minimum initial bumps that can occur when the supernatant is highly subcooled, the temperature distribution in the sludge is the lowest possible and still have some steam formation and the flow paths from the tank are the most restrictive.

The results of the computer simulations show that, with the best estimate initial temperature distribution, the normal ventilation leakage and flow paths and allowing steam condensation in the supernatant, steam bumps that can release radioactive material are not predicted for the 18 inch, 48 inch or 11 foot cases. However, the 11 foot case is close to releasing material since the steam laden sludge plume almost reached the surface of the pool even though the supernatant temperature is assumed to be only 112 °F.

Continued loss of ventilation or operation of high powered mixing pumps can increase waste and supernatant temperatures above the initial best estimate values. This will result in increasingly severe bumps that will produce significant releases through the tank leakage paths. The consequences

of energetic bumps with several layers of conservatism are presented in this report. These layers of conservatism become thinner the longer the tank is allowed to operate in this mode. The consequences of energetic bumps may not be acceptable in most of these cases.

The main conclusion one should draw from this study is that it is most prudent not to allow the tank to operate under conditions that can result in the sludge reaching the local saturation temperature and that there is a higher probability for an energetic bump to occur the longer a tank is allowed to operate under this condition.

3.0 PURPOSE

The purpose of the analyses is to provide technical basis for the steam bump phenomenon as well as to make bounding estimates of the consequences of these bumps for safety evaluation.

4.0 METHODOLOGY

Steam bump analyses have been performed using the GOTH computer code (Thurgood 1992). GOTH is a state-of-the-art transient computer program for modeling multiphase flow consisting of gas, liquid and solids. The mathematical model treats each phase as a continuum. The Navier-Stokes equations are written for each phase along with the appropriate boundary and interfacial conditions. The tank model includes the radiolytic heat generation in aqueous solution and in undissolved solid particles. It also includes the tank dome, supernatant and sludge, and in-leakage and vent paths for ventilation flow. The model has been further extended to include the complete primary ventilation system, comprised of the four tanks in the AZ tank farm, ventilation ducts, upstream and downstream de-entrainers, condensers, heater, filters and fan inlet, to assess its effect on steam bumps.

The phenomenon of tank thermal steam bumps is technically challenging since a large number of multiphase flow and heat transfer phenomena play a role in defining its potential occurrence. Steam bumps may occur in relatively low heat tanks containing settled sludge layers under certain conditions. Since it is not possible to implicitly include the full range of conditions, bounding calculations have been performed to understand the effect of important parameters on the formation and magnitude of steam bumps and to estimate the quantity of steam, liquid and solid particles that are released from the tank through the in-leakage and ventilation paths. The initial bump conditions have been assumed to occur either with the loss of the tank primary cooling system or increase of heat load due to addition of sludge which also increases the depth (i.e., conduction distance) or any process such as the operation of pumps that will result in the heat up of the sludge layer to the local saturation temperature. As the temperature reaches saturation value, steam will form and accumulate depending on the characteristics of the sludge and become buoyant relative to the supernatant leading to a rollover or geyser

formation. Previous studies (Fauske 1989, Waters 1991) have shown that for a steam bump to occur, there must be an immobile sludge with heat generating solid particles and the local temperature in the sludge must exceed/equal the saturation value. Under these conditions, a steam bump is self initiating with the formation of steam or it could be induced by mechanical means such as the operation of air lift circulators (ALC) or mixer pumps. In practice, these steam bumps are characterized with large releases of steam into the dome causing the dome pressure to rise above atmospheric pressure resulting in a release of radioactive material to the environment.

The temperature distribution in the sludge and in the supernatant when the temperature first reaches the local saturation temperature as a result of any or all of the above conditions is referred to as the best estimate temperature distribution for the waste. This temperature distribution will exist just prior to the initial bump only. Subsequent bumps will occur if the condition that has led to the increase in sludge temperature is not rectified, since each bump will transfer energy from the sludge to the supernatant and the continued heat generation in the sludge will cause the resettled sludge to heat up again. It is assumed that this process will continue and eventually the sludge and supernatant may reach the local saturation temperature. The sludge will eventually reach the saturation temperature at all elevations. This is referred to as the conservative temperature distribution. This temperature distribution could exist if the conditions that have led to the initiation of the bumps are not corrected.

Steam bump simulations have been performed using both the best estimate and the conservative initial temperature distributions. For each initial temperature distribution, calculations have also been performed with condensation suppressed to predict an upper bound, and including steam condensation based on local flow and temperature conditions to make a realistic estimate of the steam bump and its consequences.

These computer simulations have been performed using a two-dimensional tank model for the sludge, supernatant and dome space. The model includes inleakage flow path and ventilation flow paths. Appropriate flow loss coefficients have been used to obtain normal flow for the tank operating dome pressure conditions. The model has been extended to include the complete primary ventilation system to assess its effect on bumps and their consequences.

5.0 ASSUMPTIONS

Some of the following parameters that affect the magnitude of the bump and the quantity of the resultant aerosol release are considered in the analysis.

- Sludge thickness: Greater sludge depths tend to produce larger bumps with larger releases. Three sludge depths were considered in the analysis. The sludge with 18 and 48 inches of depth is assumed to have the same composition of solids and liquid and also considered to have the same heat source in the solid and liquid

waste that correspond to the current waste in tank AZ-101. The waste properties used for these two cases are given Table 1. The third case considered has a total sludge depth of 11 feet. This is assumed to be the consolidated sludge of tank C-106 and tank AY-102. The waste characteristics for this case are given in Table 2.

- Sludge Temperature Distribution: As explained above, the bump simulations were performed using both a best estimate temperature profile for an initial bump and a conservative temperature profile for simulating a bounding steam bump. The strength of the bump will be proportional to the quantity of sludge that is at the saturation temperature at the time of bump initiation. These two extremes of the sludge temperature distribution are considered for all three sludge thickness parameter cases.

- Ventilation and In-leakage Flow Paths: A large resistance to flow will reduce the quantity of steam that can be released and can significantly reduce the severity of the bump and consequent releases through the leakage paths. The effects of condensation in the system and the presence of leakage paths in other tanks connected to the same ventilation system as the bumping tank may increase the steam flow through the system. Tank bump simulations considering conservatively large leakage flow paths assume the central pump pit and four sluice pit risers are open, and simulations considering only a 6 inch equivalent in-leakage flow path in addition to the vent flow path have been performed. Also, these bump simulations have been performed considering five 4-inch diameter leakage flow paths corresponding to the drain pipes and the vent flow path. Preliminary calculations have also been performed using the AZ tank farm 702-A ventilation system, including the other double-shell tanks in the system, ventilation duct lines, condensers, filters, etc.

- The quantity of aerosols that will exit the tank are a function of the slip between the particles and the steam, the quantity of steam flow and the deposition of particles on components of the tank leakage path and ventilation components. Particle sizes assumed in the present analyses are small enough that there is essentially no slip between phases and no deposition in the system except settling in the tank waste following the release.

- Depth of Supernatant: Larger pool depths will result in higher tank bottom pressures so the corresponding saturation temperature will be higher. This means that the energy stored prior to the bump will be higher and the bump, when it happens, will be stronger. However, it also means that higher temperatures will have to be reached before steam begins to form and, if the supernatant is subcooled, there is a greater potential for the steam to condense before reaching the pool surface. Shallow pool depths may limit the ability of the sludge to rollover, preventing a large bump from occurring, provided the sludge itself is not fluidized. No attempt is made to study the effect of pool depth in the current analyses. The total depth of the waste is maintained at 30 ft in all simulations.

Table 1. Tank 101-AZ Waste Parameters.

Tank:

Primary Tank Diameter	: 75 ft.
Secondary Tank Diameter	: 80 ft.

Tank Contents:

Undissolved (dry) Solids Density	ρs = 243.4 lbm/ft3
Aqueous Solution Density	ρl = 75.5 lbm/ft3
Sludge (Liquid-Solid Mixture) Density	ρsl = 104.0 lbm/ft3
Total Waste Depth	= 30 ft.
For 18 inch Sludge Layer:	
Supernatant (Aqueous Solution) Depth	= 28.5 ft.
Sludge (Nonconvective Layer) Depth	= 1.5 ft.

Supernatant:

Heat Capacity	= 0.8 Btu/lbm-°F
Thermal Conductivity	= 0.35 Btu/hr-ft-°F
Heat Generation Rate	= 0.019 Btu/hr-lbm

Insoluble Solids:

Heat Capacity	= 0.2 Btu/lbm °F
Thermal Conductivity	= 5.0 Btu/hr ft °F
Heat Generation Rate, Unwashed Waste	= 0.37 Btu/hr-lbm
Particle Size, Washed Waste	= 1-10 μm range
	= 5 μm average
Volume Fraction of Solids, Unwashed Waste	= 17%

Table 2. Combined AY-102 and C-106 Waste Parameters.

Tank:

Primary Tank Diameter	: 75 ft.
Secondary Tank Diameter	: 80 ft.

Tank Contents:

Undissolved (dry) Solids Density	ρs = 113.9 lbm/ft3
Aqueous Solution Density	ρl = 75.5 lbm/ft3
Sludge (Liquid-Solid Mixture) Density	ρsl = 81.2 lbm/ft3
Total Waste Depth	= 30 ft.
For 11 Feet Sludge Layer:	
Supernatant (Aqueous Solution) Depth	= 19 ft.
Sludge (Nonconvective Layer) Depth	= 11 ft.
Tank AY-102 Heat Load	= 33,000 Btu/hr
Transferred C-106 Sludge Heat Load	= 92,400 Btu/hr
Total Heat Load	= 125,000 Btu/hr

Supernatant:

Heat Capacity	= 0.8 Btu/lbm^{0}F
Thermal Conductivity	= 0.35 Btu/hr-ft-^{0}F
Heat Generation Rate	= 0.0 Btu/hr-lbm

Insoluble Solids:

Heat Capacity	= 0.2 Btu/lbm ^{0}F
Thermal Conductivity	= 5.0 Btu/hr ft ^{0}F
Heat Generation Rate, Unwashed Waste	= 0.1394 Btu/hr-lbm
Particle Size, Washed Waste	= 1-10 µm range
	= 5 µm average
Volume Fraction of Solids	= 16.25%

- Sludge Viscosity: The sludge viscosity determines, in part, the ability of the sludge to trap steam bubbles and it also determines the degree to which sludge at the saturation temperature is separated from subcooled sludge and supernatant during a bump. A maximum viscosity of sludge having maximum volume fraction of particles has been assumed to be 8000 lbm/ft-s in the present analyses.

- Sludge Yield Strength: In a sludge with yield strength, larger size bubbles or a larger fraction of steam at higher pressure could be retained before it is released. The yield strength will affect how much sludge participates in the bump. A higher yield strength will allow more energy to be stored in the sludge, since the steam pressure must increase sufficiently to overcome the yield strength. However, high yield strength will also hold some sludge in place preventing it from participating in the rollover. It is assumed that the overall effect of the yield strength will reduce the magnitude of the bump. The yield strength has been assumed to be zero in the current analyses.

- Supernatant Temperature: The potential for the steam to condense and the sludge to cool before steam can reach the pool surface increases as the supernatant subcooling increases. Simulations have been performed neglecting condensation as well as including condensation in subcooled supernatant. Neglecting condensation will provide a conservative estimate of releases and a larger bump. The simulations with condensation demonstrate its effect on the magnitude of potential bump. To take credit for the condensation, it is required to establish the amount of subcooling available for any given condition.

6.0 INPUT PARAMETERS

Steam bump simulations are performed using two sludge thicknesses with the properties of the current waste in tank AZ-101 and another case of 11 ft sludge with the properties of the consolidated waste of tank C-106 and tank AY-102. Table 1 gives the waste properties used in the analysis for the first two cases. The two sludge thicknesses considered were 18 inches, which represents the current sludge level in tank AZ-101 and 48 inches, which represents a typical value used in an earlier analysis (Sathyanarayana 1994a) for thermal effects of pretreatment processes. As in previous evaluations (Sathyanarayana 1994b), the steam bump simulations have been performed using two temperature distributions in the sludge. These temperature distributions are referred to as best estimate and conservative temperature distributions.

The best estimate temperature distribution is the estimated temperature distribution for the sludge during a transient leading to local saturation temperature at the bottom. For the 18 inch sludge case, this transient is a total loss of ventilation cooling since during normal operating conditions the peak sludge temperature is less than the local saturation temperature. The loss of primary ventilation heats up the waste to the local saturation

temperature at the bottom. A one-dimensional GOTH model has been used to obtain the axial temperature distribution in the waste at the time the peak sludge temperature reaches the saturation value. Figure 1 shows the transient heat up of the waste due to the loss of ventilation cooling. The transient has been initiated from an initial steady-state temperature distribution in the tank assuming normal primary ventilation flow with an atmospheric air inlet temperature of 53.34 °F, which is the seasonal average temperature for Hanford. The best estimate axial temperature distribution in the waste with an 18 inch sludge layer when the bottom sludge reaches the local saturation temperature is shown in Figure 2. The conservative axial temperature distribution resulting from previous bumps or prolonged loss of ventilation assumes the sludge to be at the local saturation temperature at all levels in the sludge. The initial conservative axial temperature distribution is shown in Figure 3.

Operation of the tank with only the current primary ventilation system and no secondary or annulus ventilation will result in a peak temperature that will reach the saturation value for the case with 48 inches of sludge. The 48-inch sludge is comprised of the current 18 inch sludge with an added 30 inches of similar sludge settled on top of it. The sludge will heat up due to additional heat load and sludge thickness. The axial temperature distribution in the waste at the time the peak sludge temperature reaches saturation is obtained using a one-dimensional GOTH model. The transient has been initiated from an initial steady-state temperature distribution in the tank for an 18-inch sludge layer with the primary ventilation air inflow at 53.3 °F and 50% humidity. An additional 30 inches of similar sludge is then added on to the top of the 18 inch layer. The added sludge is assumed to be at the supernatant temperature. The heat up of the 48-inch layer starting from the initial axial temperature distribution of 18-inch layer is shown in Figure 4. The axial temperature distribution for the 48-inch layer at the time saturation is reached at the bottom of the layer is shown in Figure 5.

The waste temperature will further increase due to an outage of the ventilation system or due to previous bumps leading to the condition that causes the sludge to be at the local saturation temperature at all levels in the sludge. The conservative axial temperature distribution in the waste for these conditions is shown in Figure 6.

The 11 ft consolidated sludge consists of 1 ft of tank AY-102 sludge with a heat load of 33000 Btu/hr and 10 ft of transferred C-106 sludge with a heat load of 92400 Btu/hr (Sathyanarayana 1996). The transferred sludge thickness is based on the assumption that the sludge particles of tank C-106 will resettle to a particle concentration at least half as large as that which currently exists in that tank. The normal operation of the tank with consolidated sludge requires the primary ventilation flow of about 600 cfm and secondary ventilation cooling flow of 2000 cfm or greater to keep the maximum sludge temperatures below the operational safety requirements (OSR) criteria. In this configuration, the loss of secondary ventilation will lead to the bump condition sooner than loss of the primary ventilation system. The axial temperature distribution for the 11 ft sludge layer at the time saturation is reached at the bottom of the layer due to total loss of ventilation cooling (Sathyanarayana 1996) is shown in Figure 7.

Figure 1. Transient Heatup of Tank AZ-101 Waste With 18 Inches of Sludge Layer Due to Loss of Primary Ventilation Flow.

b18init
Fri Mar 1 08:23:58 1996
GOTH Version 3.4 - April 1991

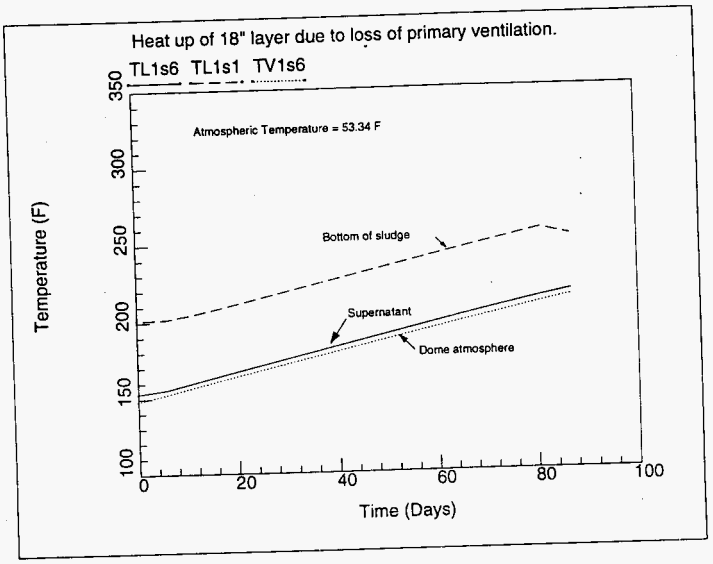

Figure 2. Best Estimate Axial Temperature Distribution in 18 Inches of Sludge Layer.

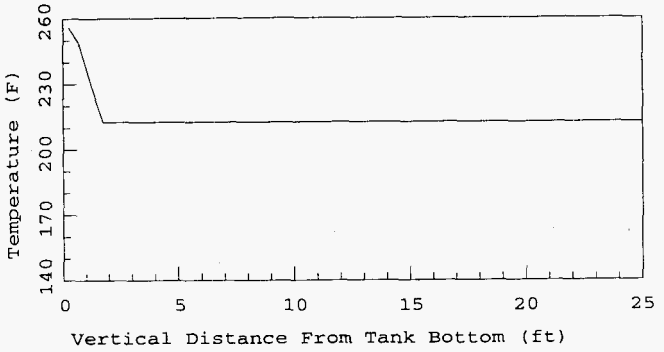

Figure 3. Conservative Axial Temperature Distribution in 18 Inches of Sludge Layer.

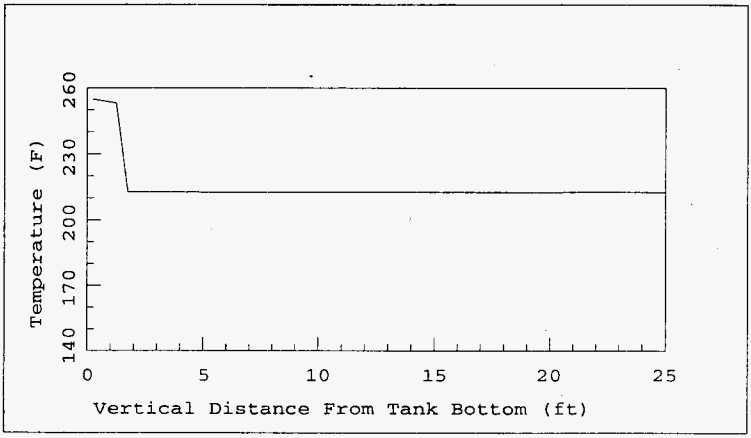

Figure 4. Transient Heatup of Tank AZ-101 Waste With 48 Inches of Sludge Layer Due to Addition of 30 Inches on Top of Current 18 Inches of Sludge.

b48init
Fri Mar 1 09:39:26 1996
GOTH Version 3.4 - April 1991

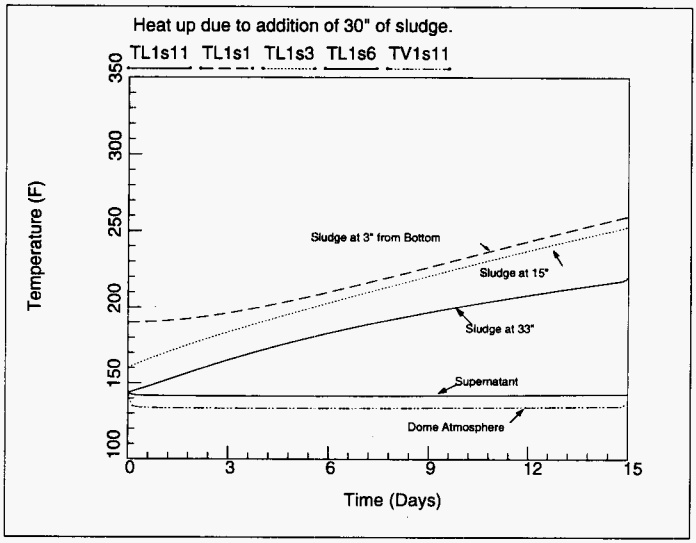

Figure 5. Best Estimate Axial Temperature Distribution in 48 Inches of Sludge Layer.

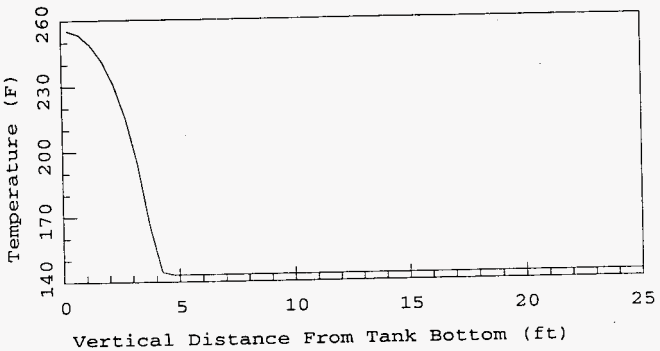

Figure 6. Conservative Axial Temperature Distribution in 48 Inches of Sludge Layer.

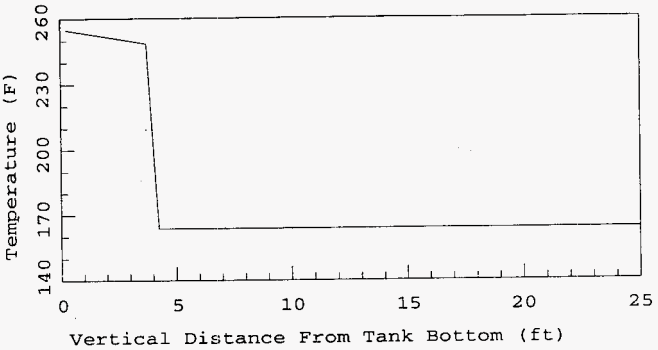

Figure 7. Best Estimate Axial Temperature Distribution in 11 Ft of Consolidated Sludge of Tank AY-102 and Tank C-106.

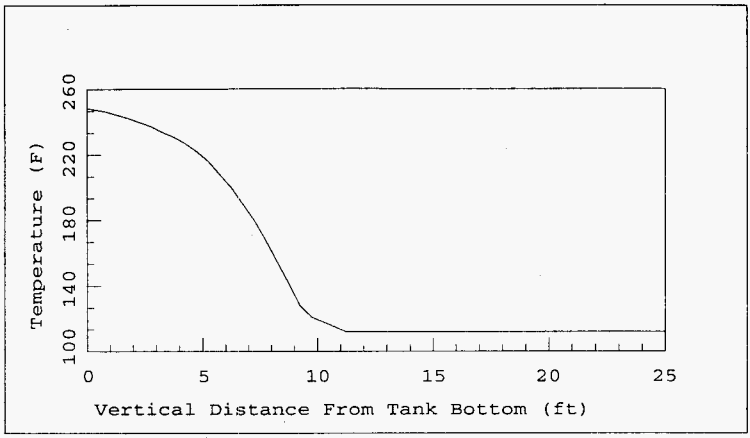

However, if the tank operating conditions are not changed from the initial bump occurrence, more bumps will continue to occur and the sludge temperature will increase throughout leading to the local saturation condition in the worst case. This leads us to consider the conservative temperature distribution to make the bounding estimate of the effects of a bump. This condition could result due to the mixing of the sludge during previous bumps (although subcooled supernatant would always act to drive the axial temperature profile back towards the best estimate temperature) or it could be reached due to prolonged ventilation outage that would cause the supernatant to heat up near its saturation temperature. This conservative temperature profile, shown in Figure 8 has the greatest potential for generating a steam bump and releasing aerosols from the tank.

Also, for each temperature distribution, two simulations were performed to get conservative and best estimate releases. In the first case, condensation between the steam and the subcooled waste is suppressed and in the later case condensation is included. Condensation is allowed to occur based on the two-phase flow regimes and temperature distributions calculated to occur in the tank. The first case where the condensation is suppressed covers the conditions when the supernatant is at local saturated temperature or when little or no mixing occurs between the supernatant and the rising hot sludge plume. It will provide an upper bound estimate on the magnitude of the bump. The best estimate release case where the condensation is allowed to occur seems more realistic. However, the results for this case need to be confirmed by additional sensitivity studies and comparison with test data.

Also the steam bump simulations have been performed using large ventilation leakage flow paths open to the atmosphere. This is believed to be a conservative assumption with respect to the severity of the steam bump for any given bump condition. This refers to the case where the flanges on the pump pit and sluice pit risers are open. The other bounding case considers a 6 inch equivalent leakage path corresponding to the case where all the risers are covered and drain lines are open along with other miscellaneous leak paths. Calculations are also performed using the leakage path area that corresponds to five, 4 inch drain lines and the ventilation flow path. In addition, preliminary simulations are also performed using the entire current ventilation system and five drain lines as leakage flow paths.

7.0 RESULTS AND DISCUSSION

The results of simulations performed using the GOTH computer code are discussed in this section. The simulations are performed with simple in-leakage and ventilation flow paths using both a conservative and best estimate initial axial waste temperature distribution for three different sludge layer thicknesses of 18 and 48 inches and 11 ft. For each sludge level, three different in-leakage flow areas corresponding to: (1) all open risers and no cover blocks, (2) with cover blocks and flanges in place but leakage through open drain pipes, and (3) with a single 6-inch diameter leakage flow path. Also, preliminary calculations are performed for evaluating the effect of the AZ/AY tank farm primary ventilation system on the tank bump using a detailed AZ tank farm 702-A ventilation system model. The first steam bump simulations were performed suppressing the condensation between the steam and liquid in

Figure 8. Conservative Axial Temperature Distribution in 11 Ft of Consolidated Sludge of Tank AY-102 and Tank C-106.

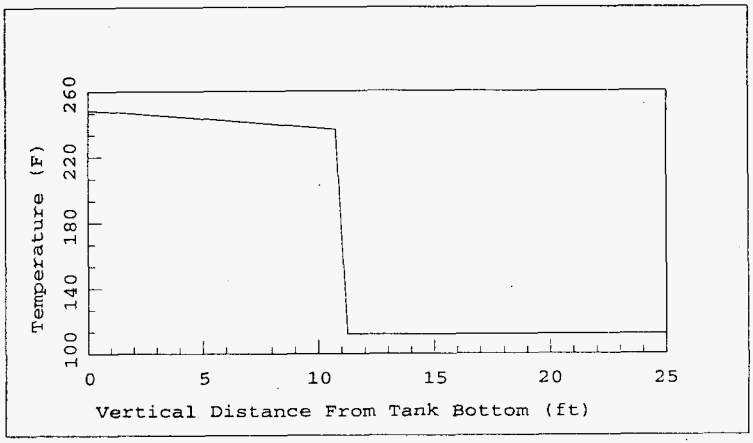

the waste to generate a conservative tank bump. Since condensation will occur in the waste if the steam bubbles come in contact with subcooled liquid, the tank bump simulations have also been performed, including the effects of condensation using the currently available models in the code. The simulations with condensation suppressed will provide conservative estimates on the size of bump and aerosol releases. Considering condensation in these simulations will provide more realistic results.

7.1 18 INCH SLUDGE LAYER OF TANK AZ-101 WASTE

The current operating conditions of the waste in tank AZ-101 keeps the peak temperature around 190 °F, which is well below local saturation temperature. The saturation conditions can only be reached if there is a loss of ventilation for an extended period of time. The axial temperature distribution is estimated assuming the loss of active ventilation cooling for the waste in tank AZ-101 using the one-dimensional GOTH model. The transient simulation estimates the heat up of the sludge, supernatant and dome air as shown in Figure 1. The temperatures are specified to be the local saturation temperature for the conservative temperature distribution,.

7.1.1 Conservative Initial Temperature and No Condensation

The simulation with the conservative initial temperature distribution and with no condensation between the steam and liquid has the greatest potential for a steam bump to occur. The steam formed in the sludge will break the waste surface and, with no condensation, will be released into the dome and exit the tank through the inleakage and vent flow areas. The results of the simulations for three different leakage flow paths are given in Table 3.

Case 1: Steam Bump With Riser Flanges and Cover Blocks Open

This simulation should be considered to be the worst possible case for the steam bump in the 18 inch thick sludge layer since the sludge is at saturation through its entire thickness and no condensation is allowed to occur. Also, the large flow paths essentially provide open ambient conditions for release. The simulation results are shown in Figures 9 through 12 by gas/vapor contour plots. The contour plots show lines of constant vapor fraction which show the separation between regions containing steam/gas and regions containing liquid or solid waste. Figure 9 shows the gas and steam distribution within the tank just prior to the initiation of the initial steam bump. The top set of vapor contour lines show the location of the pool surface. The original sludge level is shown at bottom of the tank by a dashed line. The contour lines at the bottom of the tank show the distribution of the steam in the sludge just prior to the development of the hydrodynamic instability that results in the generation of a steam bump.

The locations at which plumes begin to form are probably random, and these plumes tend to develop at more than one location for thin sludge layers and for sludge with large axial temperature gradients. The formation of multiple plumes tend to reduce the severity of bump. Figure 11 shows the formation of two plumes of superheated sludge containing steam, particles and supernatant. These plumes rise toward the surface under the influence of buoyancy, shear, and drag forces acting on the plumes. These plumes detach

Table 3. Estimate of Vent Flows for a Conservative Tank Bump in 18 Inches of Tank AZ-101 Sludge.

Parameters	Dome Flow Paths	Dome Flow Path	Dome Flow Path
	1. 42" dia-Pump Pit Path 2. 20" dia-Vent Path 3. Four 42" dia-Sluice Pits Path	1. Five 4" dia-Inleakage Paths 2. 20" dia-Vent Path	1. 6" dia-Inleakage Path 2. 20" dia-Vent Path
1. Tank Dome Peak Pressure, psia	15	15.7	15.5
2. Vapor Flow			
Flow path 1, lbm	150	130	35
Flow path 2, lbm	--	610	360
Flow path 3, lbm	1000	NA	
3. Liquid Flow			
Flow path 1, lbm	2000	56	132
Flow path 2, lbm	--	--	--
Flow path 3, lbm	--	NA	NA
4. Particle Flow			
Flow path 1, lbm	150	1.3	7
Flow path 2, lbm	--	--	--
Flow path 3, lbm	--	NA	NA

Figure 9. Steam Concentration Contours in Tank AZ-101 Waste With 18 In. of Sludge Just Prior to Initiation of Steam Bump.

b18con-18 inch original waste, conservative temperature at atmospheric pressure. No condensat
Fri Mar 15 14:28:20 1996
GOTH Version 3.4 - April 1991

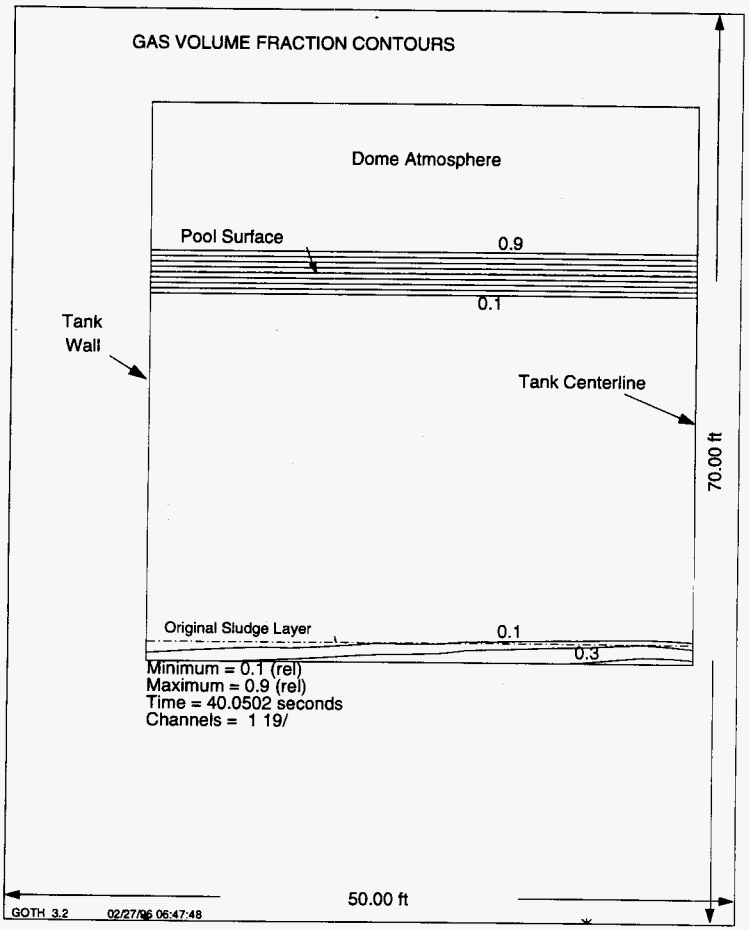

Figure 10. Development of Hydrodynamic Instability in Sludge Just Prior to Initiation of Steam Bump.

b18con-18 inch original waste, conservative temperature at atmospheric pressure. No condensat
Tue May 28 14:20:43 1996
GOTH Version 3.4 - April 1991

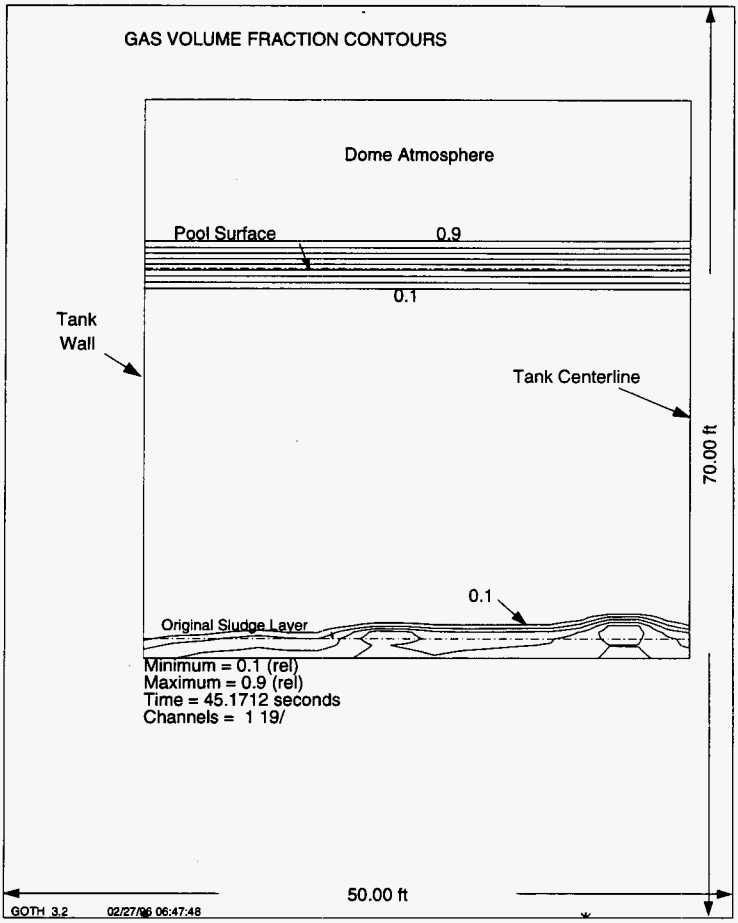

Figure 11. Formation of Superheated Sludge Plumes in Tank AZ-101 Waste With 18 In. of Sludge.

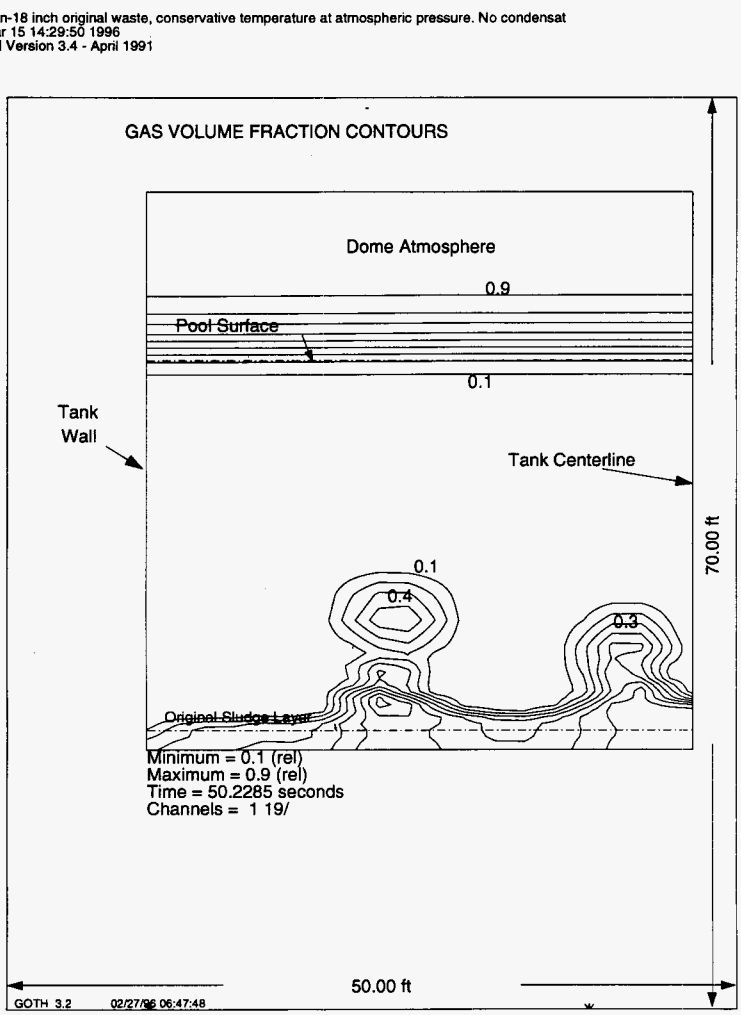

Figure 12. Repetitive Bumps Which Eventually Disperse Liquid Droplets and Solid Particles From Tank Dome Through Leakage and Ventilation Flow Paths.

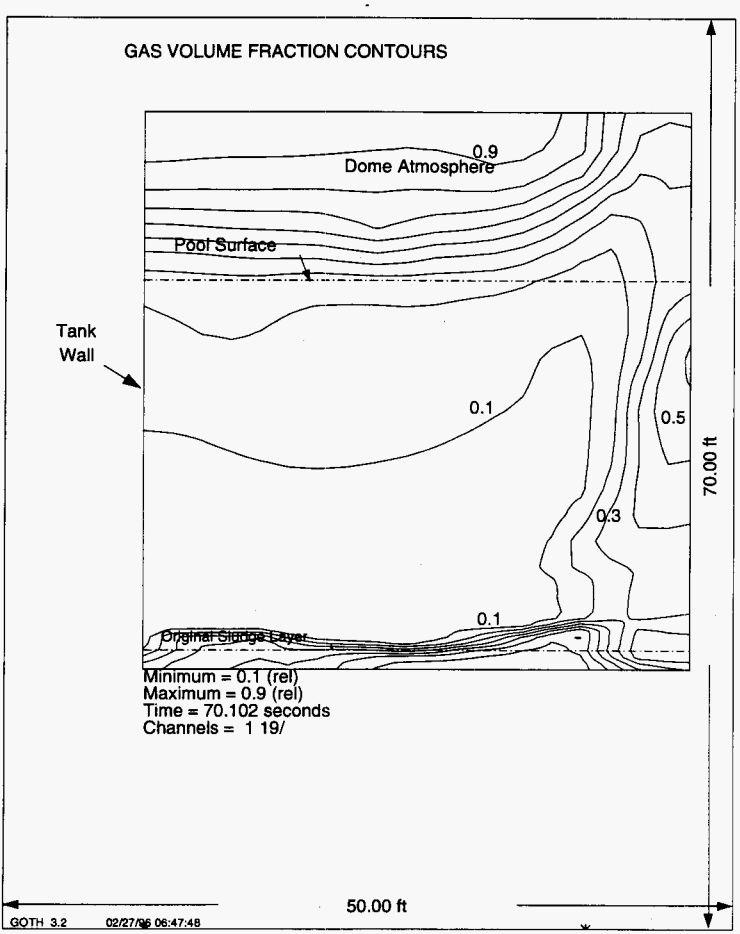

from the sludge and rise toward the surface of the waste breaking it and carrying with it liquid and solid particle aerosols into the dome space. Figure 12 shows a single plume at 70 seconds of transient breaking the waste surface and releasing liquid and solid particles into the dome and leakage flow and ventilation paths. Figures 13 and Figure 14 show the quantity of liquid droplets and solid particles flowing through the vents.

It should be recognized that bumps will continue to occur until ventilation is restored and the tank cooled sufficiently to reduce the peak temperature of the sludge below the local saturation value. The total amount of aerosols released to the atmosphere depends on the time allowed for the bumps to occur and the exact nature of each bump. Bumping may be interrupted for a period of time while solids which have been mixed with the supernatant due to previous bumps resettle and reform the sludge layer, but will resume as the temperature builds up.

Case 2: Five 4 inch Drain Pipes as Leakage Flow Paths

This case is very similar to the previous case except the inleakage flow path area is changed to reflect the total area corresponding to five 4 in. diameter drain pipes. All five flow paths are combined into one leakage path located at the pump pit riser location i.e., center of the dome. This flow path is much more restrictive than that in case 1 above. Figures 15 and 16 show the vapor contours in the sludge as the steam is formed and released during the bump. In this case the dome peak pressure is 15.7 psia and size and duration of the bump smaller than for the open risers case. The vapor, liquid and particle flow through the flow paths are shown in Figures 17 through 19, respectively. The integrated mass flow of releases are shown in Table 3.

Case 3: Simple 6 inch leakage Path at Dome Center

This simulation is very similar to the above case with an inleakage flow area corresponding to a 6 in. diameter vent which provides 600 cfm flow under normal operating conditions. The reduced vent flow area for this case generates the plume closer to the center of the tank than the above case and the inleakage flow path is located at the center of the tank above the dome; larger releases of particle and liquid occur. Figures 20 through 22 show the development of tank bump with vapor contours in the waste. The resulting vapor, liquid and particle flows through the dome flow paths are shown in Figures 23, 24 and 25, respectively. This simulation is also performed for a vent flow duct diameter of 24 in. instead of 20 in. keeping the inleakage flow area at a 6 in. equivalent duct diameter and it has resulted in a tank bump occurring right at the center of the tank as shown in Figures 26 through 28 and the plume hitting the inleakage path. The gas flow through the leakage and vent flow paths is shown in Figure 29. This simulation has resulted in liquid and particle releases as shown in Figures 30 and 31 of 740 and 41 lbm through the inleakage path respectively.

Figure 13. Liquid Droplet Flow Out Through Inleakage Flow Path Due to Steam Bump.

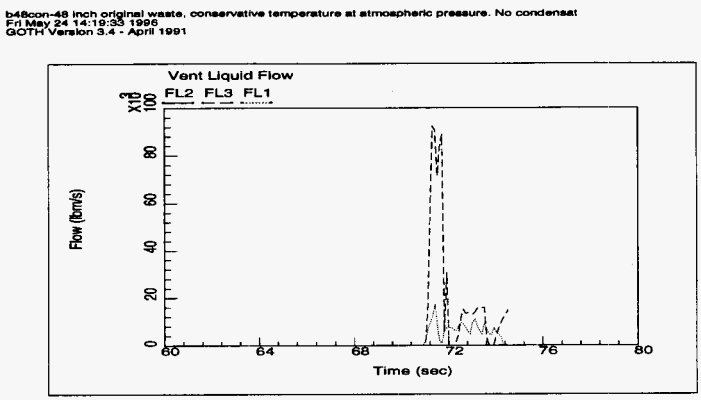

Figure 14. Solid Particle Flow Out Through Inleakage Flow Path Due to Steam Bump.

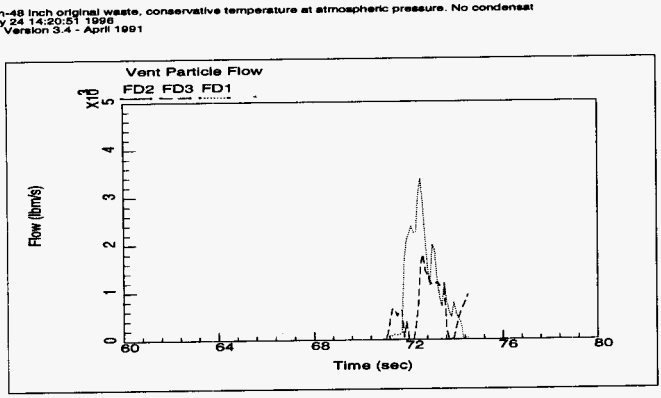

Figure 15. Steam Concentration Contours in 18-Inch Sludge of Tank AZ-101 Waste and Inleakage Flow Paths Through Drain Pipes.

b18c92sv-18 inch original waste, conservative temperature at atmospheric pressure. No condensat
Fri Apr 26 10:48:15 1996
GOTH Version 3.4 - April 1991

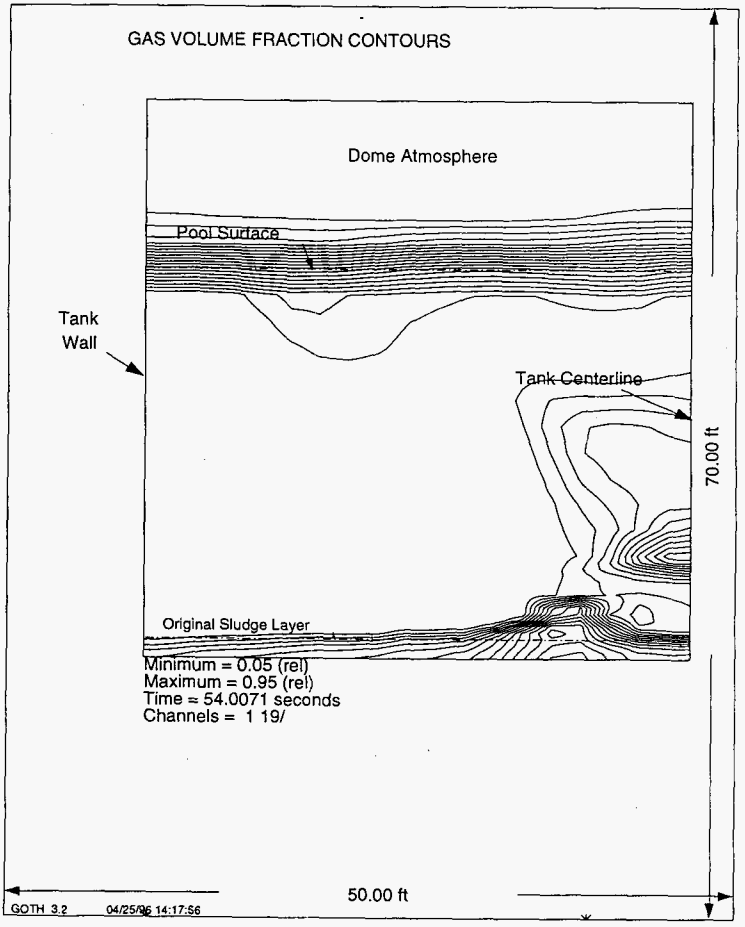

Figure 16. Steam Concentration Contours in 18-Inch Sludge of Tank AZ-101 Waste and Inleakage Flow Paths Through Drain Pipes.

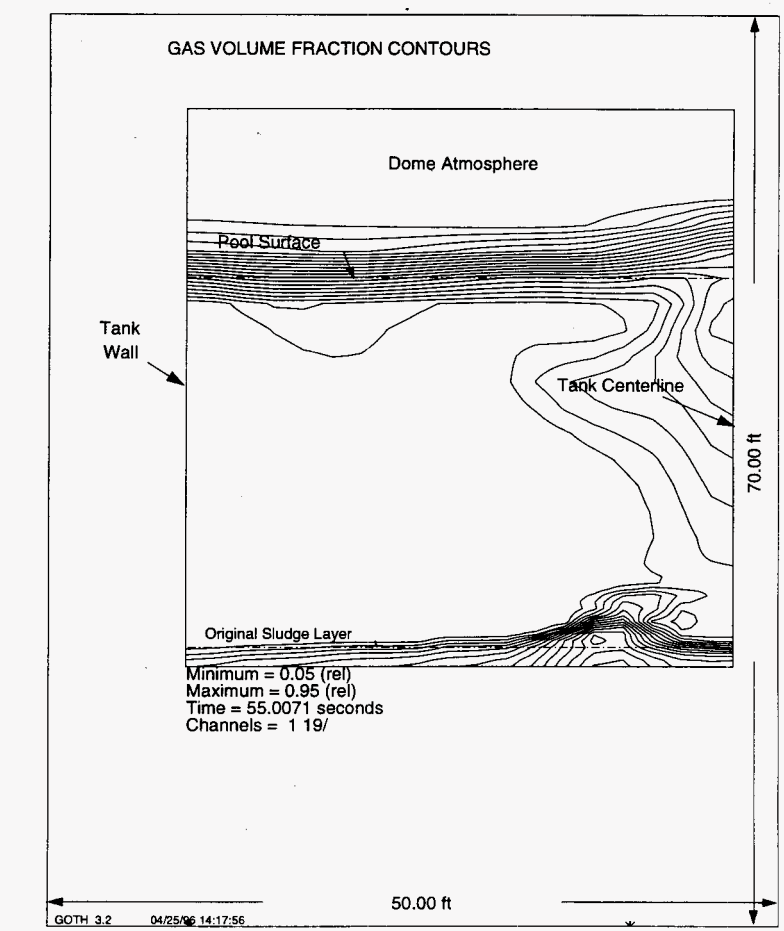

Figure 17. Gas/Flow Through Inleakage and Ventilation Flow Paths.

b18c92sv-18 inch original waste, conservative temperature at atmospheric pressure. No condensat
Fri Apr 26 10:37:13 1996
GOTH Version 3.4 - April 1991

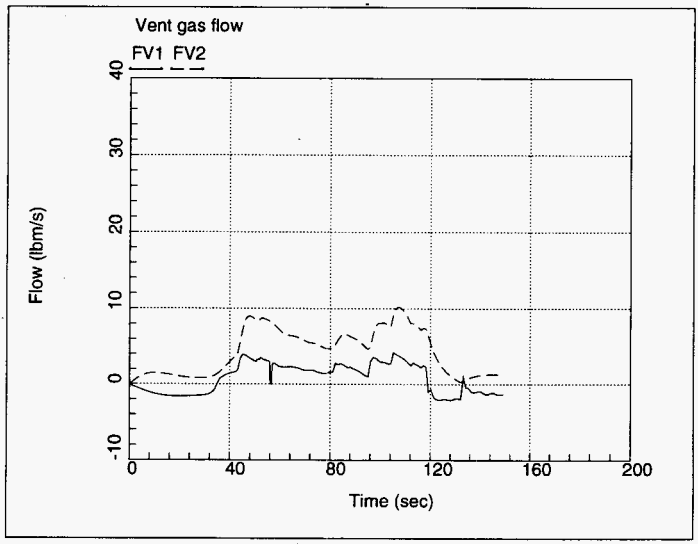

Figure 18. Liquid Droplets Flow Through Inleakage Flow Path.

b18c92sv-18 inch original waste, conservative temperature at atmospheric pressure. No condensat
Fri Apr 26 10:36:02 1996
GOTH Version 3.4 - April 1991

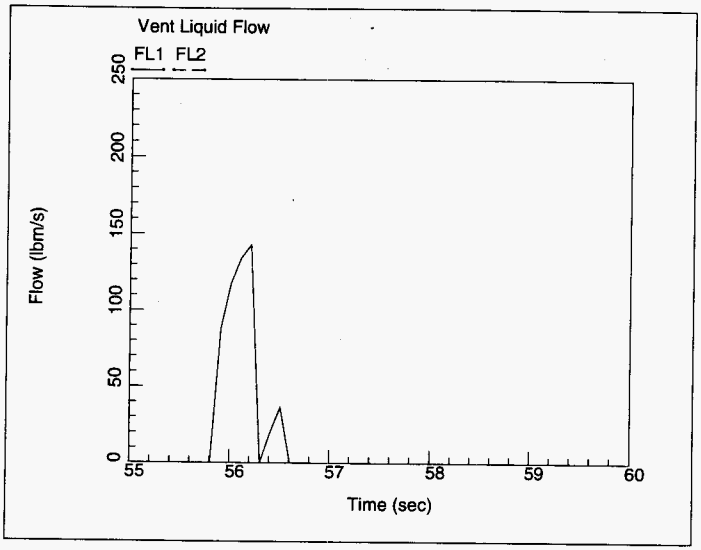

Figure 19. Solid Particle Flow Through Inleakage Flow Path.

b18c92sv-18 inch original waste, conservative temperature at atmospheric pressure. No condensat
Fri Apr 26 10:36:33 1996
GOTH Version 3.4 - April 1991

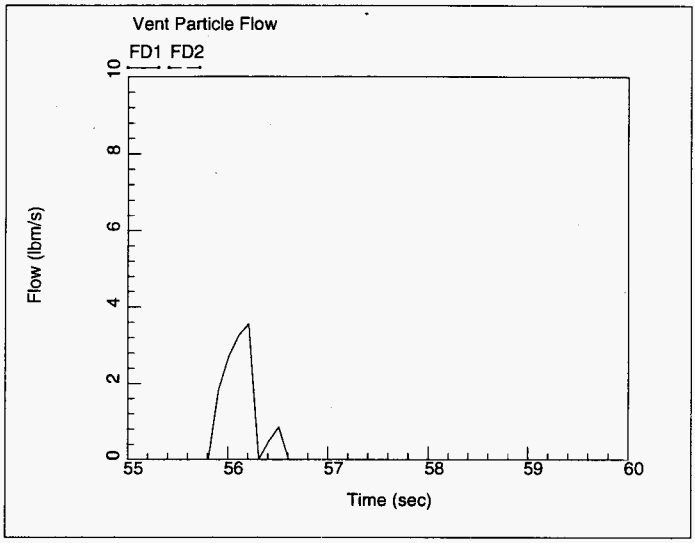

Figure 20. Steam Concentration Contours in 18-Inch Sludge of Tank AZ-101 Waste With 6-Inch Diameter Inleakage Flow Path.

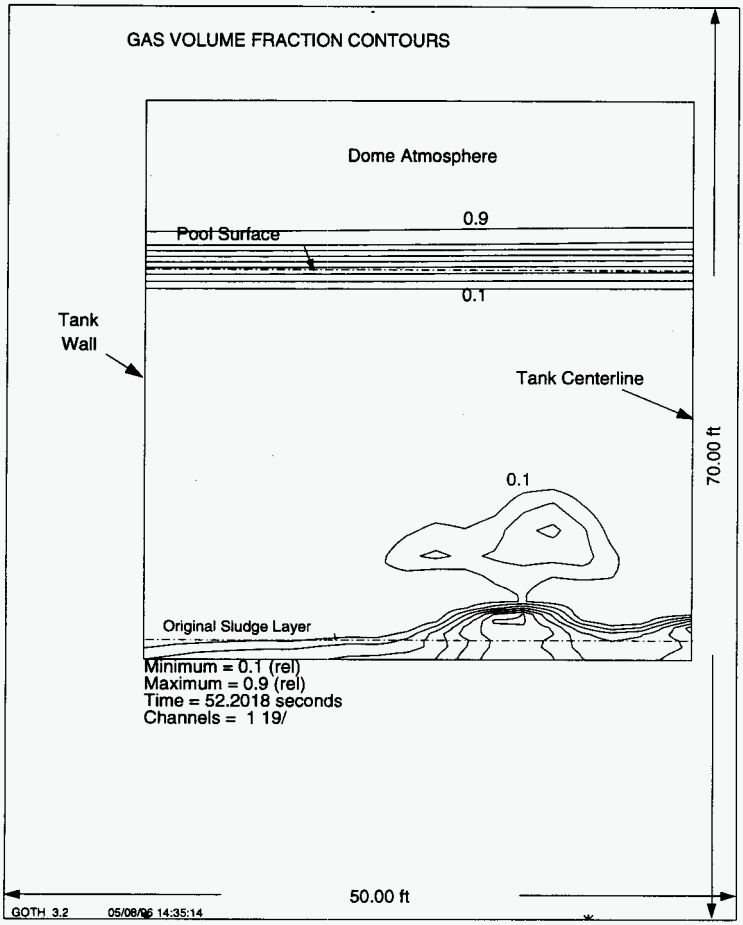

Figure 21. Steam Concentration Contours in 18-Inch Sludge of Tank AZ-101 Waste With 6-Inch Diameter Inleakage Flow Path.

b18conv2-18 inch original waste, conservative temperature at atmospheric pressure. No condensat
Thu May 9 09:25:23 1996
GOTH Version 3.4 - April 1991

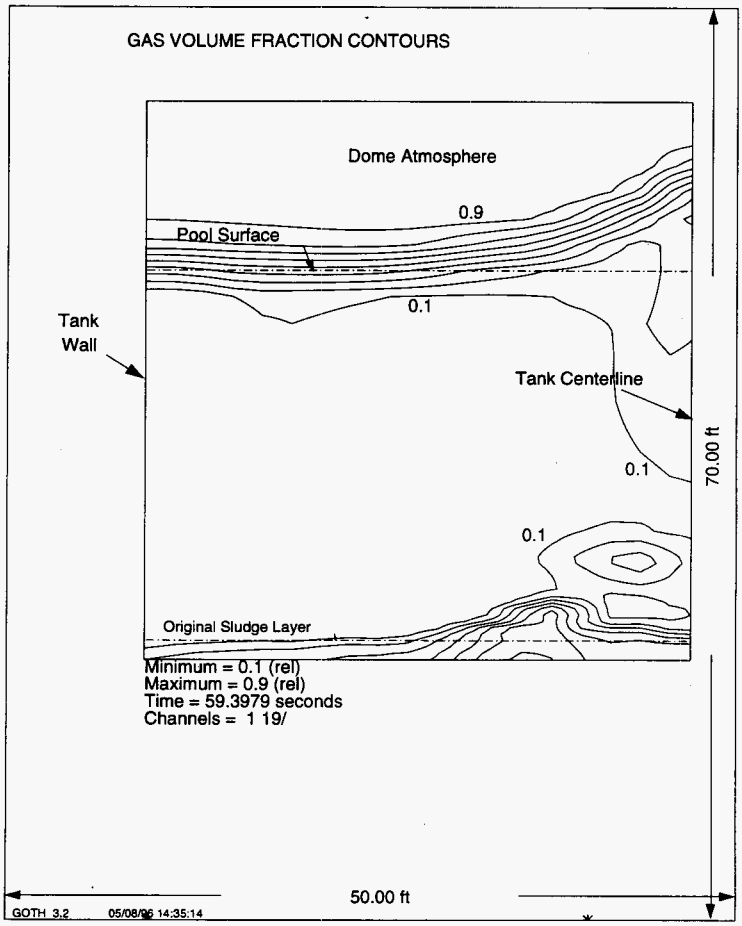

Figure 22. Steam Concentration Contours in 18-Inch Sludge of Tank AZ-101 Waste With 6-Inch Diameter Inleakage Flow Path.

b18conv2-18 inch original waste, conservative temperature at atmospheric pressure. No condensat
Thu May 9 09:42:50 1996
GOTH Version 3.4 - April 1991

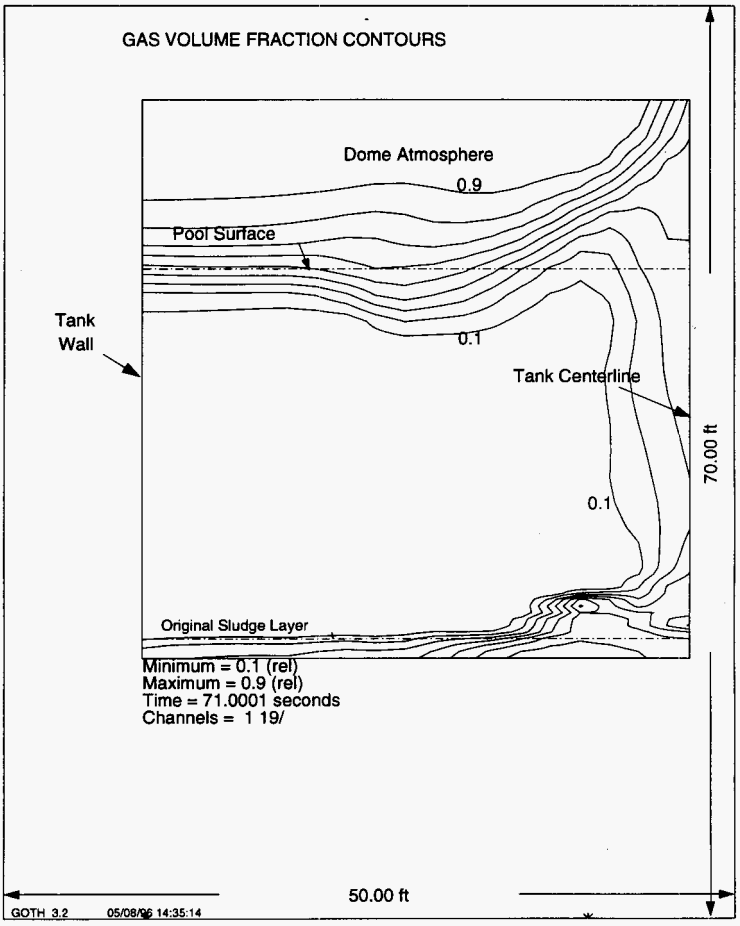

Figure 23. Gas/Steam Flow Through Inleakage and Ventilation Flow Paths.

b18conv2-18 inch original waste, conservative temperature at atmospheric pressure. No condensat
Thu May 9 09:52:39 1996
GOTH Version 3.4 - April 1991

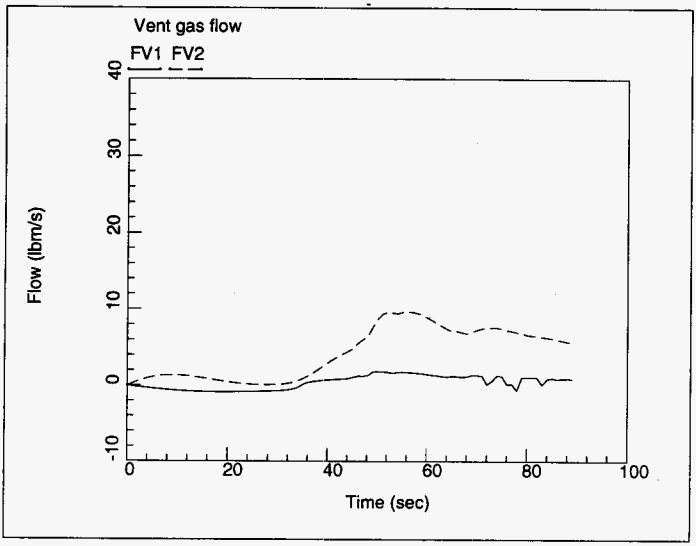

Figure 24. Liquid Droplets Flow Through Inleakage Flow Path.

b18conv2-18 inch original waste, conservative temperature at atmospheric pressure. No condensat
Thu May 9 09:52:03 1996
GOTH Version 3.4 - April 1991

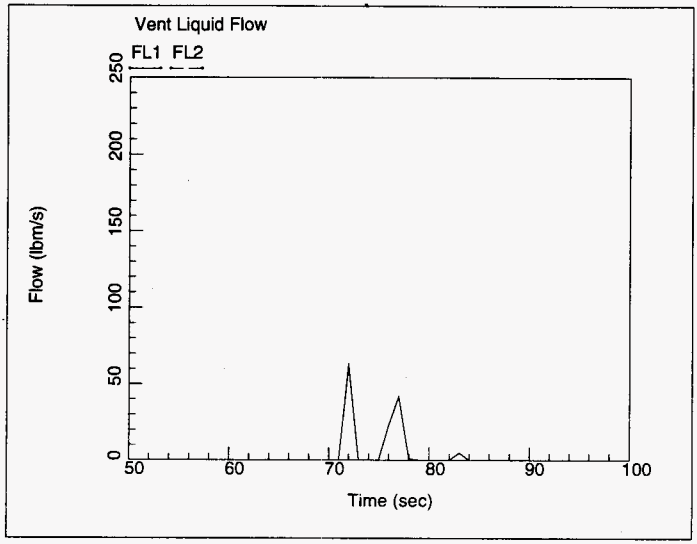

Figure 25. Solid Particle Flow Through Inleakage Flow Path.

b18conv2-18 inch original waste, conservative temperature at atmospheric pressure. No condensat
Thu May 9 09:52:22 1996
GOTH Version 3.4 - April 1991

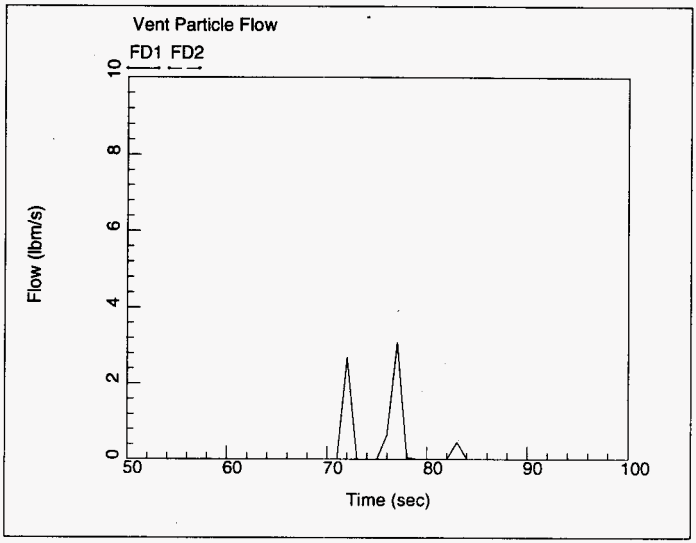

Figure 26. Steam Concentration Contours in 18-Inch Sludge of Tank AZ-101 Waste With 6-Inch Diameter Inleakage Flow Path and 24-Inch Ventilation Duct.

b18consv-18 inch original waste, conservative temperature at atmospheric pressure. No condensat
Thu Apr 25 13:40:39 1996
GOTH Version 3.4 - April 1991

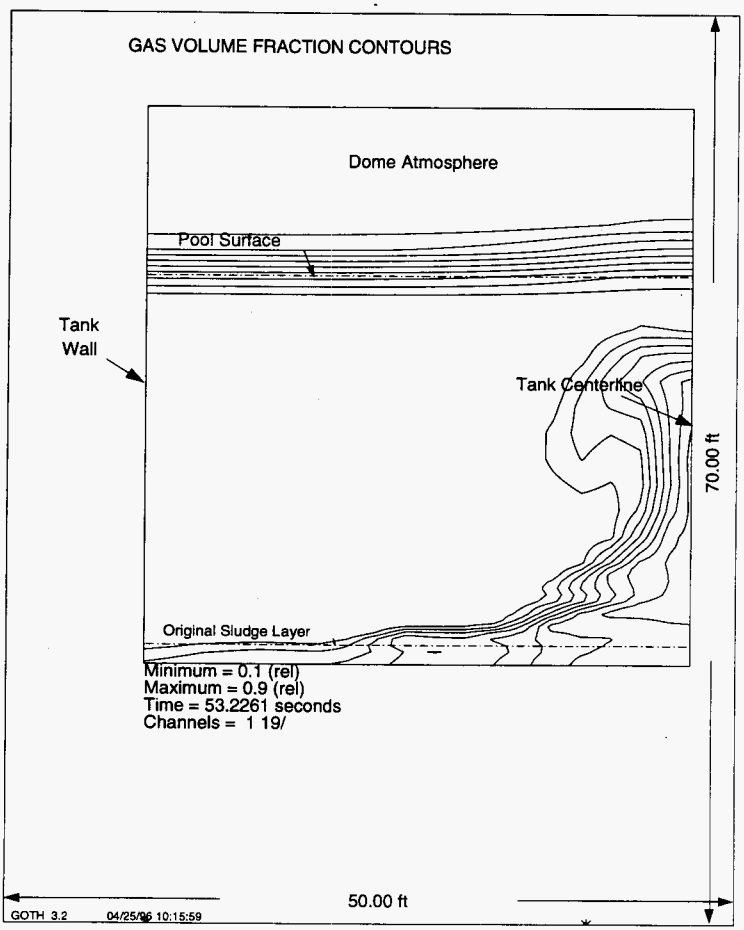

Figure 27. Steam Concentration Contours in 18-Inch Sludge of Tank AZ-101 Waste With 6-Inch Diameter Inleakage Flow Path and 24-Inch Ventilation Duct.

b18consv-18 inch original waste, conservative temperature at atmospheric pressure. No condensat
Thu Apr 25 13:41:21 1996
GOTH Version 3.4 - April 1991

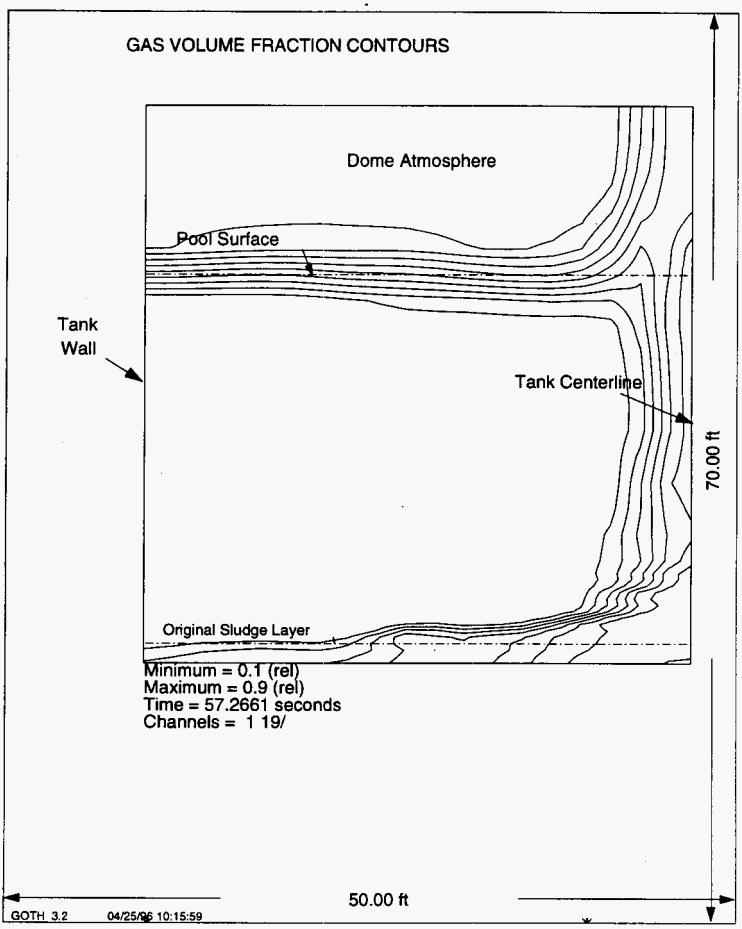

Figure 28. Steam Concentration Contours in 18-Inch Sludge of Tank AZ-101 Waste With 6-Inch Diameter Inleakage Flow Path and 24-Inch Ventilation Duct.

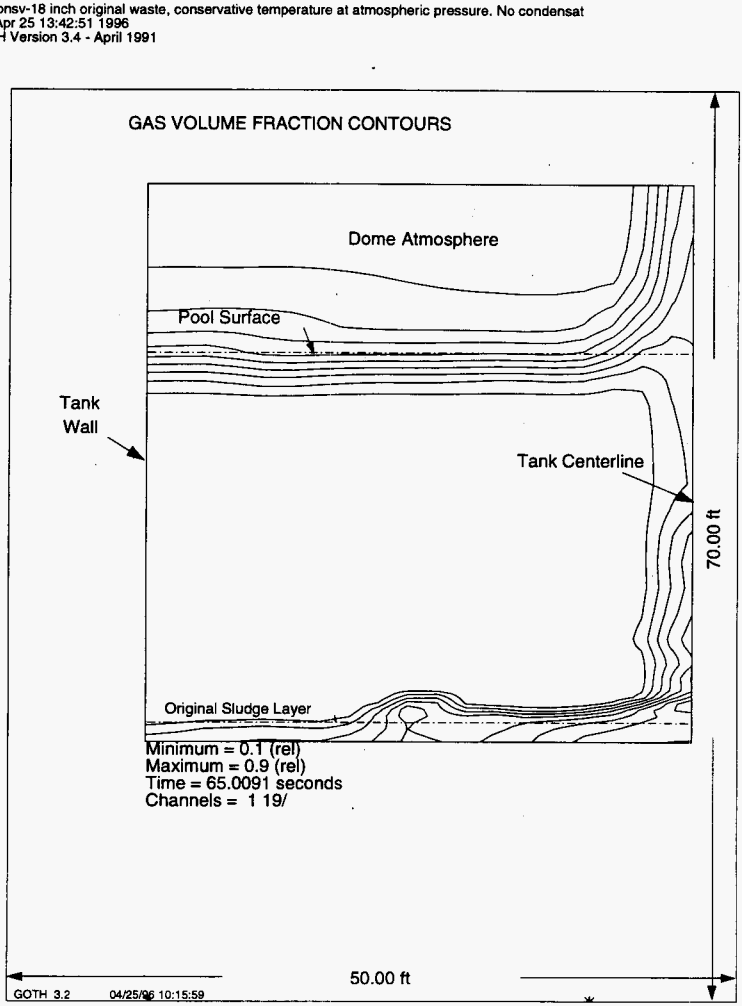

Figure 29. Gas/Steam Flow Through Inleakage and Ventilation Flow Paths.

b18consv-18 inch original waste, conservative temperature at atmospheric pressure. No condensat
Thu Apr 25 09:38:56 1996
GOTH Version 3.4 - April 1991

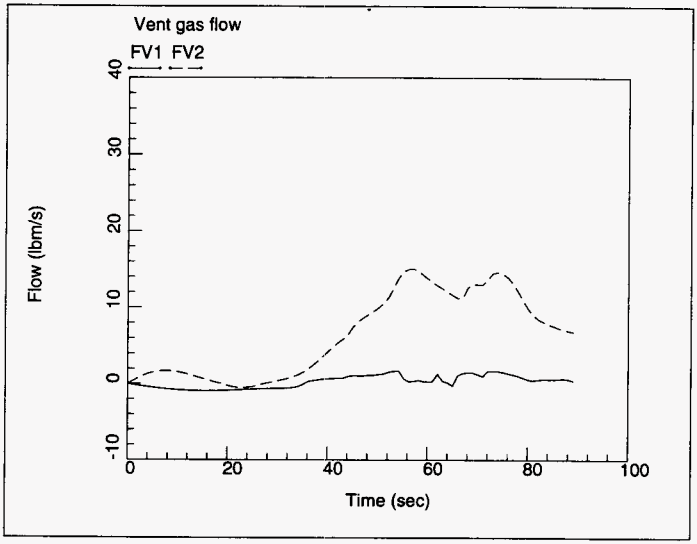

Figure 30. Liquid Droplets Flow Through Inleakage Flow Path.

b18conv1-18 inch original waste, conservative temperature at atmospheric pressure. No condensat
Thu May 9 14:41:19 1996
GOTH Version 3.4 - April 1991

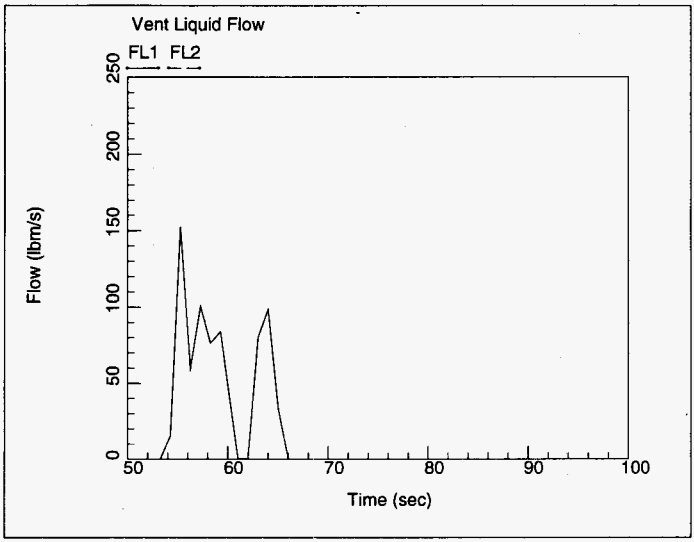

Figure 31. Solid Particle Flow Through Inleakage Flow Path.

b18conv1-18 inch original waste, conservative temperature at atmospheric pressure. No condensat
Thu May 9 14:42:18 1996
GOTH Version 3.4 - April 1991

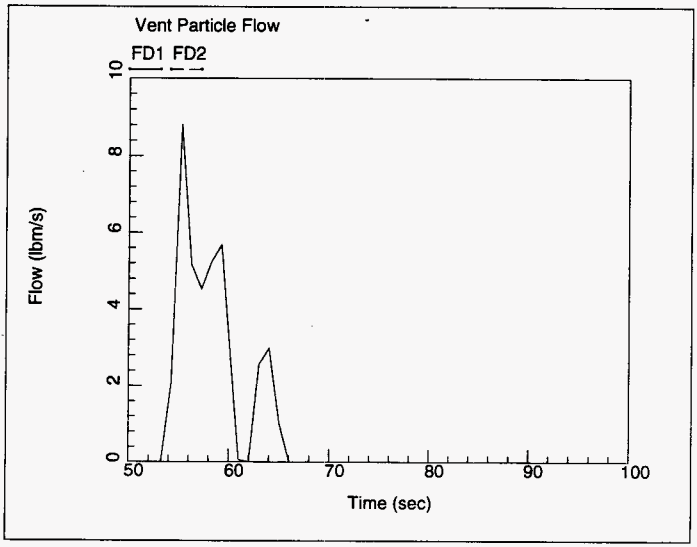

7.1.2 Conservative Initial Temperature with Condensation

The tank bump calculation for the 18 inch AZ-101 sludge was performed, including the effect of condensation of steam in the waste. In this case, the condensation is allowed in the 213 °F supernatant based on the degree of mixing, the two-phase flow regime, and interfacial mass transfer. The vapor concentration profile in the waste just prior to the initiation of initial steam bump is shown in Figure 32. The vapor contour profile shows that due to the condensation of steam at the sludge/supernatant interface, the volume of steam in the sludge at this instant is less than that in the previous case where condensation was suppressed. .The condensation at the interface suppresses the development of the hydrodynamic instability since the strength of the instability or the volume of vapor for this layer thickness is not strong enough to overcome condensation caused by introducing steam and superheated sludge into the node above the sludge which is filled with subcooled supernatant. This suppression of the instability may be numerical, indicating that smaller mesh sizes may be required to calculate the heat transfer between the sludge and supernatant in cells containing the sludge interface. However, for thin sludge layers the bump strength appears to be weak, and it is quite possible that mixing at the sludge interface will allow subcooled supernatant to condense the steam before a steam/sludge plume can develop. The instability attempts to form a plume, but it is suppressed by condensation as shown in Figure 33 (compare with Figure 11). Mixing of sludge and supernatant at the sludge/supernatant interface caused by the flows induced by the instability cause the collapse of the steam void in the sludge (see Figure 34). Therefore, for this case with condensation, the results show that the steam bump does not occur. It is likely, that collapse of the steam void is, in part, caused by the mesh size and the numerical model. However, clearly the strength of the instability in thin sludge layers is weak and the bumps that are produced are weak. So it is very likely that the plumes formed in this layer will breakup and condense if there is a thick layer of subcooled supernatant on top of the sludge.

7.1.3 Best Estimate Initial Temperature and No Condensation

The calculations described above utilized an initial temperature distribution equal to the local saturation temperature in the sludge. This initial temperature distribution led to the strongest possible bump for a given sludge thickness. In this section, results are presented for the case where the best estimate temperature distribution leads to a steam bump in the 18 inch sludge layer of tank AZ-101. This temperature distribution corresponds to the time when the sludge at the bottom of the tank first reaches saturation during the transient heat up due to a ventilation outage. Bumps generated from this temperature profile will be smaller for this case, since less sludge is at the saturation temperature so less energy is stored in the sludge.

Case 1: Steam Bump with Open Risers and Cover Blocks

The waste temperature is initialized with temperature distribution as shown in Figure 2. The heatup is assumed due to ventilation system outage. The vapor concentration contours in the sludge just prior to and during the plume development are shown in Figures 35 and 36. Clearly, the plumes formed

Figure 32. Steam Concentration Contours in Sludge Just Prior to Initiation of Steam Bump.

b18conc-18 inch original waste, conservative temperature at atmospheric pressure. Condensat
Wed May 22 14:36:07 1996
GOTH Version 3.4 - April 1991

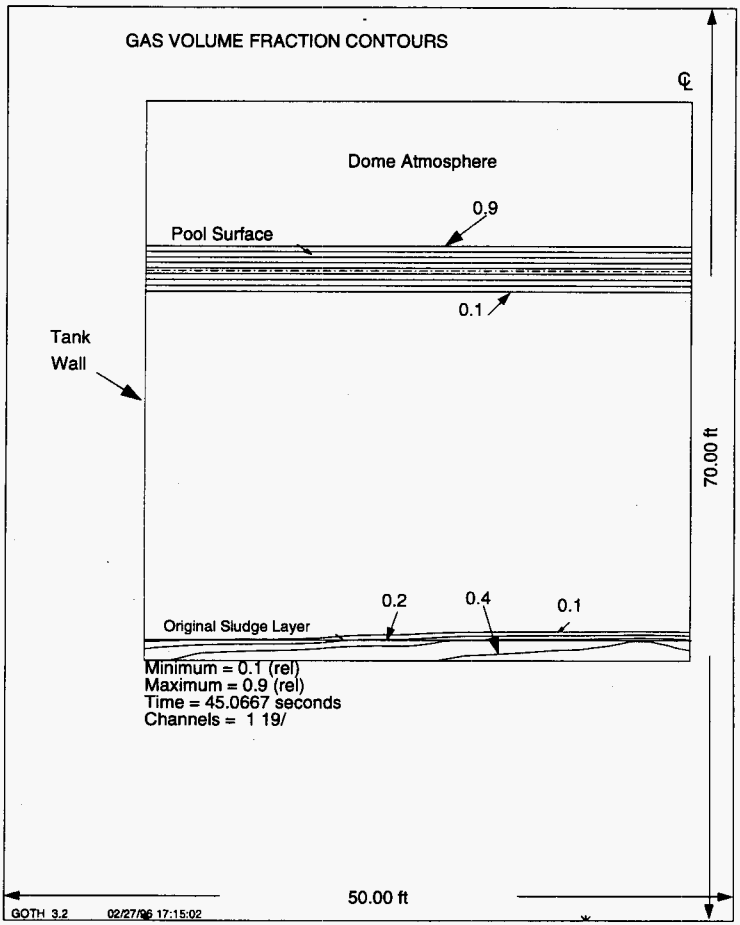

Figure 33. Steam Concentration Contours in Sludge Showing the Suppression of Plume Formation by Condensation.

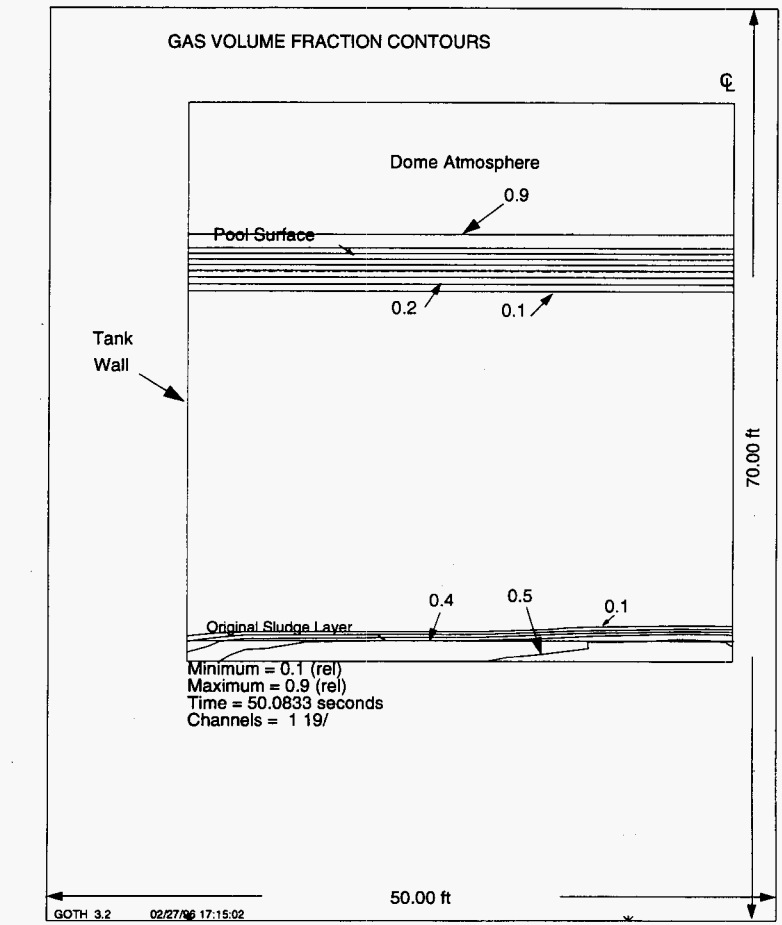

Figure 34. Steam Concentration Contours in Sludge Indicating the Collapse of Steam Bubble Due to Mixing at Sludge/Supernatant Interface.

b18conc-18 inch original waste, conservative temperature at atmospheric pressure. Condensat
Wed May 22 14:40:15 1996
GOTH Version 3.4 - April 1991

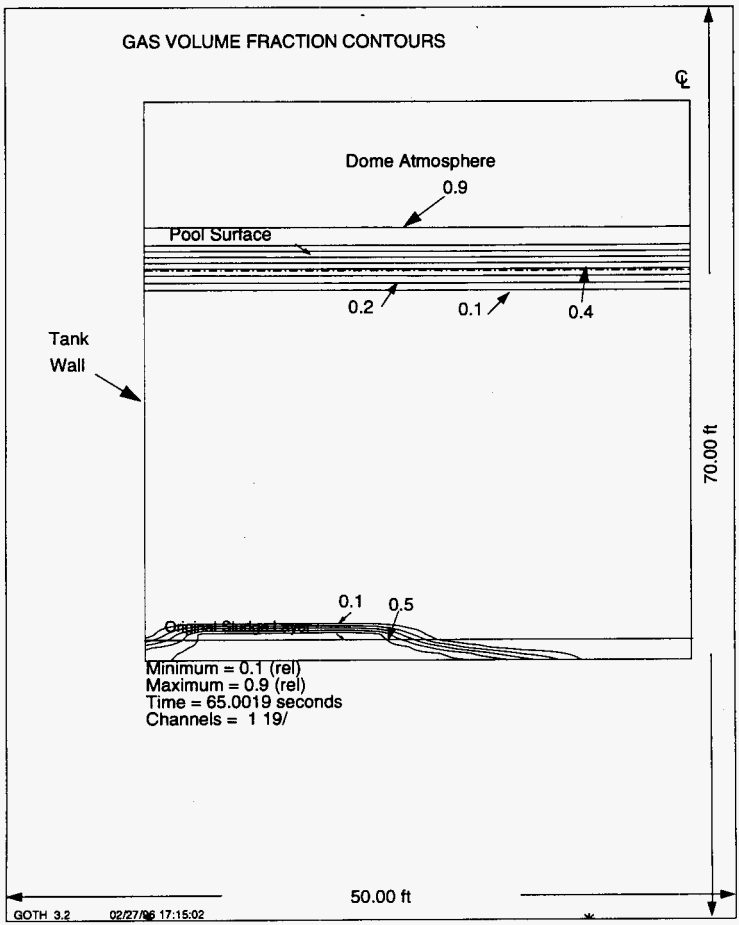

Figure 35. Steam Concentration contours In Sludge Just prior to Plume Formation For Best Estimate Initial Temperature Profile.

b18be-18 inch original waste, conservative temperature at atmospheric pressure. No condensat
Fri May 24 11:25:57 1996
GOTH Version 3.4 - April 1991

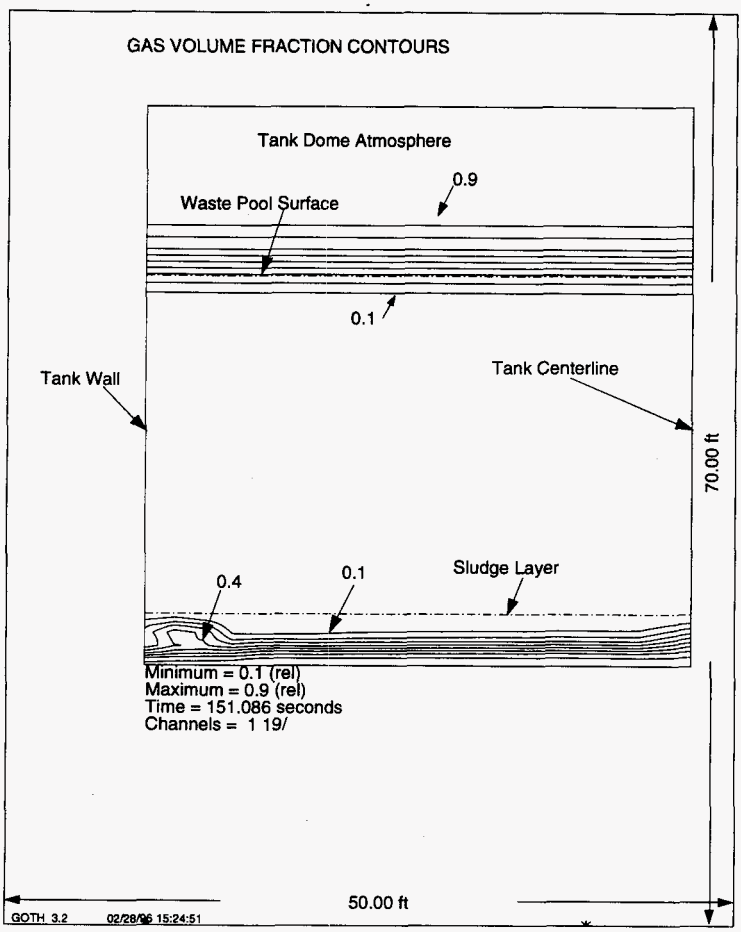

Figure 36. Steam Concentration Contours In Sludge Showing Plume Formation.

b18be-18 inch original waste, conservative temperature at atmospheric pressure. No condensat
Fri May 24 11:25:37 1996
GOTH Version 3.4 - April 1991

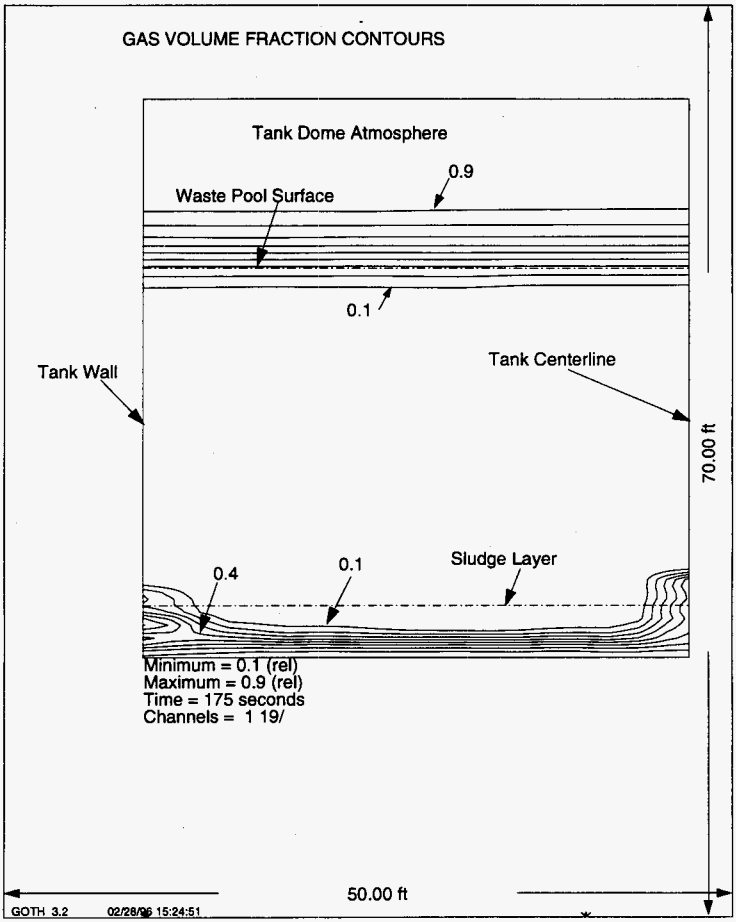

in this case are smaller than in the case where the simulation has been initiated with the conservative temperature distribution. Also, the time delay before plumes begin to form is nearly 2 minutes longer. The detachment of the plumes and the size of sludge/steam bubbles is smaller than those formed for the conservative case and does not create much of a disturbance as they approach the surface (see Figures 37 and 38). Little steam was able to leave the supernatant and there was no significant dispersal of aerosols to the tank dome atmosphere.

The steam bump was not predicted starting with this temperature distribution in the sludge even under conditions of suppressed condensation effects and with large vent openings. This simulation shows that even if the saturation temperature is reached at some location in the sludge and if the large portion of sludge is below saturation conditions, then steam bump does not seem to be possible provided appropriate steps are taken to prevent any further heat up of the sludge.

7.2 48-INCH SLUDGE LAYER OF AZ-101 WASTE

It is assumed that the four feet of sludge considered here is currently made up of 18 inches of tank AZ-101 sludge at thermal equilibrium with the supernatant at present operating conditions of primary ventilation system on and with no secondary ventilation system and added thirty inches of additional sludge having the same waste characteristics. This additional sludge is assumed to settle immediately to the bottom of the tank on top of the existing 18 inch sludge layer. The sludge will heat up due to the increased heat load and sludge thickness even with the primary ventilation system operating. The sludge will reach the local saturation temperature for a sludge layer of 4 ft. thickness under current operating conditions (Sathyanarayana 1994b). Steam bump simulations using the conservative and best estimate axial temperature distribution and with three different vent models are performed and the results are discussed in this section. The effect of condensation was also investigated for this sludge thickness case.

7.2.1 Conservative Initial Temperature and No Condensation

The tank waste subjected to initial bumps, mechanical mixing and/or prolonged outage of ventilation system can lead to temperature distribution as shown in Figure 6 for 48 inch sludge. The steam bumps with such an initial distribution of sludge temperature are discussed in this section. Steam bump calculations for 48 inch sludge are performed not allowing condensation between the steam and the supernatant for three different inleakage flow path areas. The potential range of vent and leakage flows from the tank dome space for steam bumps calculated using a conservative temperature distribution in the sludge and different inleakage flow path areas are shown in Table 4. These calculations assume that no condensation is possible between steam and supernatant.

Case 1: Steam Bump With Riser Flanges and Cover Blocks Open

This simulation should be considered a worst possible case for the generation of a steam bump in 48 inch sludge since the sludge is at the local

Figure 37. Steam Concentration Contours In Sludge Indicating the Detachment of Plume.

b18be-18 inch original waste, conservative temperature at atmospheric pressure. No condensat
Fri May 24 11:25:26 1996
GOTH Version 3.4 - April 1991

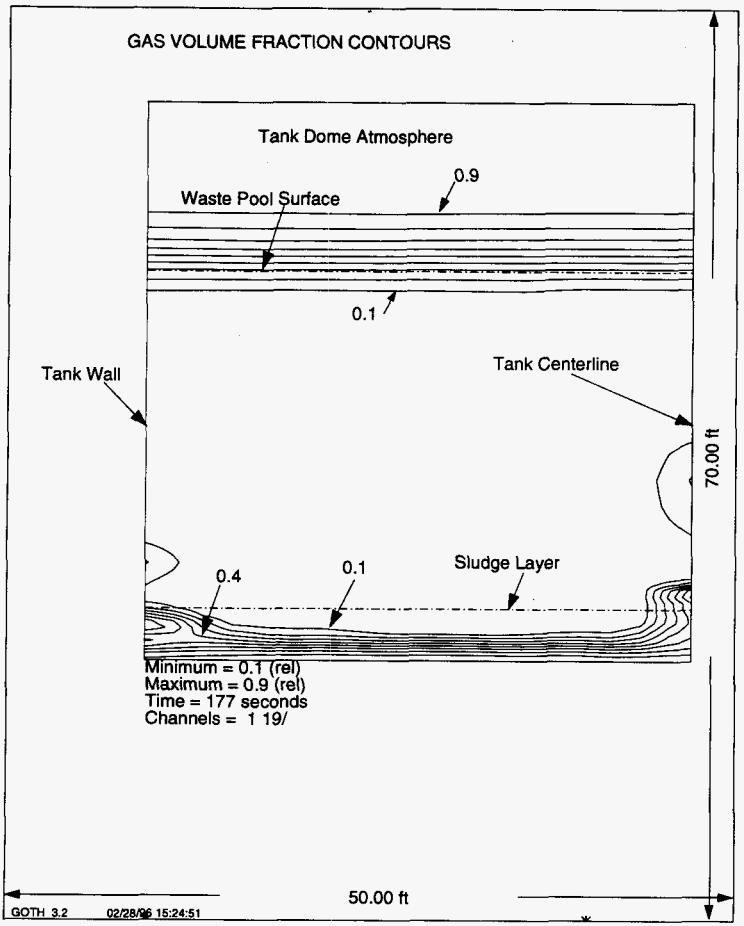

Figure 38. Steam Concentration Contours In Sludge Indicating the Steam Bubble Approaching Pool Surface.

b18be-18 inch original waste, conservative temperature at atmospheric pressure. No condensat
Fri May 24 11:25:15 1996
GOTH Version 3.4 - April 1991

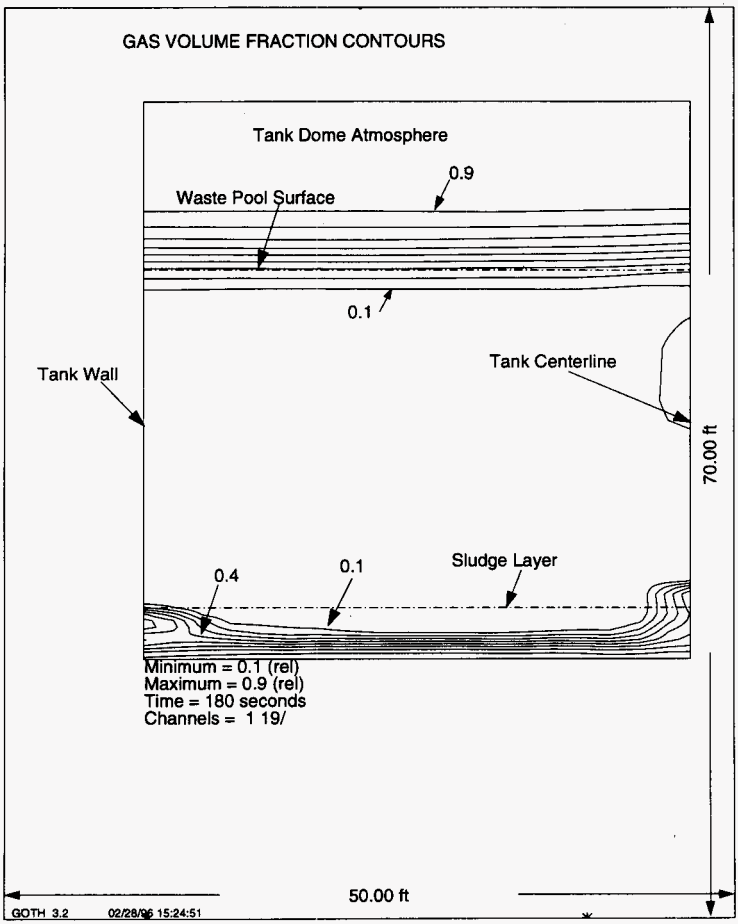

Table 4. Estimate of Vent Flows for a Conservative Tank Bump in 48 Inches of Tank AZ-101 Sludge.

Parameters	Dome Flow Paths	Dome Flow Path	Dome Flow Path
	1. 42" dia-Pump Pit Path 2. 20" dia-Vent Path 3. Four 42" dia-Sluice Pits Path	1. Five 4" dia-Inleakage Paths 2. 20" dia-Vent Path	1. 6" dia-Inleakage Path 2. 20" dia-Vent Path
1. Tank Dome Peak Pressure, psia	22.5	17.3	19.5
2. Vapor Flow Flow path 1, lbm Flow path 2, lbm Flow path 3, lbm	 150 -- 1050	 120 460 NA	 160 1200 NA
3. Liquid Flow Flow path 1, lbm Flow path 2, lbm Flow path 3, lbm	 24000 -- 76000	 640 -- NA	 3900 00
4. Particle Flow Flow path 1, lbm Flow path 2, lbm Flow path 3, lbm	 4000 -- 2300	 85 -- NA	 165 -- NA

saturation temperature throughout and the four sluice pits and one pump pit risers open to ambient pressure. This provides the maximum energy for producing a steam bump that will rise through the waste and release aerosols into the dome space.

The steam concentration contours just prior to the initiation of the bump is shown in Figure 39. The top contour lines show the location of the pool surface. Above these lines is the gas in the dome atmosphere and below is the supernatant liquid. The dashed line at the bottom shows the original location of the 48 inch sludge layer before steam started to accumulate in the sludge. The contour lines at the bottom of the tank show the distribution of the steam in the tank just prior to the development of the hydrodynamic instability that results in the formation of a steam bump. Figure 40 shows the development of the hydrodynamic instability. The location at which the plumes begin to form is probably random, although as shown in Figure 11, multiple points of instability tend to develop for thin layers and for the sludge layer that have significant radial temperature gradients. The formation of multiple separated instabilities tend to reduce the severity of the bump. A strong single point of instability develops for this case and results in a very high energy bump releasing large quantities of liquid and particles.

The formation of a single plume of superheated sludge containing steam, particles and supernatant is shown in Figure 41. The plume rises toward the pool surface under the influence of buoyancy, shear and drag forces acting on it. The plume detaches from the sludge layer within seconds of being formed and rises to the surface of the waste (see Figure 42) where it flows through as shown in Figure 43 and generates liquid and solid particle aerosols in the tank dome space. Plumes continue to form, break free and rise to the surface. Each plume is sufficiently large to disperse liquid droplets and solid particles in the dome space to the elevation of leakage and vent flow inlets as shown in Figure 43 and 44. This results in a release of liquid droplets and solid particles from the dome space to the tank surroundings and ventilation system (see Figures 45 and 46). Almost all the liquid and solid particle flow is to the tank surroundings because of large leakage flow area.

It should be noted that an explicit calculation of the total amount of aerosols released to the atmosphere depends on the time allowed for the bumps to continue and on the exact nature of each bump. Bumping may be interrupted for a period of time while solids that have been mixed with the supernatant due to previous bumps resettle and reform the sludge layer, but bumps will resume as soon as this occurs.

The peak sludge temperature reaches the saturation value due to the addition of 30 inches of similar sludge while operating the primary ventilation system normally. The supernatant will heat up due to added heat load and reach an equilibrium. For these simulations a supernatant temperature of 163 °F was used. The supernatant is likely to reach saturation if the primary ventilation system is lost, resulting in conditions nearly the same as those used in these calculations. This condition can be avoided by assuring that the ventilation system remains operational or it is restored or by keeping the waste mixed with a mixing pump well before the sludge temperatures for bump initiation are reached. Operation of mixing pumps will also heat the tank contents, and there may be limits on how long the pumps may be operated for both ventilation on and ventilation off cases.

Figure 39. Steam Concentration Contours For 48 inch Sludge Just Prior to Initiation of Steam Bump.

b48con-48 inch original waste, conservative temperature at atmospheric pressure. No condensat
Fri May 24 14:04:29 1996
GOTH Version 3.4 - April 1991

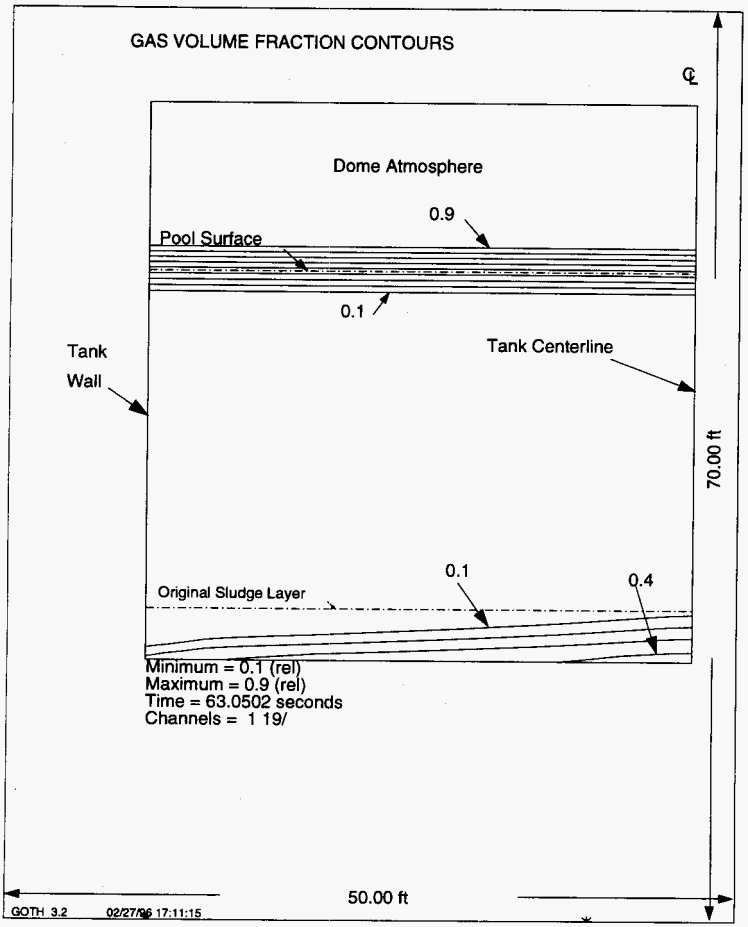

Figure 40. Steam Concentration Contours In 48 inch Sludge Indicating Hydrodynamic Instability Just Prior to Initiation of Steam Bump.

b48con-48 inch original waste, conservative temperature at atmospheric pressure. No condensat
Fri May 24 14:08:07 1996
GOTH Version 3.4 - April 1991

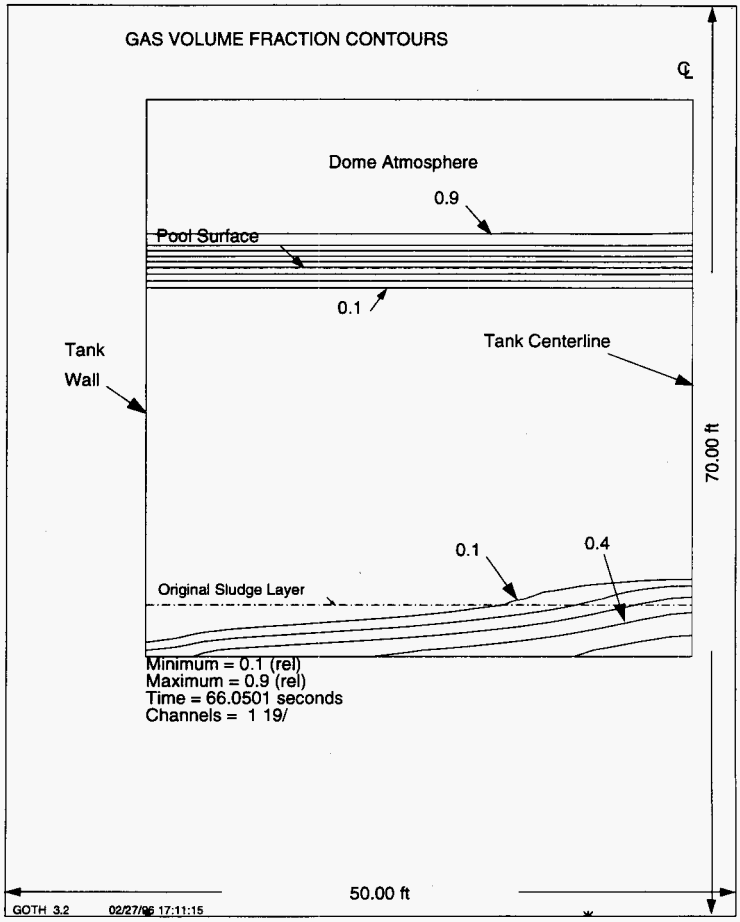

Figure 41. Steam Concentration Contours In Sludge Indicating the Formation of Superheated Sludge Plume.

b48con-48 inch original waste, conservative temperature at atmospheric pressure. No condensat
Fri May 24 14:10:22 1996
GOTH Version 3.4 - April 1991

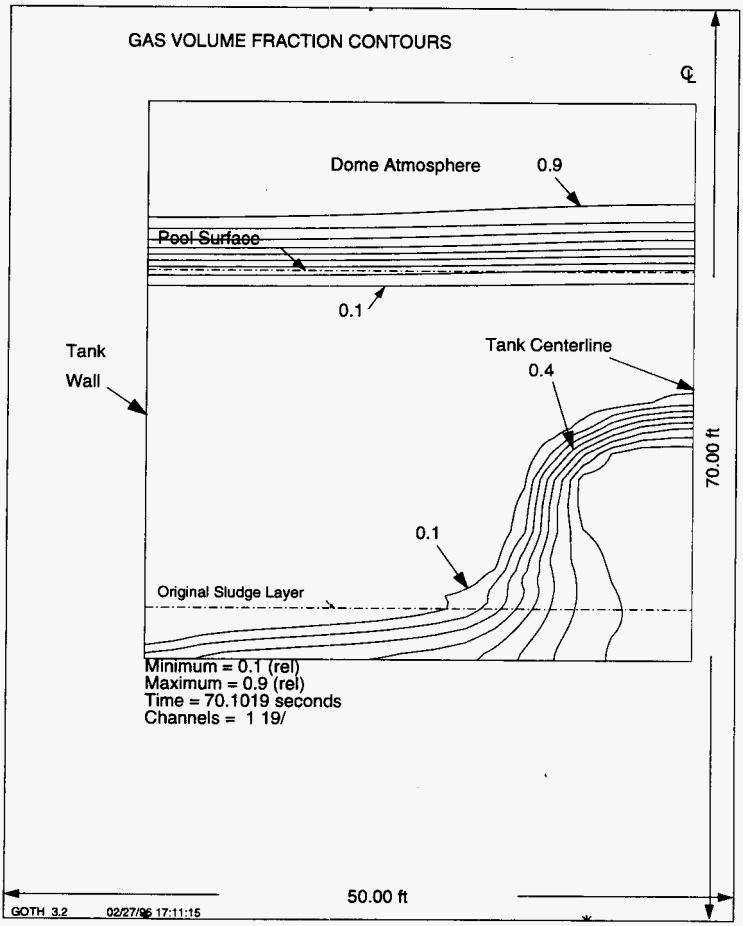

Figure 42. Steam Concentration Contours In Sludge Showing Plume Rise to Supernatant Surface.

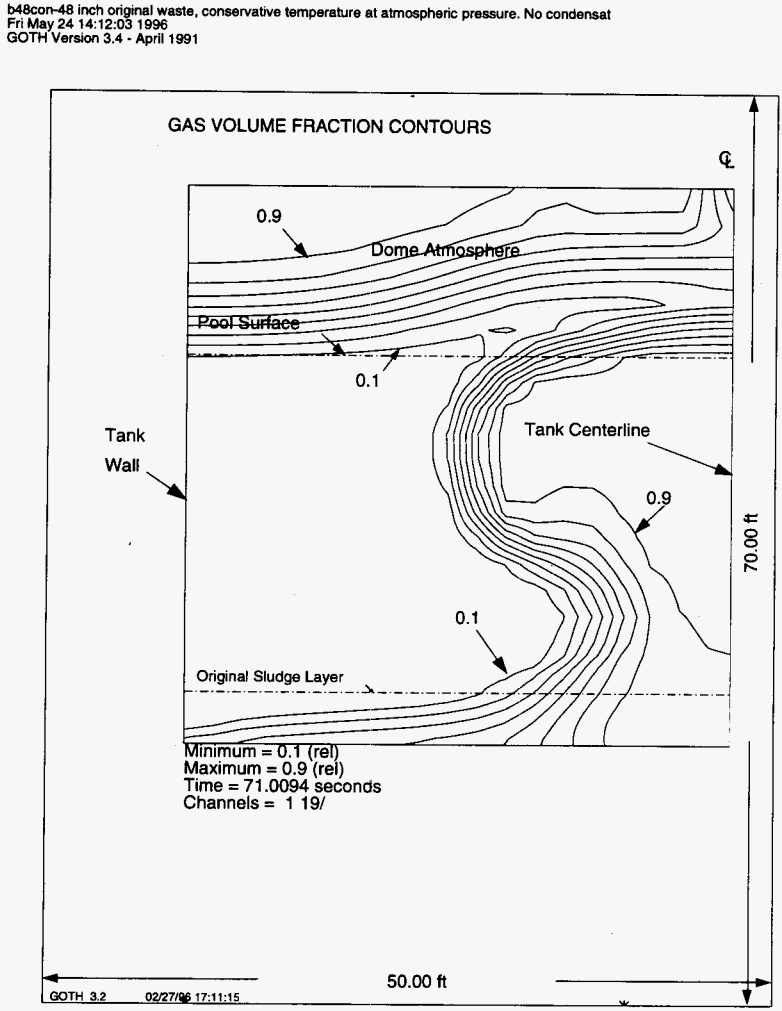

Figure 43. Steam Concentration Contours In Sludge Indicating Hot Sludge and Steam Bubble Breaks Pool Surface.

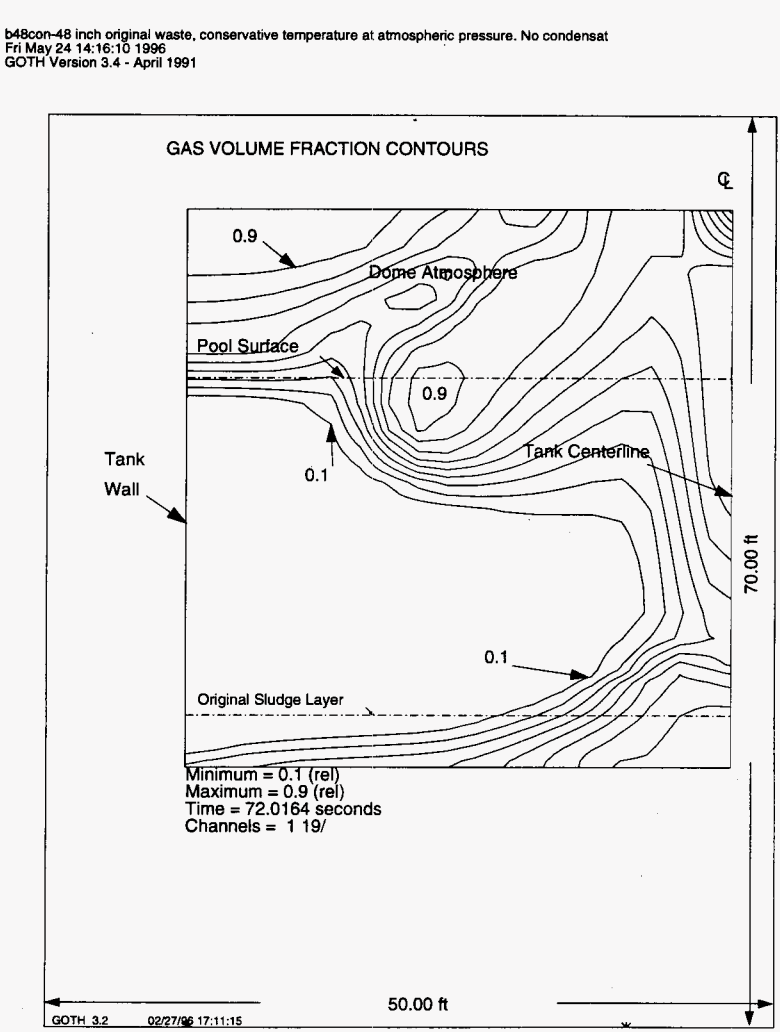

Figure 44. Steam Bump Releasing Liquid Droplets and Solid Particles through Inleakage and Ventilation Flow Paths.

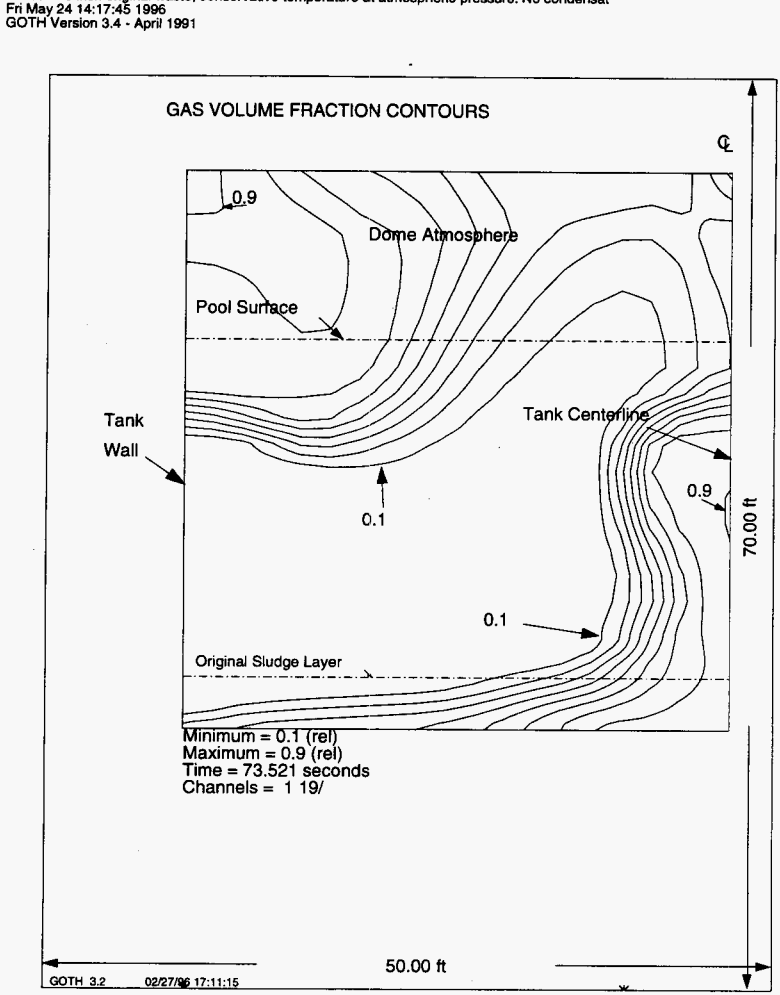

Figure 45. Liquid Droplet Flow Out Through Inleakage Flow Path Due to Steam Bump.

b48con-48 inch original waste, conservative temperature at atmospheric pressure. No condensat
Fri May 24 14:19:33 1996
GOTH Version 3.4 - April 1991

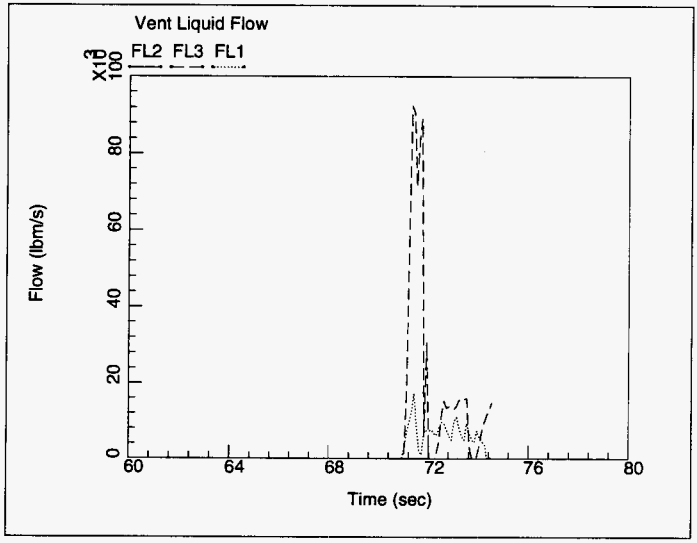

Figure 46. Solid Particle Flow Out Through Inleakage Flow Path Due to Steam Bump.

b48con-48 inch original waste, conservative temperature at atmospheric pressure. No condensat
Fri May 24 14:20:51 1996
GOTH Version 3.4 - April 1991

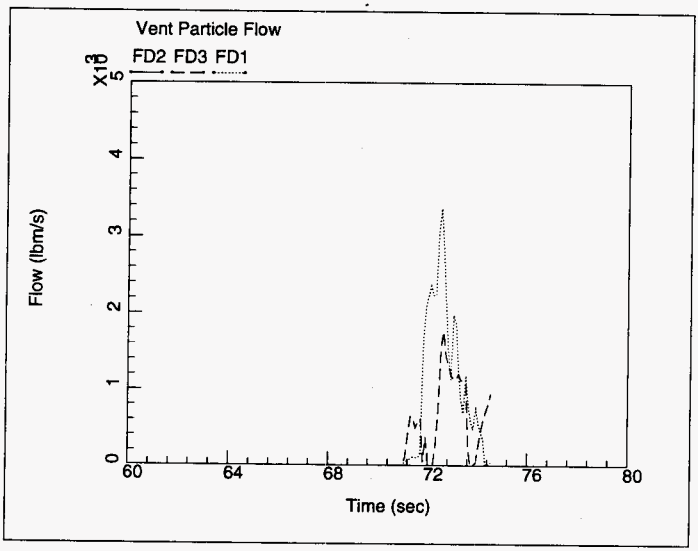

Case 2: Steam Bump with Five 4 inch Drain Pipes as Leakage Flow Paths

This simulation is similar to the above except the leakage flow path area is smaller, corresponding to the total area of five 4 inch diameter drain pipes. The steam concentration contours shown in Figures 47 through 49 indicate that the plume formation starts a few seconds later and the size of the plume is smaller. This is because less high temperature waste gets to the surface and less liquid flashing occurs because of the more restrictive leakage flow path. The combined effect of less steam in the dome and smaller leakage flow paths creates a peak pressure of 17.3 psia in the dome. Figure 50 shows the dome pressure variation during the steam bump event. For this steam bump event, the liquid droplet and solid particle flows through the leakage and vent flow paths are shown in Figures 51 and 52, respectively. The integrated values of steam/gas, liquid and particle flows are given in Table 4. It can be seen from Figure 50 that a smaller second bump follows the large first bump. There is no material release predicted due to the second bump.

Case 3: Steam Bump with 6 inch Leakage Flow Paths.

In this simulation, the leakage flow area is set to a 6 inch equivalent diameter, which for steady operating conditions, provides normal operating ventilation flow for the tank dome pressure of−2 in. water gauge. The pressure variation in the dome shown in Figure 53 suggests that there is a smaller bump first and then it is followed by a relatively larger bump. The steam concentration contours shown in Figures 54 through 56 indicate that the instability in sludge was developed at the center of the tank and it developed into a plume as in a previous case (see Figure 47) but smaller in size. The plume approaches and flows through the pool surface releasing liquid and solid particles into the dome and subsequently into the atmosphere. The integrated mass flow of releases due to this first bump are much smaller than the values shown in Table 4 as they refer to combined releases for both the bumps. The liquid and solid particle releases were about 200 and 60 lbs, respectively for the first bump. Figures 57 through 59 show the development of the second bump which has its instability started in the middle of the radius and it is larger in size. The vapor, liquid, and particle flows through the leakage and ventilation paths are shown in Figure 60, 61 and 62, respectively.

7.2.2 Conservative Initial Temperature With Condensation.

This case is identical to the case presented in the previous section except that condensation is allowed to occur in the 163.8 °F supernatant. The primary ventilation flow is assumed to continue to operate normally for this case. The steam concentration profile just prior to initiation of the steam bump is shown in Figure 63. The steam void profile just prior to the development of the hydrodynamic instability and the formation of superheated sludge/steam plume are shown in Figures 64 and 65, respectively. The formation of the plume is delayed by about 2 seconds as compared to the case without condensation and the size of the plume is reduced due to the effects of condensation. Figure 66 shows the detachment of the plume from the sludge surface. The neck of the plume is much smaller due to the effects of subcooled supernatant rushing in behind the bubble, condensing steam and cooling the sludge. The steam bubble breaking the pool surface is shown in Figure 67. It should be noted that the supernatant is significantly subcooled

Figure 47. Steam Concentration Contours In Sludge Indicating the Formation of Superheated Sludge Plume.

b48c92sv-48 inch original waste, con temp, atm press. No condensation. Simple Vent.
Fri Apr 26 10:10:41 1996
GOTH Version 3.4 - April 1991

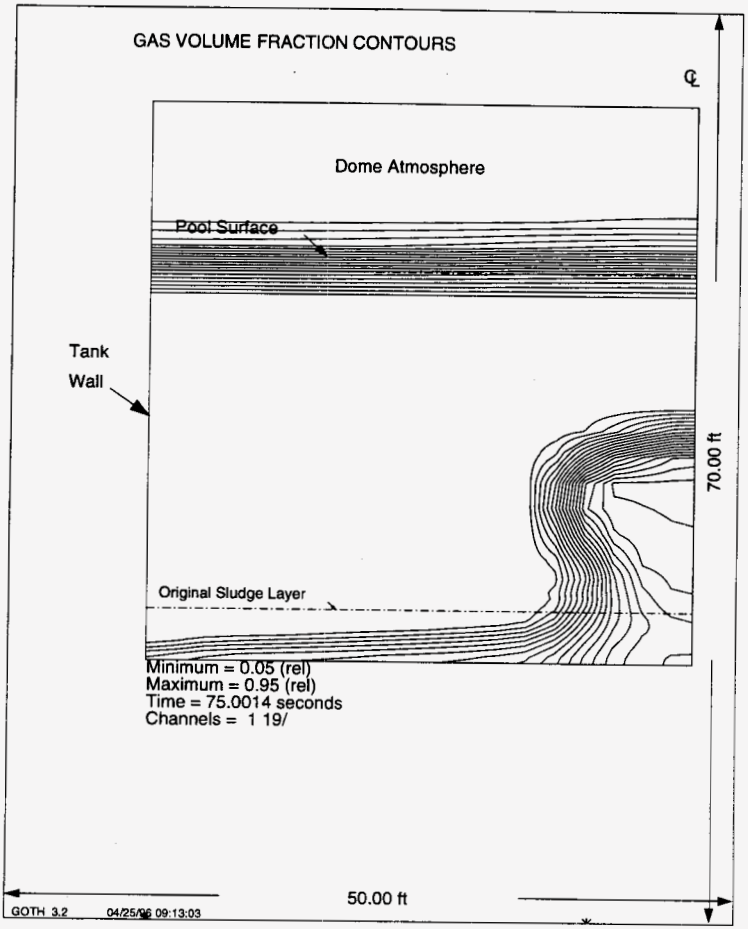

Figure 48. Steam Concentration Contours In Sludge Showing Plume Rise to Supernatant Surface.

b48c92sv-48 inch original waste, con temp, atm press. No condensation. Simple Vent.
Fri Apr 26 10:10:53 1996
GOTH Version 3.4 - April 1991

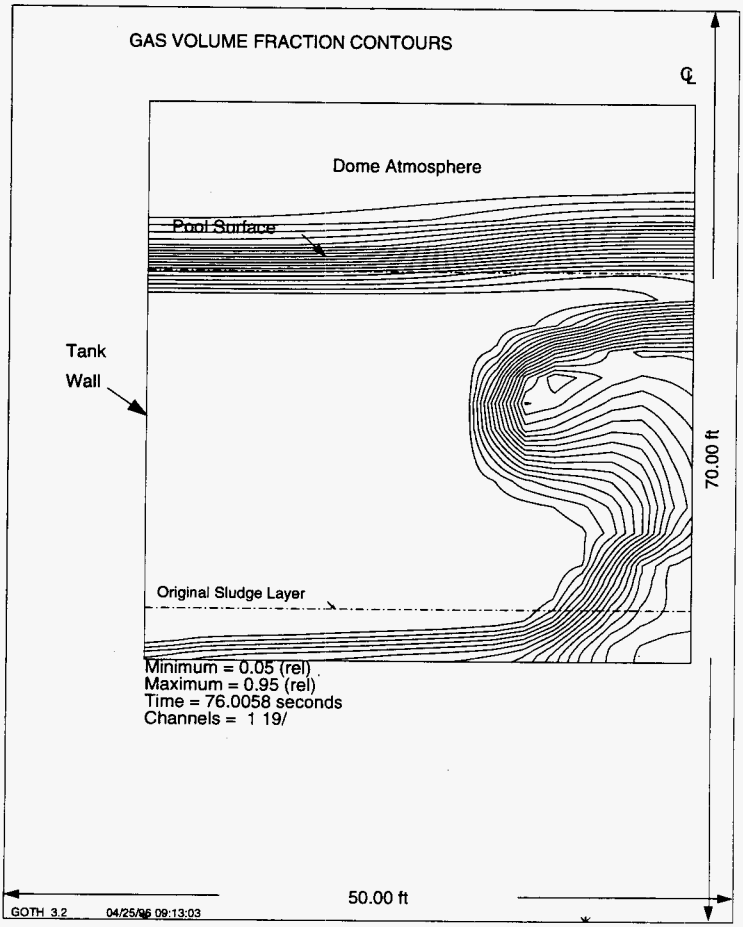

Figure 49. Steam Concentration Contours In Sludge Indicating Hot Sludge and Steam Bubble Breaks Pool Surface.

b48c92sv-48 inch original waste, con temp, atm press. No condensation. Simple Vent.
Fri Apr 26 10:11:04 1996
GOTH Version 3.4 - April 1991

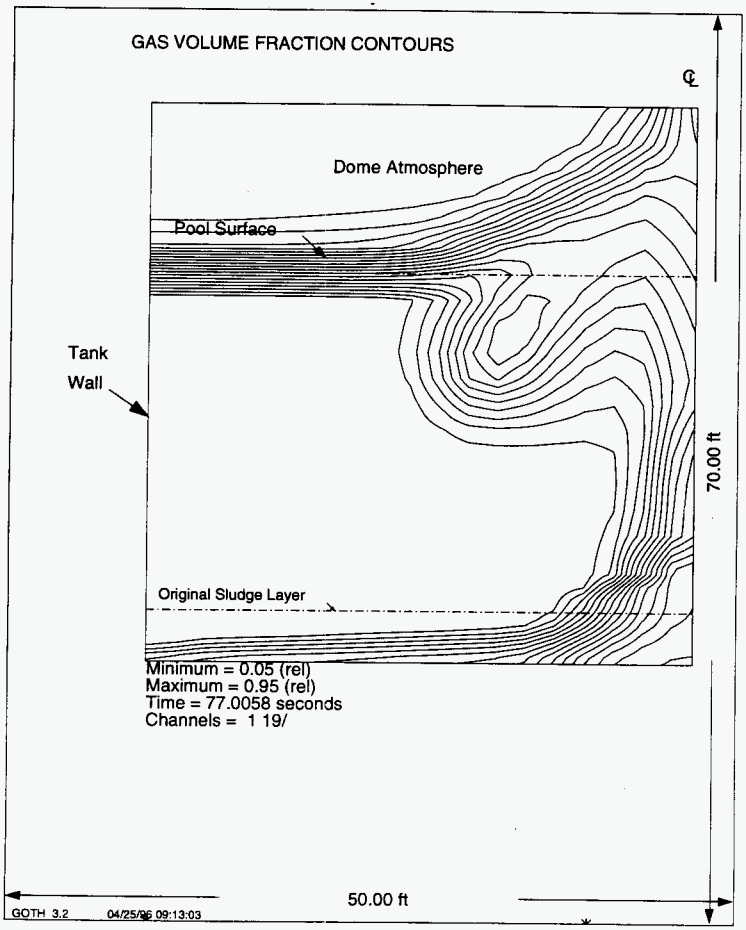

Figure 50. Dome Pressure Variation During Steam Bump For 48 Inch Sludge With Conservative Initial Temperature and Drain Pipes as Dome Leak Paths.

b48c92sv-48 inch original waste, con temp, atm press. No condensation. Simple Vent.
Thu May 30 09:31:29 1996
GOTH Version 3.4 - April 1991

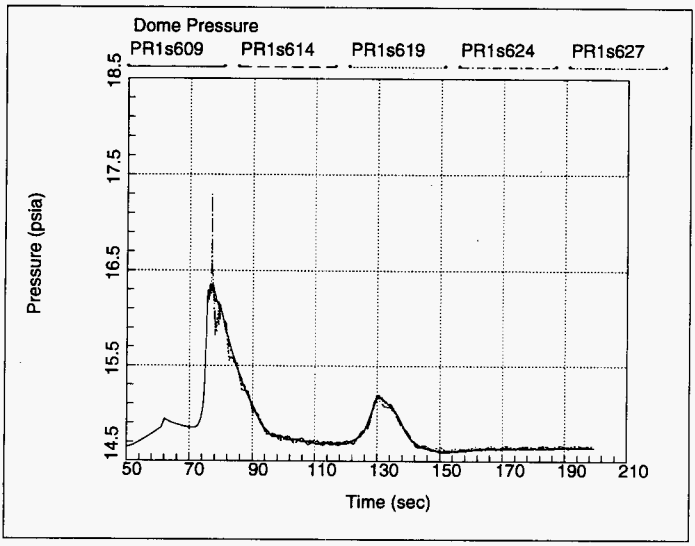

Figure 51. Liquid Droplet Flow Out Through Inleakage Flow Path Due to Steam Bump.

b48c92sv-48 inch original waste, con temp, atm press. No condensation. Simple Vent.
Tue May 28 22:16:37 1996
GOTH Version 3.4 - April 1991

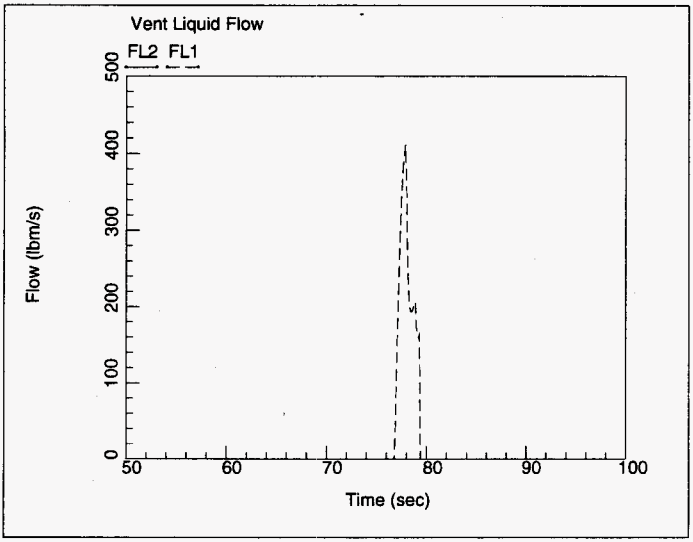

Figure 52. Solid Particle Flow Out Through Inleakage Flow Path Due to Steam Bump.

b48c92sv-48 inch original waste, con temp, atm press. No condensation. Simple Vent.
Tue May 28 22:16:43 1996
GOTH Version 3.4 - April 1991

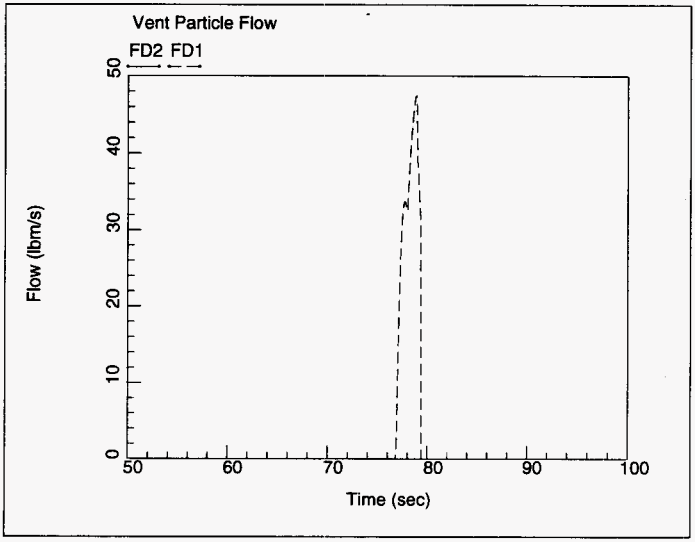

Figure 53. Dome Pressure Variation During Steam Bump For 48 inch Sludge With Conservative Initial Temperature and 6 Inch Diameter Dome Leak Paths.

k48consv-48 inch original waste, con temp, atm press. No condensation. Simple Vent.
Wed May 29 08:18:23 1996
GOTH Version 3.4 - April 1991

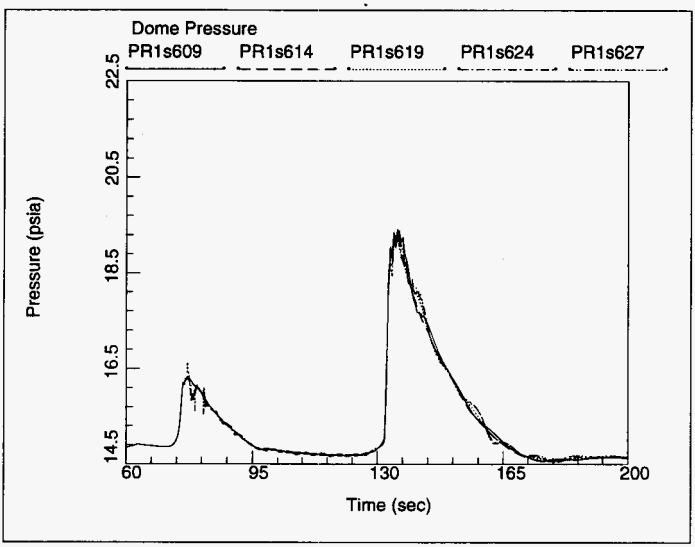

Figure 54. Steam Concentration Contours In Sludge Indicating the Formation of Superheated Sludge Plume for First Steam Bump.

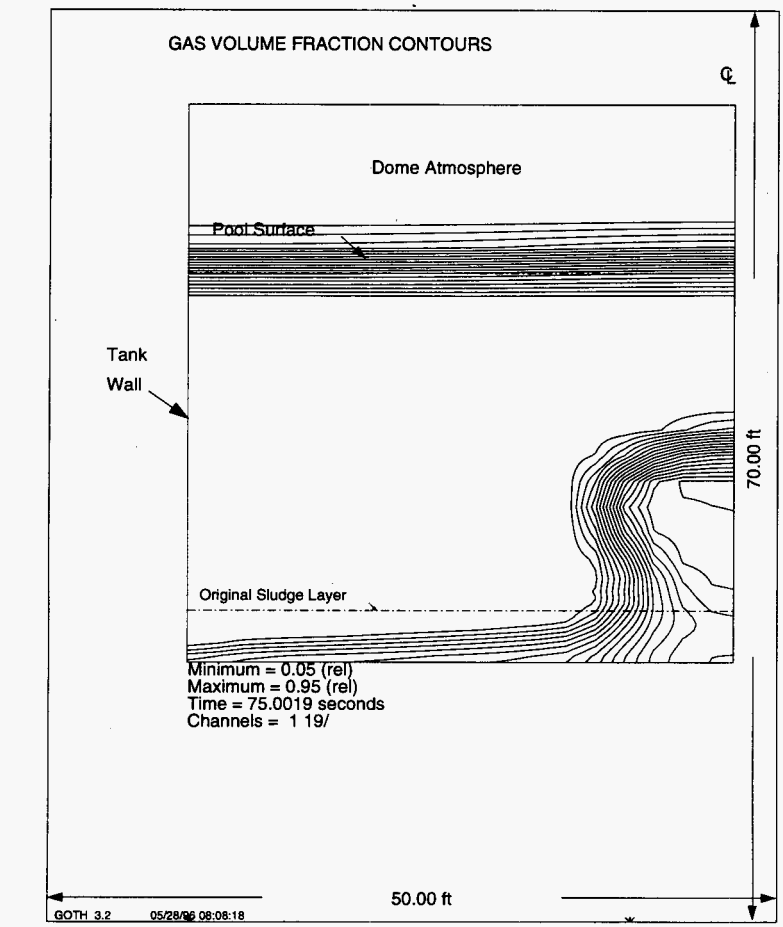

Figure 55. Steam Concentration Contours In Sludge Showing Plume Rise to Supernatant Surface For First Steam Bump.

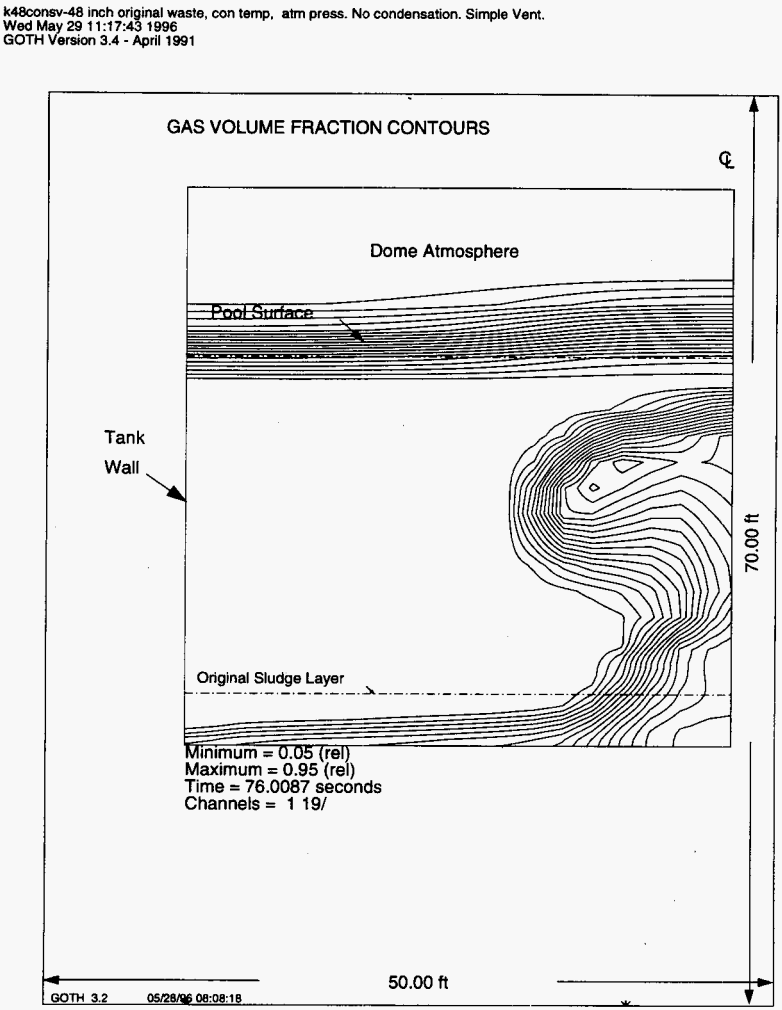

Figure 56. Steam Concentration Contours In Sludge Indicating Hot Sludge and Steam Bubble Breaks Pool Surface For First Steam Bump.

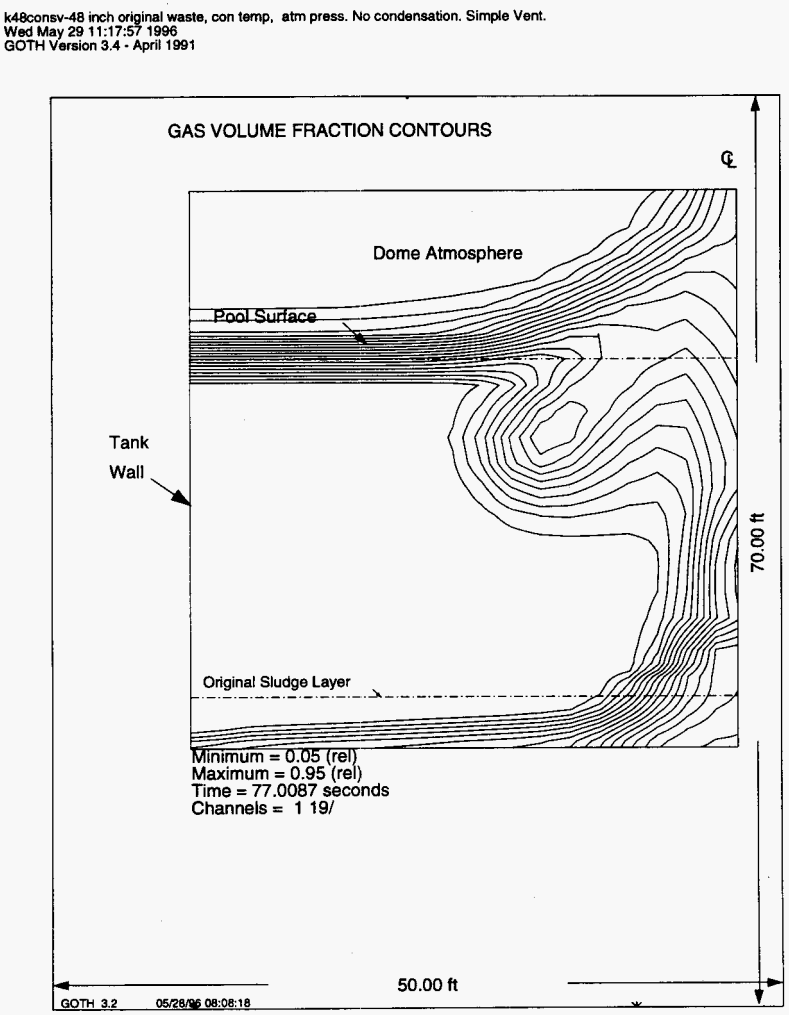

Figure 57. Steam Concentration Contours In Sludge Indicating the Formation of Superheated Sludge Plume for Second Steam Bump.

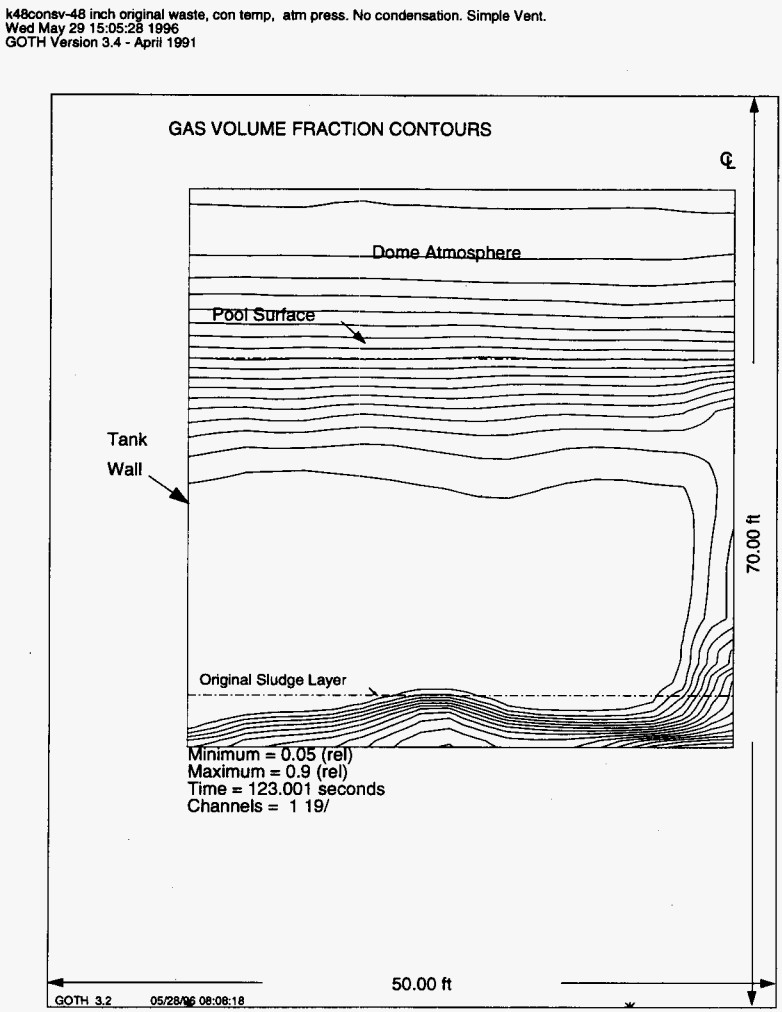

Figure 58. Steam Concentration Contours In Sludge Showing Development of Plume Rising to Supernatant Surface For Second Steam Bump.

k48consv-48 inch original waste, con temp, atm press. No condensation. Simple Vent.
Wed May 29 13:26:19 1996
GOTH Version 3.4 - April 1991

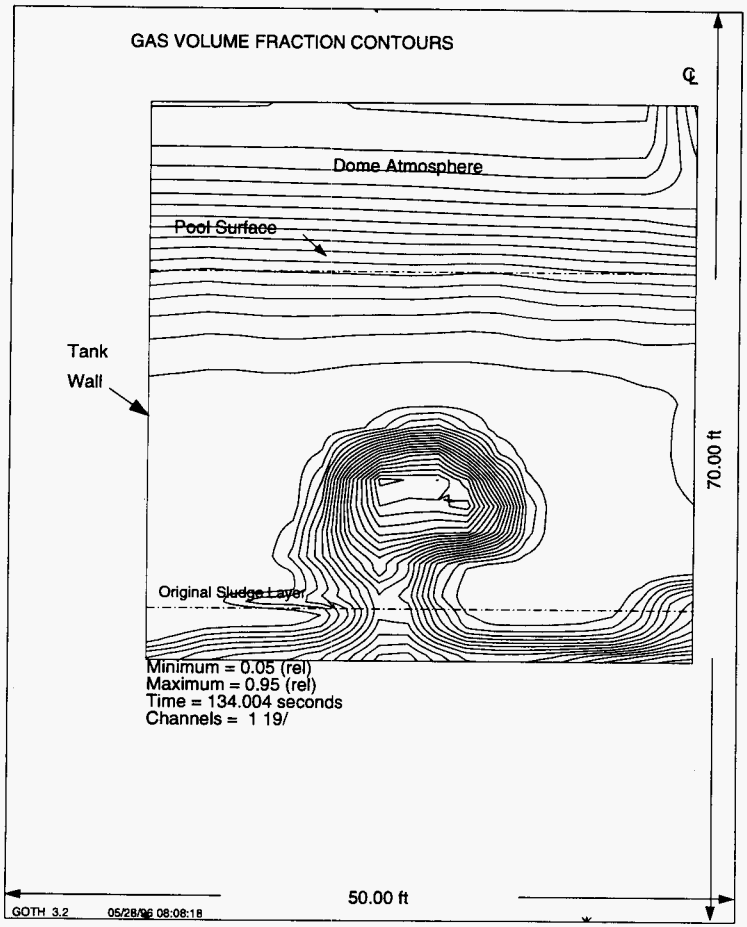

Figure 59. Steam Concentration Contours In Sludge Indicating Hot Sludge and Steam Bubble Breaks Pool Surface For Second Steam Bump.

k48consv-48 inch original waste, con temp, atm press. No condensation. Simple Vent.
Wed May 29 13:26:37 1996
GOTH Version 3.4 - April 1991

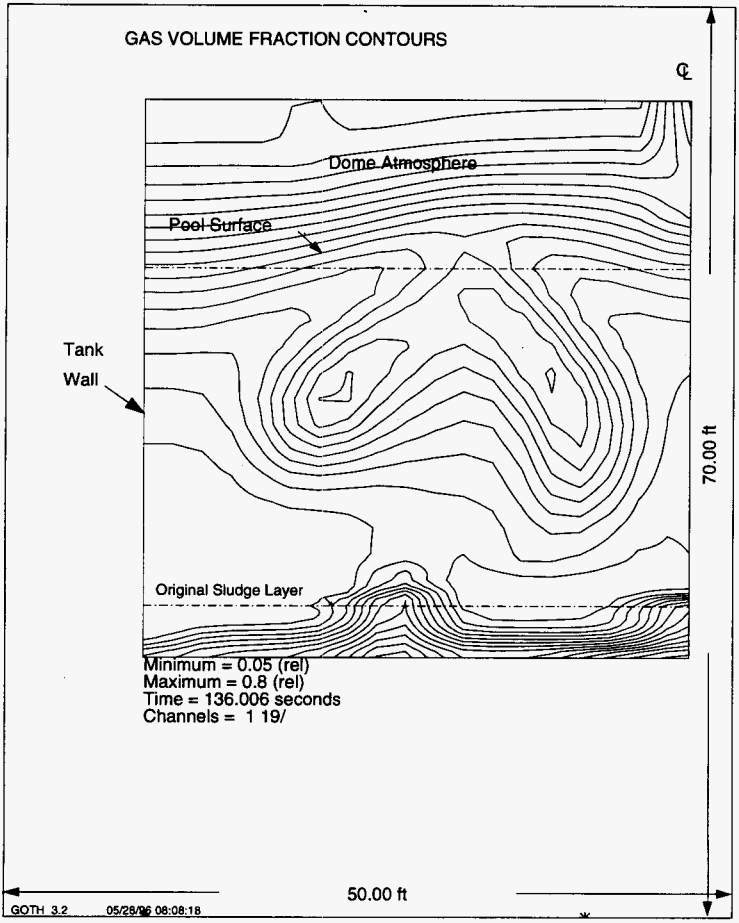

Figure 60. Steam/Gas Flow Out Through Inleakage and Vent Flow During the Steam Bump.

k48consv-48 inch original waste, con temp, atm press. No condensation. Simple Vent.
Wed May 29 08:19:06 1996
GOTH Version 3.4 - April 1991

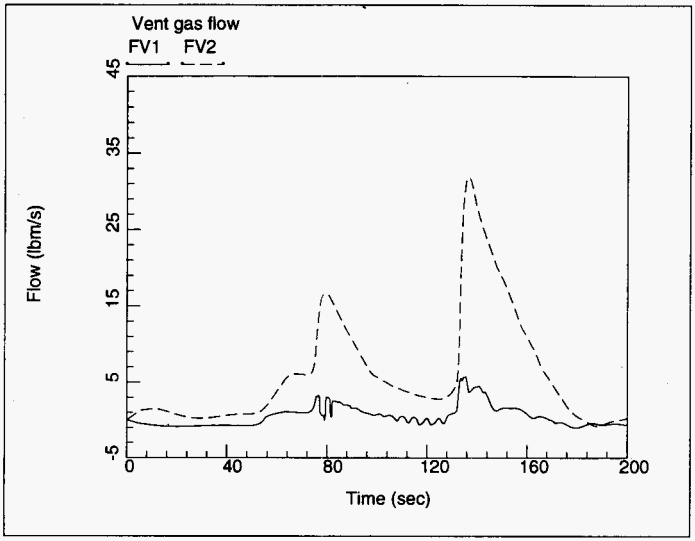

Figure 61. Liquid Droplet Flow Out Through Inleakage Flow Path Due to Steam Bump.

k48consv-48 inch original waste, con temp, atm press. No condensation. Simple Vent.
Wed May 29 08:19:46 1996
GOTH Version 3.4 - April 1991

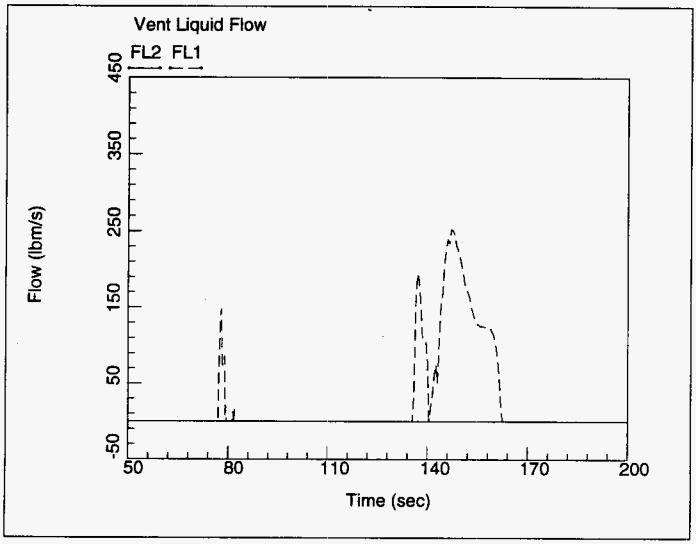

Figure 62. Solid Particle Flow Out Through Inleakage Flow Path Due to Steam Bump.

k48consv-48 inch original waste, con temp, atm press. No condensation. Simple Vent.
Wed May 29 08:19:59 1996
GOTH Version 3.4 - April 1991

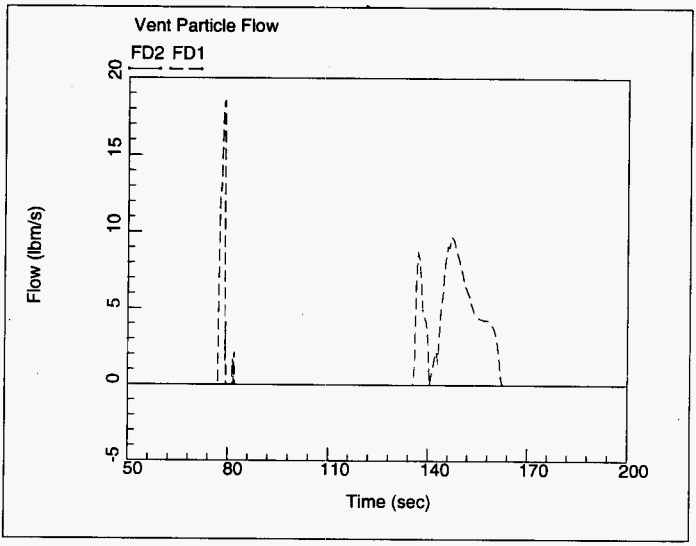

Figure 63. Steam Concentration Profile In 48 Inch Sludge Just Prior To Initiation of Steam Bump Including Condensation.

b48conc-48 inch original waste, conservative temperature at atmospheric pressure. Condensat
Thu May 30 08:17:07 1996
GOTH Version 3.4 - April 1991

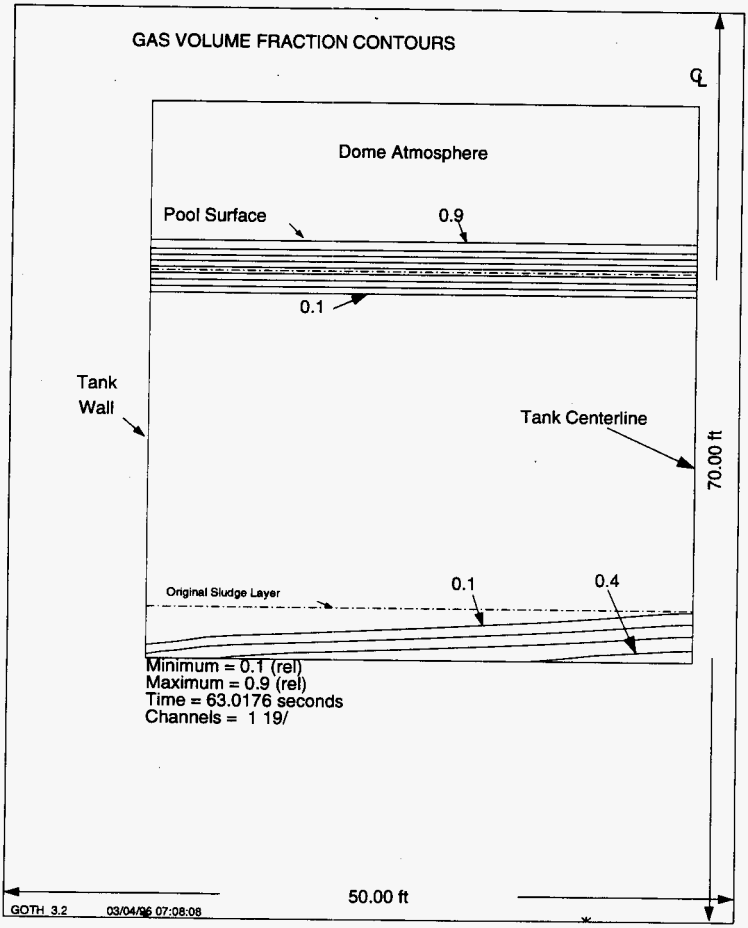

Figure 64. Steam Concentration Profile In 48 Inch Sludge Showing Development of Hydrodynamic Instability Just prior To Initiation of Steam Bump Including Condensation.

b48conc-48 inch original waste, conservative temperature at atmospheric pressure. Condensat
Thu May 30 08:19:29 1996
GOTH Version 3.4 - April 1991

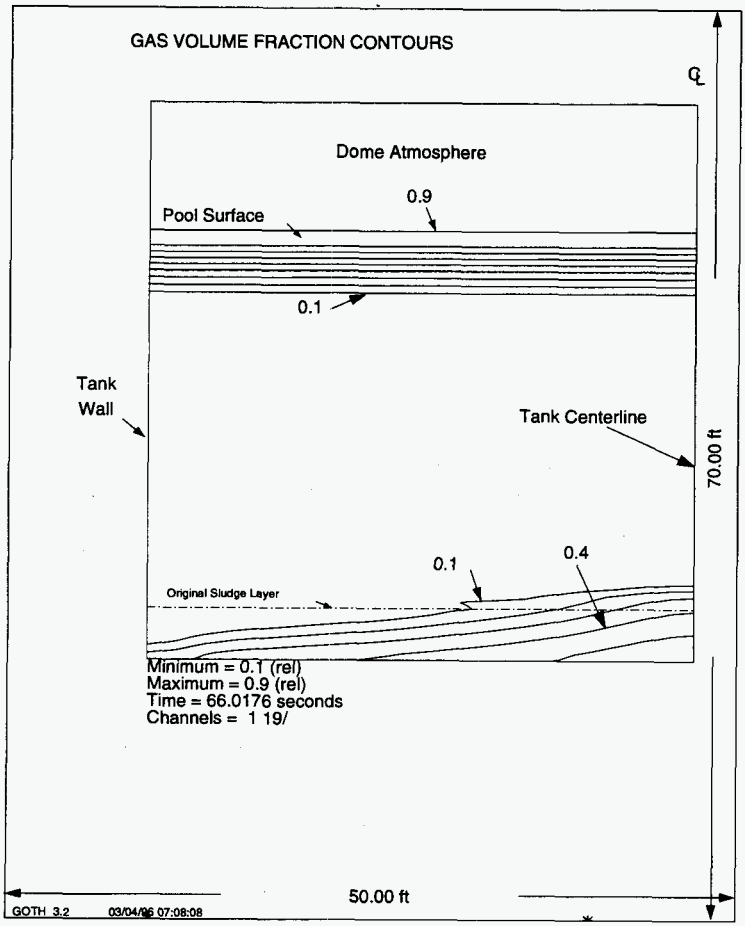

Figure 65. Steam Concentration Profile In 48 Inch Sludge During the Formation of Superheated Sludge Plume for Steam Bump Including Condensation.

b48conc-48 inch original waste, conservative temperature at atmospheric pressure. Condensat
Thu May 30 08:21:51 1996
GOTH Version 3.4 - April 1991

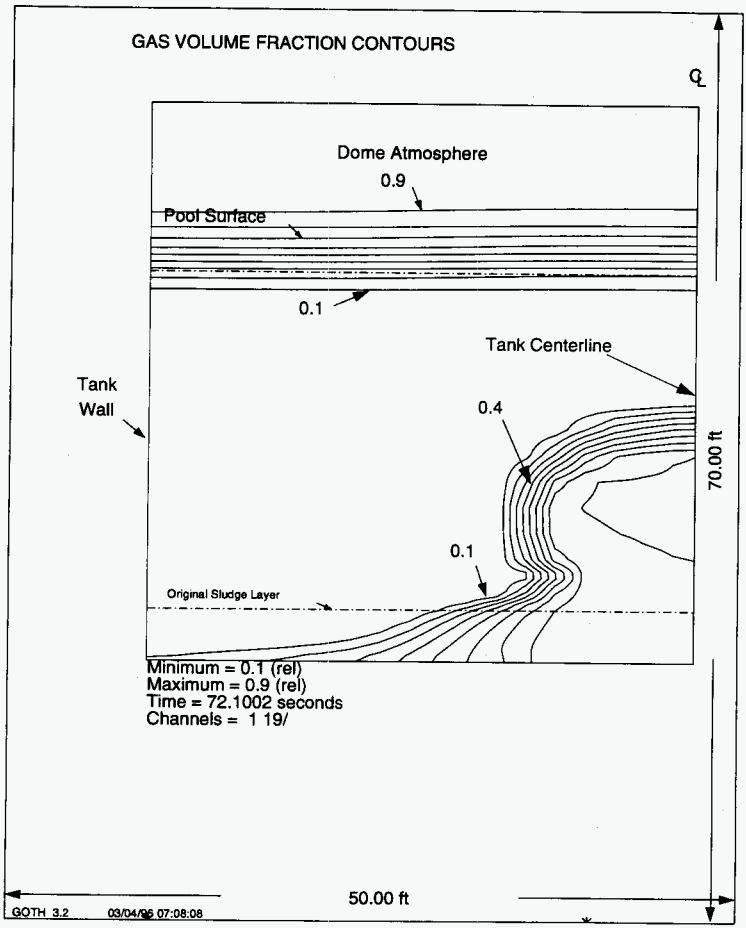

Figure 66. Steam Concentration Profile In 48 Inch Sludge Indicating the Steam/Sludge Plume Detachment for Steam Bump Including Condensation.

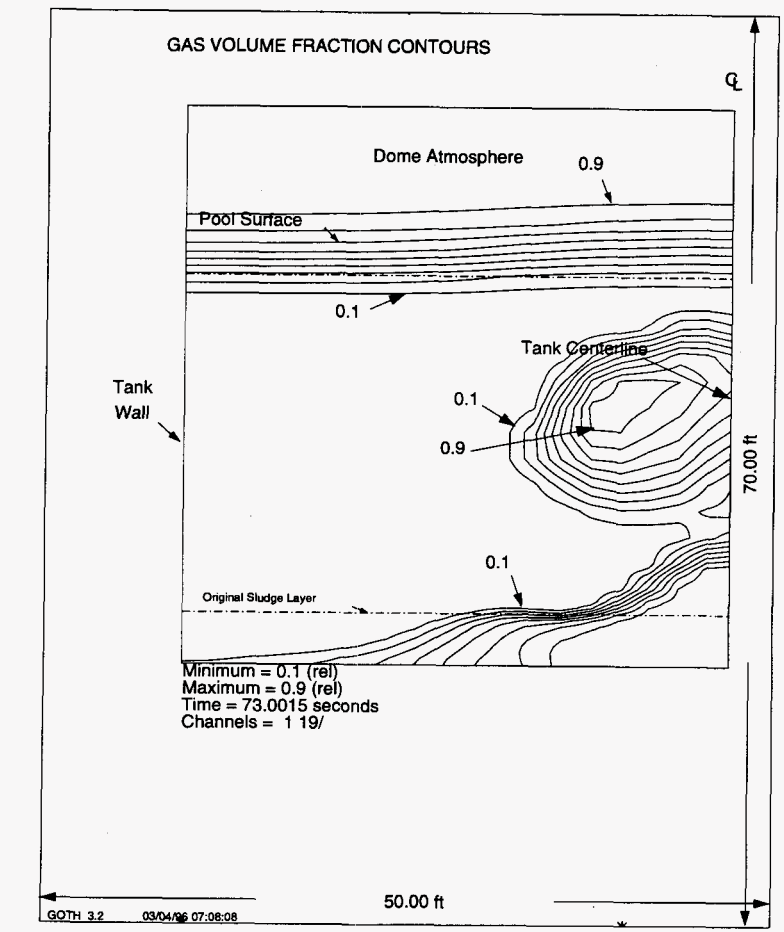

Figure 67. Steam Concentration Profile In 48 Inch Sludge Showing The Hot Sludge and Steam Bubble Breaks Pool Surface.

b48conc-48 inch original waste, conservative temperature at atmospheric pressure. Condensat
Thu May 30 08:28:30 1996
GOTH Version 3.4 - April 1991

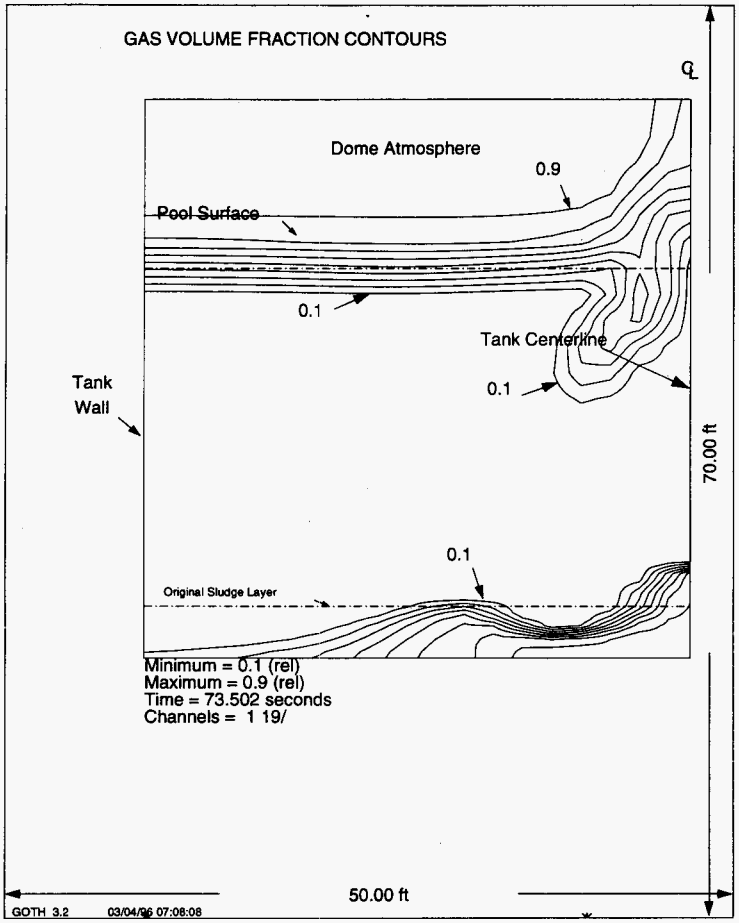

in this case. However, if primary ventilation is lost in addition to the increased heat and sludge loading, then the supernatant will heat up reducing the amount of subcooling. This will significantly reduce the ability of supernatant to condense the steam. Figures 68 and 69 show the mass flow of liquid and solid particles through the inleakage and vent flow paths to the atmosphere from the dome. In addition, the supernatant in this case has a depth of 26 ft. Reducing the depth would allow less time for the steam/sludge bubble to condense before breaking the surface. Additional studies need to be performed to define the effects of supernatant subcooling and depth on steam bump severity.

7.2.3 Best Estimate Initial Temperature And No Condensation

The best estimate temperature distribution resulting from the transient heat up of the sludge following the addition of 30 inches of similar sludge to the current 18 inches of sludge in tank AZ-101 is the initial condition for the simulations presented in this section. The temperature distribution is realistic for the initial steam bump that would occur following the addition of waste. Subsequent steam bumps may be initiated from a temperature distribution that is more like the conservative temperature distribution, as considered in the previous section.

Case 1: Steam Bump With Riser Flanges and Cover Blocks Open

This steam bump simulation is evaluated with the best estimate initial temperature distribution with no condensation of steam by the supernatant even though the supernatant is highly subcooled. The purpose of this simulation is to evaluate a more realistic initial bounding steam bump that can occur for this temperature distribution. Figure 70 shows the steam void profile just prior to the initiation of the hydrodynamic instability leading to the steam bump. The steam concentration contour lines are closer together than for the conservative case since the steam is concentrated nearer the bottom of the tank because of the axial temperature gradient in the sludge. A much longer time is required for the instability to develop compared to the conservative temperature profile case because more steam must accumulate before the sludge becomes neutrally buoyant.

It is typical with the best estimate initial temperature distribution cases, that the instability developed at two points, one at the tank centerline and the other near the wall. While it is not clear why this occurs, it may be due to the large amount of steam required to reach neutral buoyancy, the wall shear and the viscosity of the sludge. As the instability develops, plumes of superheated sludge and steam form on the surface of the sludge as shown in Figure 71. As these plumes rise through the supernatant, hot sludge carried upwards in the plume flashes into steam due to the drop in local pressure at higher elevations. This causes the plume to grow in size and to accelerate as it rises. Since condensation is not allowed in this simulation, the plume continues to accelerate and grow until the shear relationship for the sludge cause the neck at the bottom of the plume to narrow, Figure 72, and the plume separates from the remainder of the sludge. Finally the sludge/steam bubble breaks the pool surface (see Figure 73) dispersing liquid droplets and solid particles into the dome atmosphere. In this simulation, the aerosol cloud does not reach the elevation of the leakage and vent flow paths before the steam flow subsides. No release of aerosols

Figure 68. Liquid Droplet Flow Out Through Inleakage Flow Path Due to Steam Bump.

b48conc-48 inch original waste, conservative temperature at atmospheric pressure. Condensat
Thu May 30 08:29:15 1996
GOTH Version 3.4 - April 1991

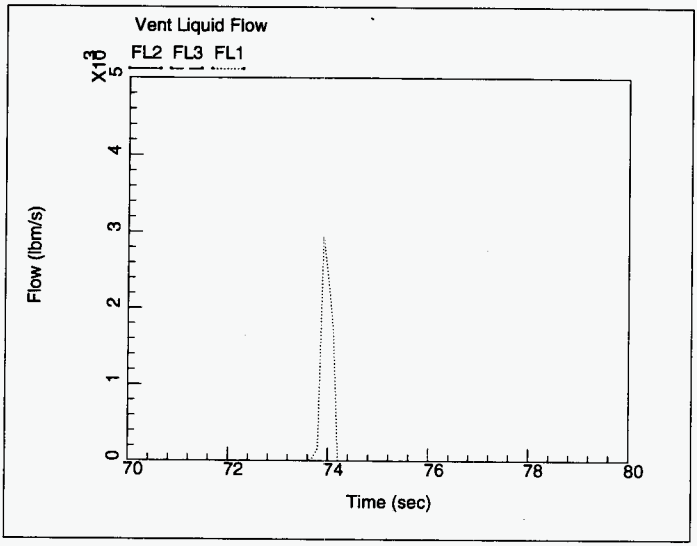

Figure 69. Solid Particle Flow Out Through Inleakage Flow Path Due to Steam Bump.

b48conc-48 inch original waste, conservative temperature at atmospheric pressure. Condensat
Thu May 30 08:29:51 1996
GOTH Version 3.4 - April 1991

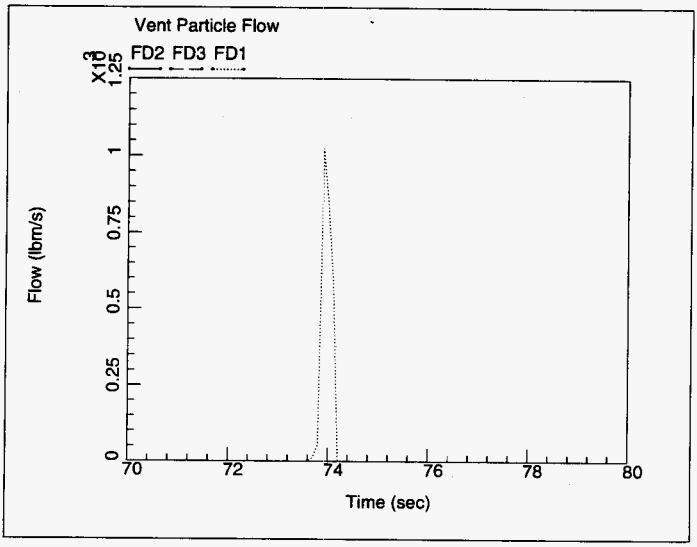

Figure 70. Steam Concentration Profile In 48 Inch Sludge Showing Development of Hydrodynamic Instability Just Prior to Initiation of Steam Bump.

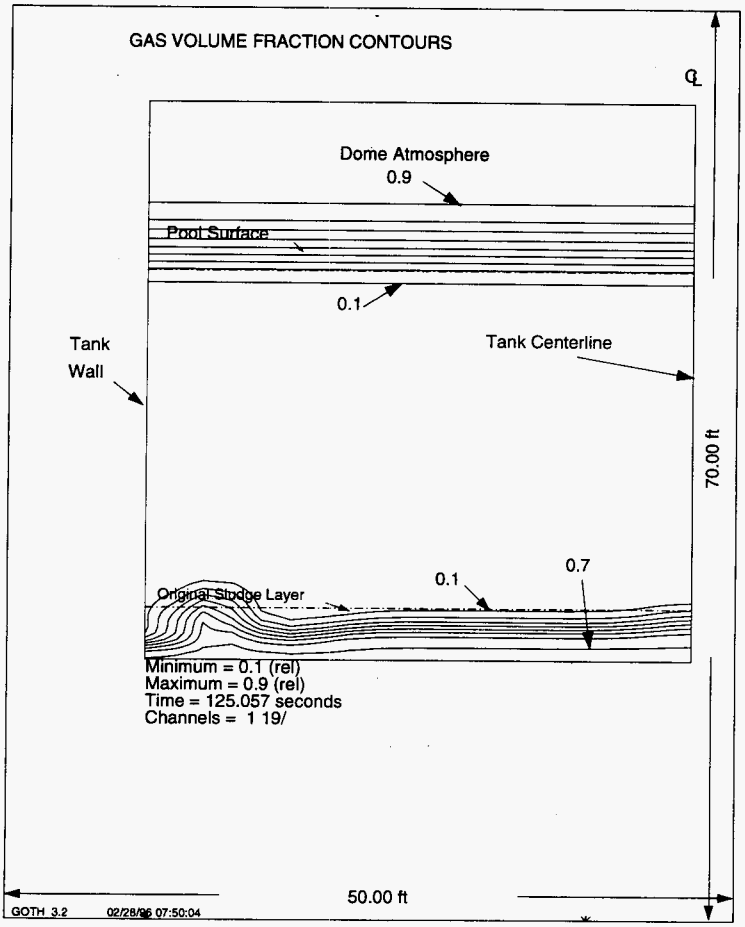

Figure 71. Steam Concentration Profile In 48 Inch Sludge During the Formation of Superheated Sludge Plume For Steam Bump.

b48be - 48 inch layer with be temperature distribution and no condensation
Thu May 30 08:49:17 1996
GOTH Version 3.4 - April 1991

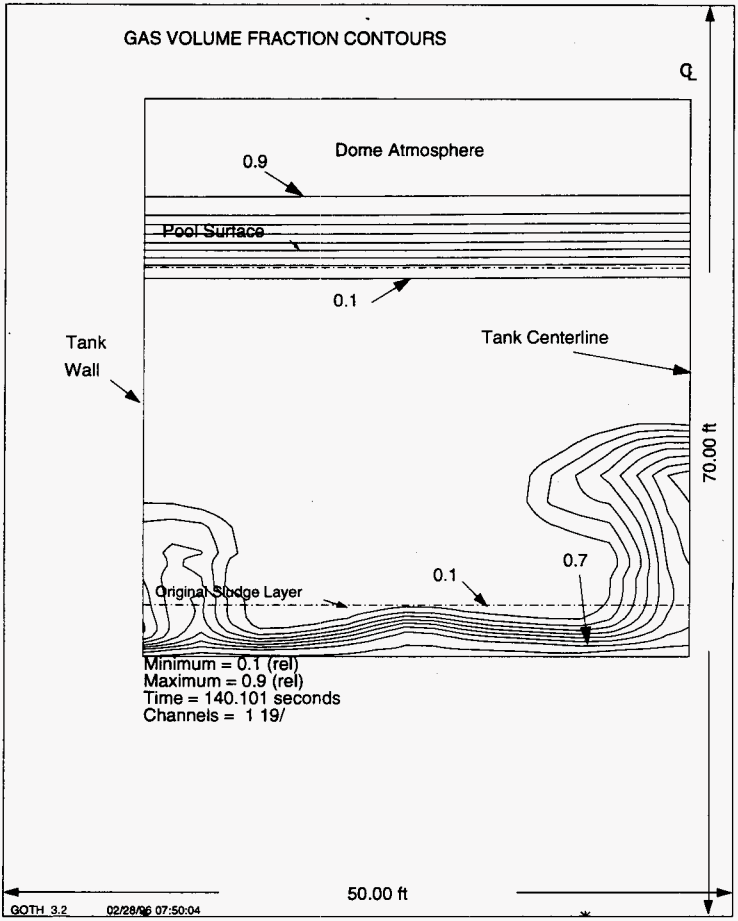

Figure 72. Steam Concentration Profile In 48 Inch Sludge Indicating the Steam/Sludge Plume Detachment For Steam Bump.

b48be - 48 inch layer with be temperature distribution and no condensation
Thu May 30 08:50:39 1996
GOTH Version 3.4 - April 1991

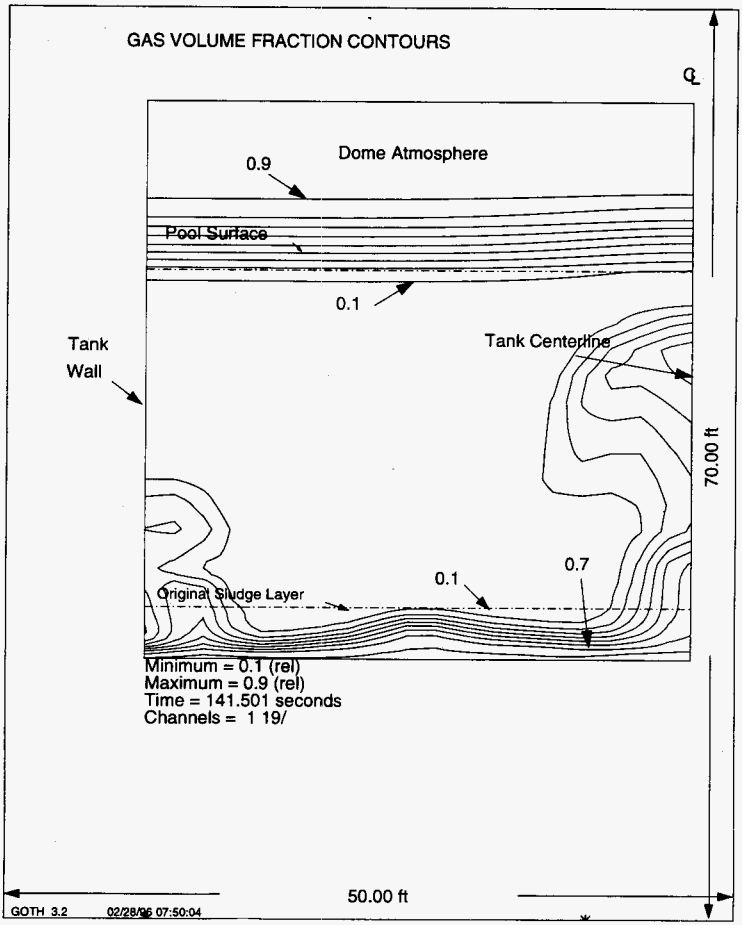

Figure 73. Steam Concentration Profile In 48 Inch Sludge Showing The Hot Sludge and Steam Bubble Breaks Pool Surface.

b48be - 48 inch layer with be temperature distribution and no condensation
Thu May 30 08:51:49 1996
GOTH Version 3.4 - April 1991

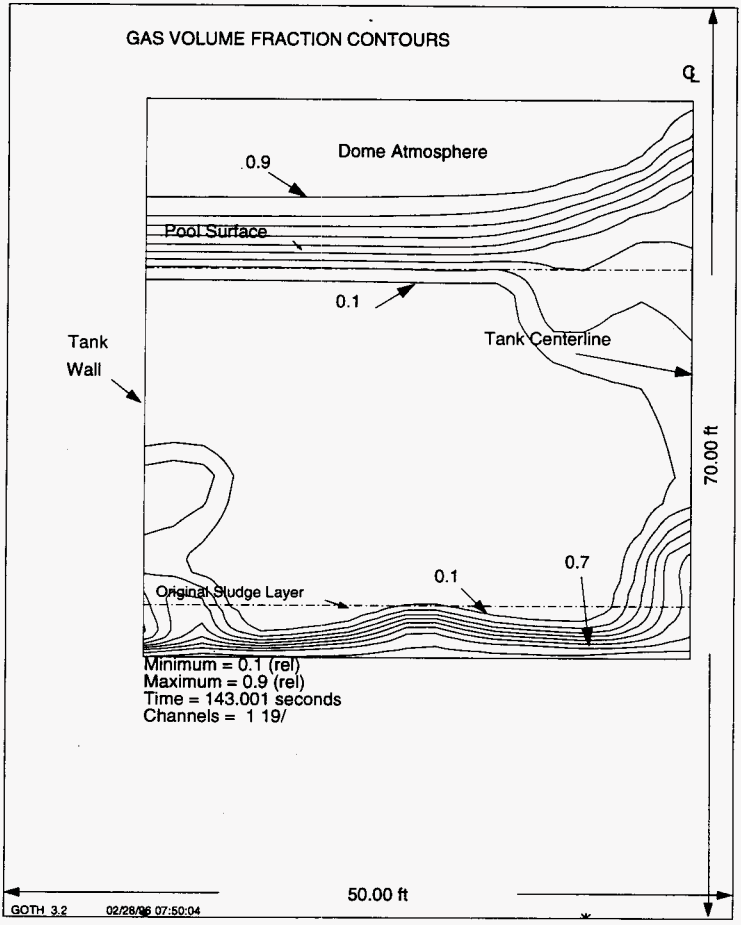

outside of the tank has been calculated. However, it is likely that small particles would eventually be carried out through the ventilation system by the normal ventilation flow.

7.2.4 Best Estimate Initial Temperature With Condensation

The initial conditions for this simulation are identical to those of the previous calculation except that the subcooled supernatant is allowed to condense the steam. The supernatant temperature is 143.1 °F, which is the temperature the supernatant would reach at the time the sludge first reaches the local saturation temperature following the addition of 30 inches of sludge. The steam void distribution shown in Figure 74 corresponds to the time at which hydrodynamic instability develops. It is more suppressed compared to the case where no condensation was allowed (Figure 70). Fluid motion induced in the sludge by this instability causes subcooled sludge and supernatant to mix with the saturated sludge, condensing the steam which in turn collapses the steam bubble as shown in Figure 75.

The plume has not developed for this case, so no aerosol releases are predicted. The evaporation rate from the pool surface increases for a period of time following the event to allow the energy absorbed by the supernatant in condensing the steam to be dissipated. No steam bubbles would be expected to reach the sludge surface. However, some noncondensible gases that may also have been trapped in the sludge would be released and these would break the surface of the pool.

7.3 11 FEET OF CONSOLIDATED SLUDGE OF TANK C-106 AND TANK AY-102

In order to eliminate the safety concerns of tank C-106, a single-shell tank containing high heat waste with a maximum heat load of 132,400 Btu/hr, the Department of Energy is proposing a remedial action to transfer this waste into a double-shell tank (AY-102). Currently, tank AY-102 contains 32,000 gallons (~1 ft.) of sludge with an estimated heat load of about 33,000 Btu/hr. The thermal hydraulic analysis (Sathyanarayana and Fryer 1996) conducted to provide a technical basis supporting consolidation of waste has recommended a transfer of 157,000 gallons of tank C-106 sludge (4.75 ft containing 92,400 Btu/hr) into tank AY-102. The consolidated sludge after the transfer of C-106 waste will have about 11 ft of nonconvective sludge with a total heat load of 125,000 btu/hr. The consolidated sludge can be operated below required temperature limits by operating floor cooling channels of the secondary ventilation system with high flow rates of more than 2000 cfm. These operational requirements are based on the assumption that the transferred tank C-106 sludge will achieve a particle volume fraction no less than 50% of that currently in tank C-106 after settling to the nonconvective condition. Also, the tank waste level must be maintained at 30 ft level in order to keep the required margin for the peak sludge temperatures. The maximum sludge temperature estimated with 2000 cfm flow through the floor cooling channels and the air entering at steady state average summer meteorological conditions is 201 °F and the peak temperature occurs at 3.75 ft above the tank floor. As the cooling air flow rate is reduced, the peak sludge temperature will increase and the peak temperature location will move closer to the tank bottom. The loss of floor cooling channel flow will heat up the sludge and the sludge peak temperatures will reach saturation value in about 60 days (Sathyanarayana and Fryer 1996).

Figure 74. Steam Concentration Profile In 48 Inch Sludge Showing Development of Hydrodynamic Instability Just prior To Initiation of Steam Bump Including Condensation.

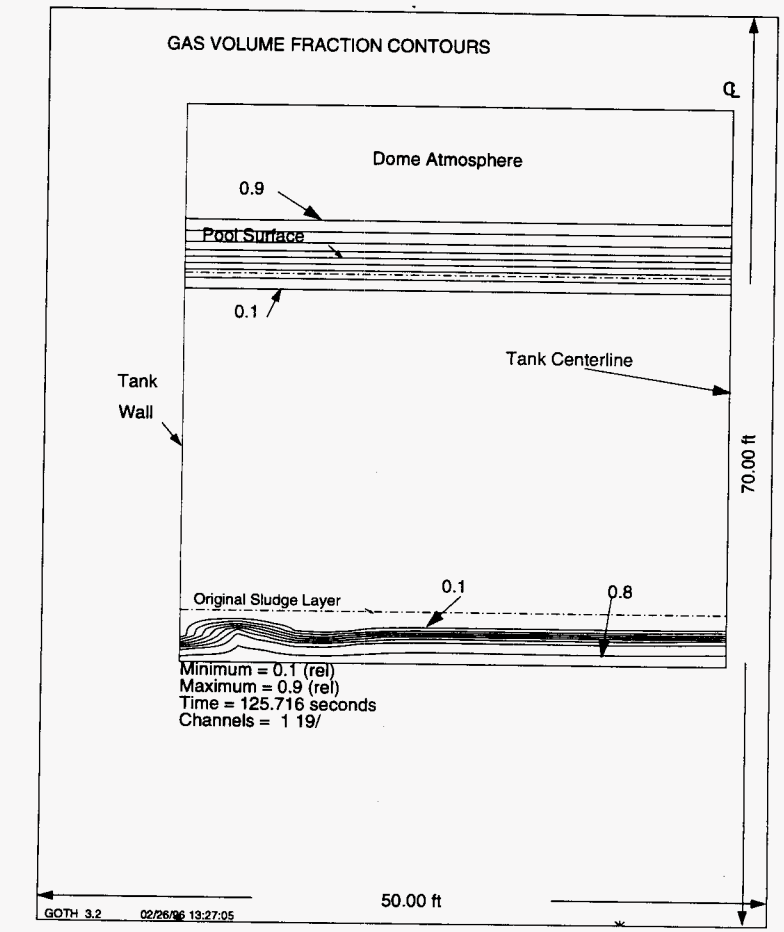

Figure 75. Steam Concentration Profile In 48 Inch Sludge Showing Collapse of Steam Voids By Condensation.

b48bec - 48 inch layer with be temperature distribution with condensation
Thu May 30 08:58:16 1996
GOTH Version 3.4 - April 1991

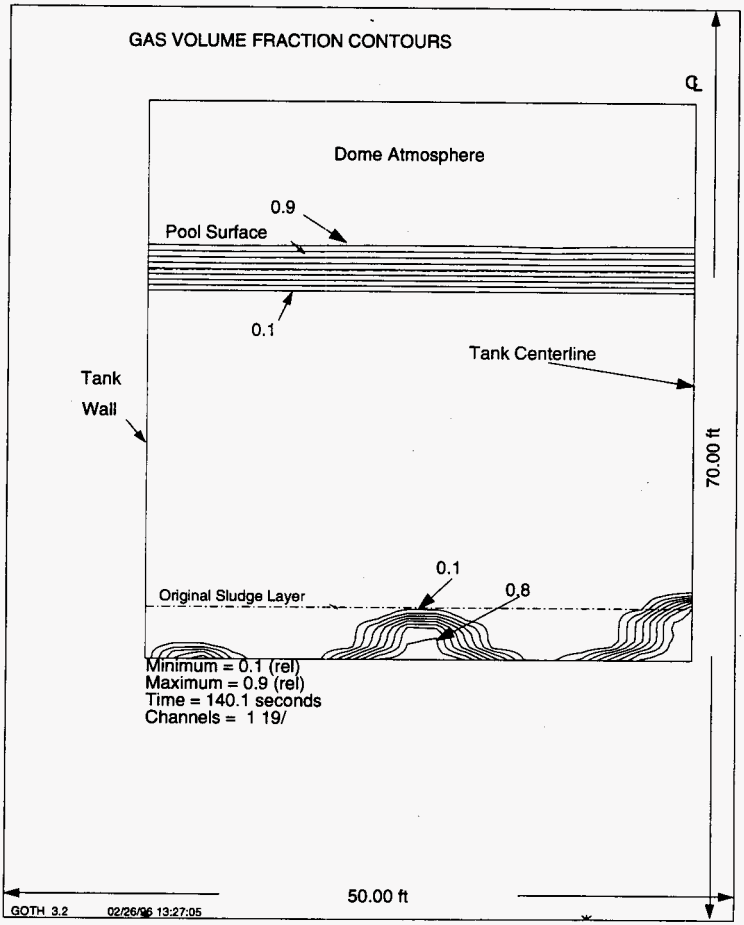

7.3.1 Conservative Initial Temperature and No Condensation

The sludge temperature was initialized as shown in Figure 8.. The steam condensation in liquid waste was suppressed to estimate a very conservative bump and waste releases. The simulation considers 11 ft of sludge and 19 ft of supernatant with three different inleakage paths. The results of simulations for expected quantities of releases corresponding to three different inleakge flow paths are shown in Table 5. The wide open risers and pits will provide extremely violent bumps so the release quantities are significantly higher. The size of the plume produced can be seen in Figures 76 through 78 where the vapor volume fraction contours are plotted. The tank dome pressure, vapor flow, liquid droplets and particle flow are shown in Figures 79 through 82. Even after 125 seconds into the transient, the waste releases continue and so the integrated mass flow values shown in Table 5 are up to that transient time only. The waste releases can even be higher if such a steam bump occurs. The reduced leakage flow path area has reduced waste releases considerably. The peak dome pressure depends on the amount of steam in the dome which in turn depends on the amount of high temperature liquid waste that is carried to the pool surface with the plume. The maximum peak pressure in the dome can be as high as that of tank bottom hydrostatic pressure. Figure 83 and 84 show the vapor volume fraction contours indicating the size of the steam bump and the vapor flow through the inleakage and vent flow paths, respectively for the case of five drain pipes as leakage flow paths. In this case, the size of the bump and also the releases are smaller than the open pits and riser case. By further reducing the inleakage flow path to 6 inch equivalent diameter, the results of the steam bump are shown in Figure 85 and 86 illustrating the size of the bump and the vapor flow through the vent and leakage paths, respectively. In all the three cases the dome pressure as shown in Figure 79 remain higher for a longer time as the dome atmosphere contains a large fraction of liquid droplets and particles. No effort is made to determine the duration of positive pressure in the dome.

7.3.2 Conservative Initial Temperature With Condensation

The same steam bump simulations described in the previous section have been repeated allowing the condensation process to take place as calculated by the code. The results of these simulations for the release of radioactive material are shown in Table 6. The reduced inleakage flow path show drastically reduced radioactive release quantities. It should be noted that these release quantities correspond only up to the time the particular simulation was performed. In some cases, the simulation was not run sufficiently long for the total release to be calculated for any given occurrence of steam bump. Therefore, these material release quantities only represent order of magnitudes values and provide a good measure for comparison with respect to a given parameter variation. In this case the parameter is the inleakage flow path area. For open risers and pit cases, the plume development in the waste, as shown in Figure 87 and Figure 88, shows the rise of the plume and breaking the pool surface and carrying the waste into the dome. However, the plume is suppressed quickly due to the condensation effect as shown in Figure 89. This process can repeat itself as long as the cooling of the waste is not restored. Figures 90 and 91 show the liquid droplet and solid particle flows through the inleakage and vent paths. As in earlier cases with large leakage paths, most of the material flows through the inleakage paths.

Table 5. Estimate of Vent Flows for a Conservative Tank Bump in 11 Feet of Combined Tank AY-102 and C-106 Sludge.

Parameters	Dome Flow Paths	Dome Flow Paths	Dome Flow Paths
	1. 42" dia.-Pump Pit 2. 20" dia.-Vent 3. Four 42" dia.-Sluice Pits	1. Five of 4" dia.-Inleakage Paths 2. 20" dia.-Vent Path	1. 6" dia.-Inleakage Path 2. 20"dia.-Vent Path
1. Tank Dome Peak Pressure, psia	27	25	25
2. Vapor Flow Path 1. Flow, lbm Path 2. Flow, lbm Path 3. Flow, lbm	 400 -- 5100	 250 1900 NA	 200 2000
3. Liquid Flow Path 1. Flow, lbm Path 2. Flow, lbm Path 3. Flow, lbm	 300,000 lbm -- 1.1×10^6 lbm	 21500 - NA	 10500 - NA
4. Particle Flow Path 1. Flow, lbm Path 2. Flow, lbm Path 3. Flow, lbm	 29,000 lbm -- 68,000 lbm	 2100 -- NA	 1000 50 NA

Table 6. Estimate of Potential Vent Flows for a Tank Bump Including Condensation in 11 Feet of Combined Tank AY-102 and C-106 Sludge.

Parameters	Dome Flow Paths	Dome Flow Paths	Dome Flow Paths
	1. 42" dia.-Pump Pit 2. 20" dia.-Vent 3. Four 42" dia.-Sluice Pits	1. Five of 4" dia.-Inleakage Paths 2. 20" dia.-Vent Path	1. 6" dia.-Inleakage Path 2. 24"dia.-Vent Path
1. Tank Dome Peak Pressure, psia	28	30	32
2. Vapor Flow			
Path 1. Flow, lbm	150	80	20
Path 2. Flow, lbm	--	420	300
Path 3. Flow, lbm	1600	NA	NA
3. Liquid Flow			
Path 1. Flow, lbm	21,000 lbm	2500	30
Path 2. Flow, lbm	--	-	-
Path 3. Flow, lbm	0.1 x 10^6 lbm	NA	NA
4. Particle Flow			
Path 1. Flow, lbm	2900 lbm	260	2.5
Path 2. Flow, lbm	--	--	-
Path 3. Flow, lbm	3300 lbm	NA	NA

Figure 76. Steam Concentration Contours in 11 ft of Sludge Showing the Formation of Super Heated Sludge Plume.

b11con-11 foot washed waste, conservative temperature at atmospheric pressure. No condensat
Thu May 30 15:31:32 1996
GOTH Version 3.4 - April 1991

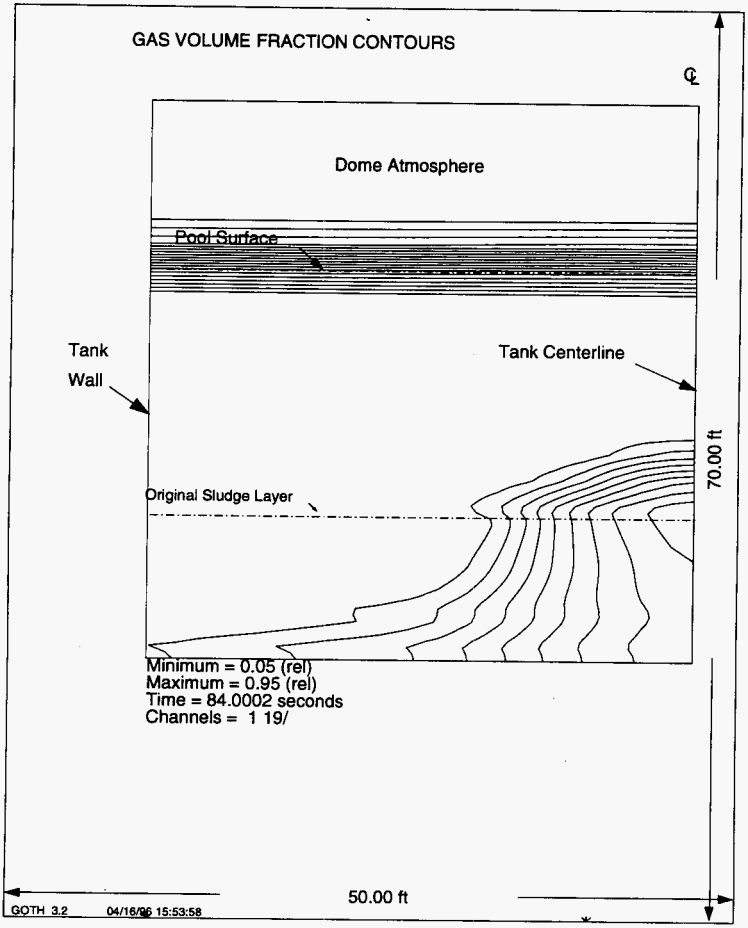

Figure 77. Steam Concentration Contours in 11 ft of Sludge Showing the Plume Rise to Supernatant Surface.

b11con-11 foot washed waste, conservative temperature at atmospheric pressure. No condensat
Thu May 30 15:33:02 1996
GOTH Version 3.4 - April 1991

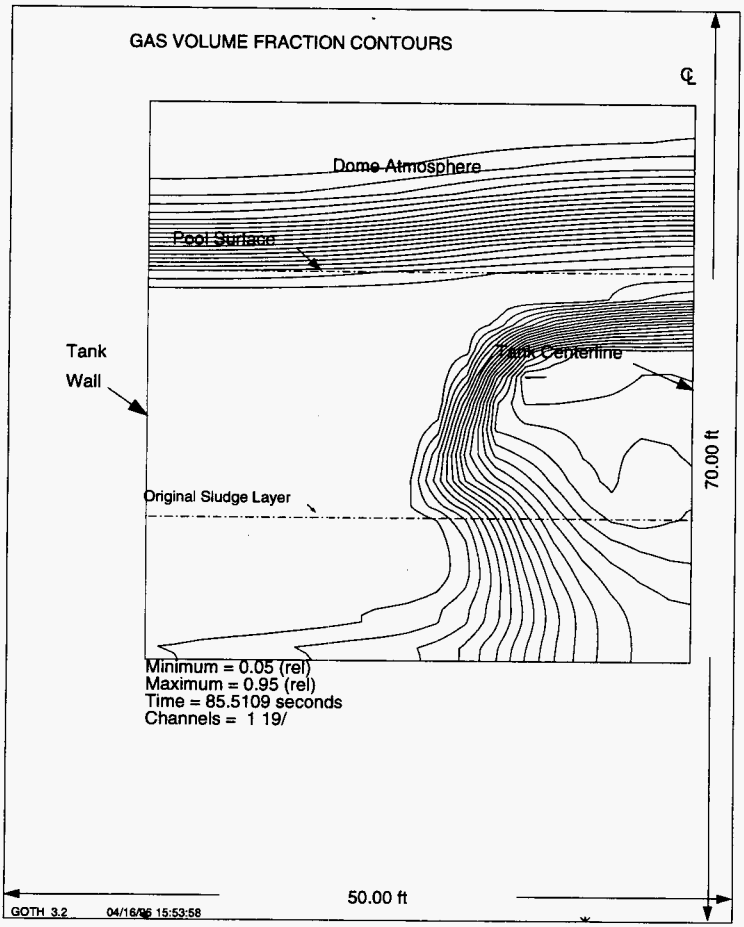

Figure 78. Steam Concentration Contours in 11 ft of Sludge Indicating Hot Sludge and Steam Bubble Breaks the Pool Surface.

b11con-11 foot washed waste, conservative temperature at atmospheric pressure. No condensat
Fri Apr 12 15:26:13 1996
GOTH Version 3.4 - April 1991

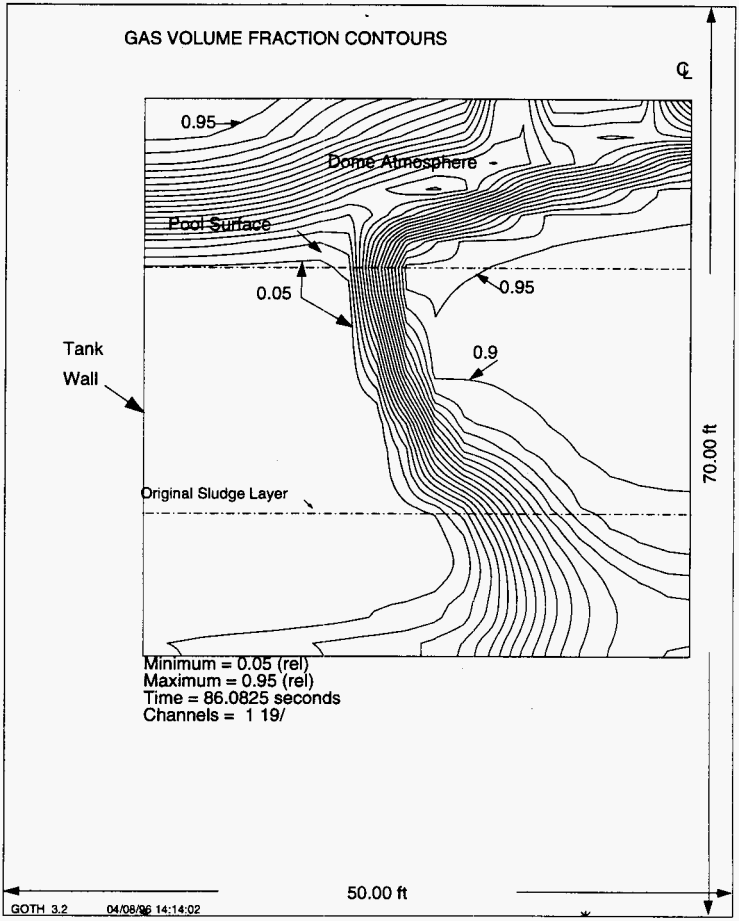

Figure 79. Dome Pressure Variation During the Steam Bump for 11 ft of Sludge for Conservative Initial Temperature and no Condensation.

b11con-11 foot washed waste, conservative temperature at atmospheric pressure. No condensat
Wed Apr 17 08:45:13 1996
GOTH Version 3.4 - April 1991

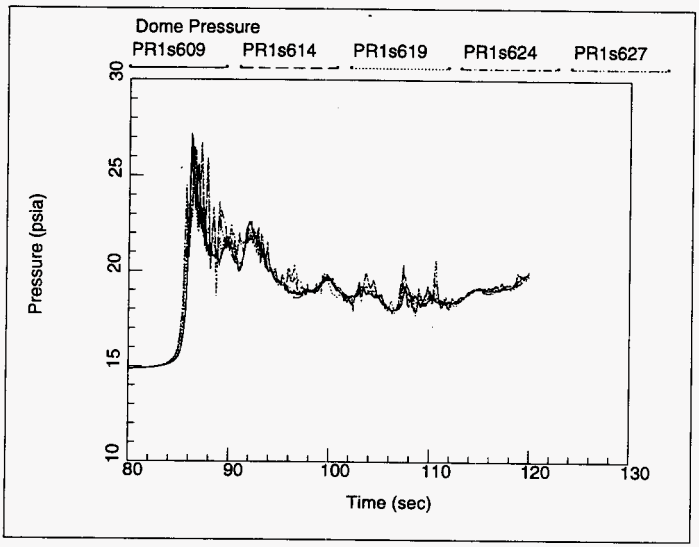

Figure 80. Gas/Steam Flow Through Inleakage and Vent Flow Paths During the Steam Bump.

b11con-11 foot washed waste, conservative temperature at atmospheric pressure. No condensat
Mon Jun 3 14:47:31 1996
GOTH Version 3.4 - April 1991

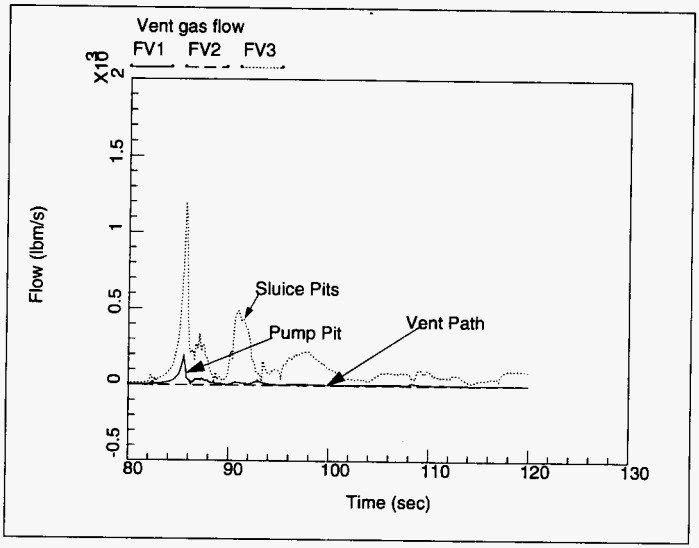

Figure 81. Liquid Droplet Flow Out Through Inleakage and Vent Flow Paths During the Steam Bump.

b11con-11 foot washed waste, conservative temperature at atmospheric pressure. No condensat
Wed Apr 17 08:47:23 1996
GOTH Version 3.4 - April 1991

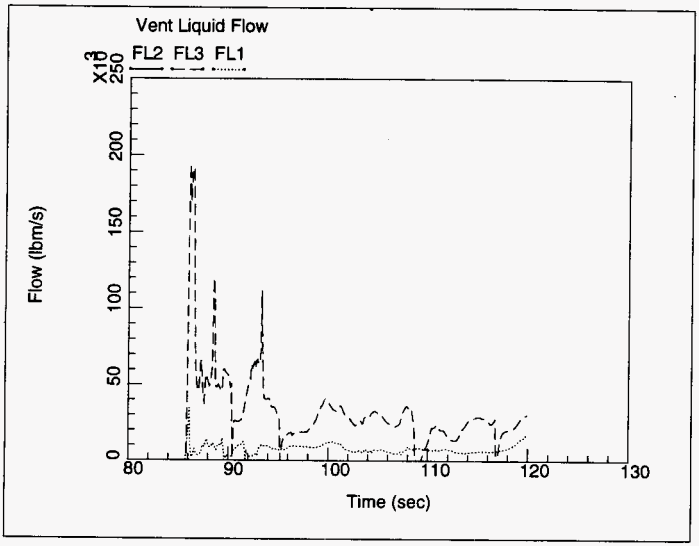

Figure 82. Solid Particle Flow Out Through Inleakage and Vent Flow Paths During the Steam Bump.

b11con-11 foot washed waste, conservative temperature at atmospheric pressure. No condensat
Wed Apr 17 08:48:52 1996
GOTH Version 3.4 - April 1991

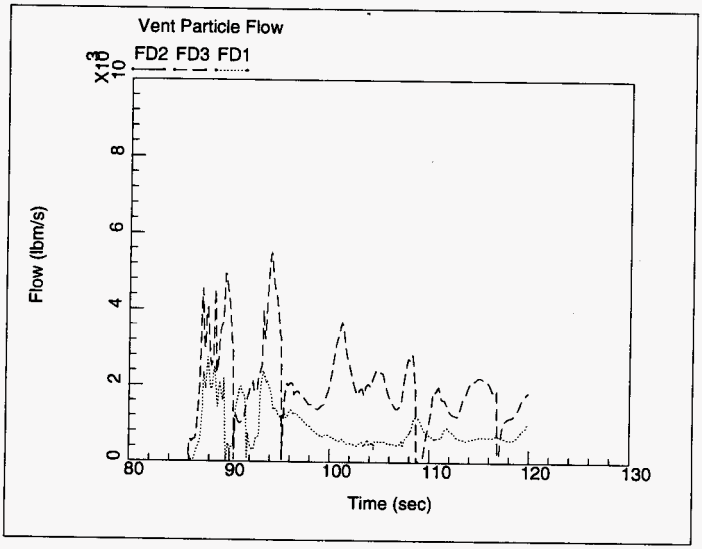

Figure 83. Steam Concentration Contours in 11 ft of Sludge Indicating Hot Sludge and Steam Bubble Break the Pool Surface With Drain Pipes as Inleakage Flow Paths.

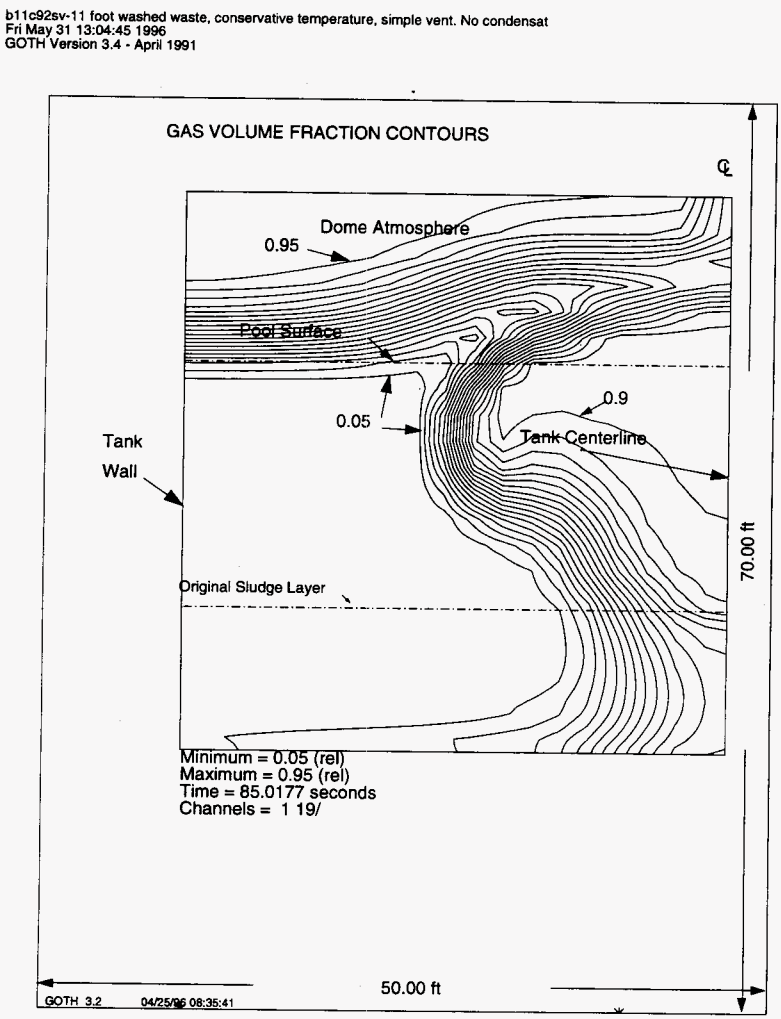

Figure 84. Gas/Steam Flow Through Inleakage and Vent Flow Paths During the Steam Bump With Drain Pipes as Inleakage Flow Paths.

b11c92sv-11 foot washed waste, conservative temperature, simple vent. No condensat
Mon Jun 3 14:23:45 1996
GOTH Version 3.4 - April 1991

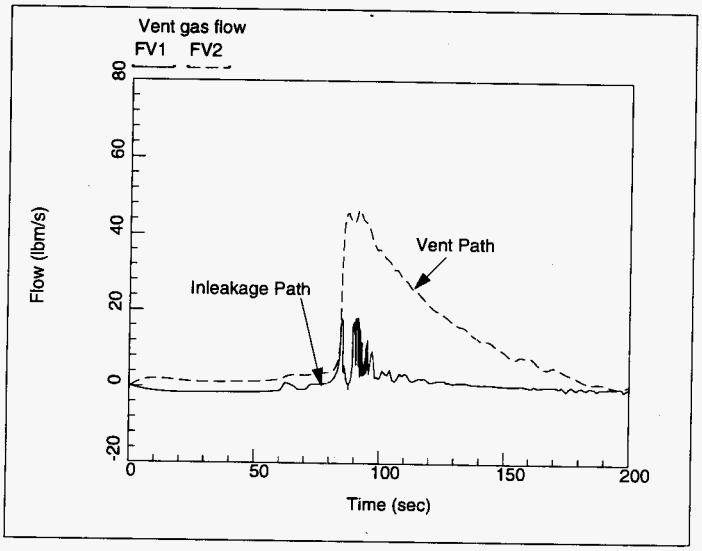

Figure 85. Steam Concentration Contours in 11 ft of Sludge Indicating Hot Sludge and Steam Bubble Break the Pool Surface With 6 Inch Diameter Inleakage Flow Path.

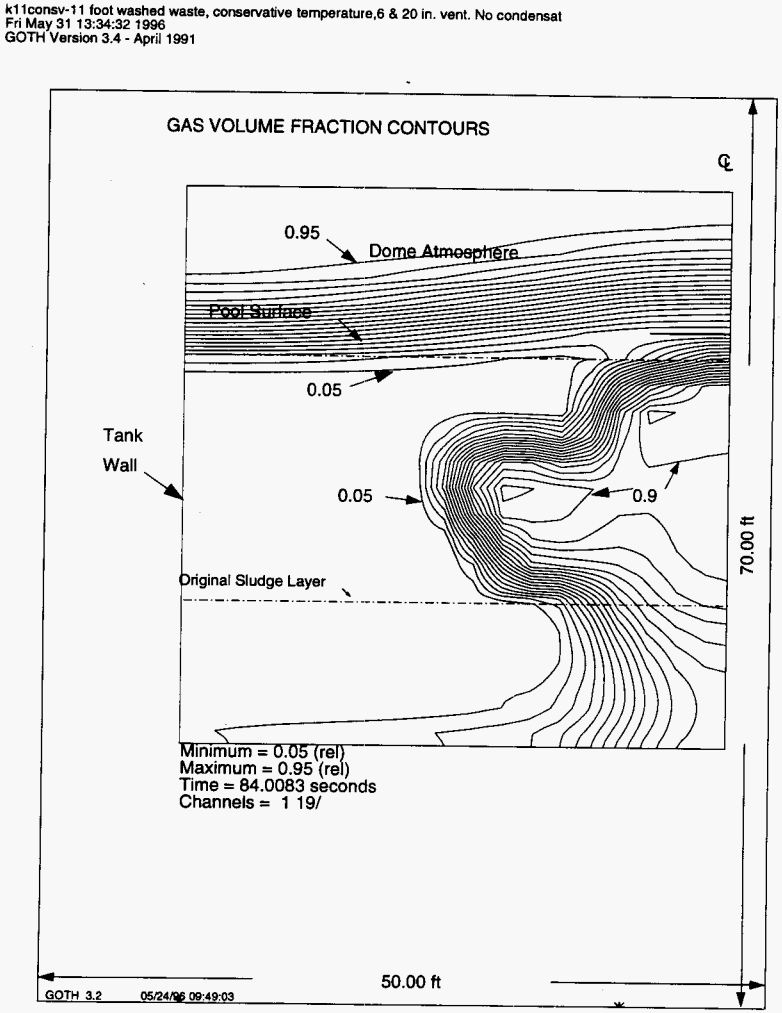

Figure 86. Gas/Steam Flow Through Inleakage and Vent Flow Paths During the Steam Bump With 6 Inch Diameter Inleakage Flow Path.

k11consv-11 foot washed waste, conservative temperature,6 & 20 in. vent. No condensat
Mon Jun 3 14:20:18 1996
GOTH Version 3.4 - April 1991

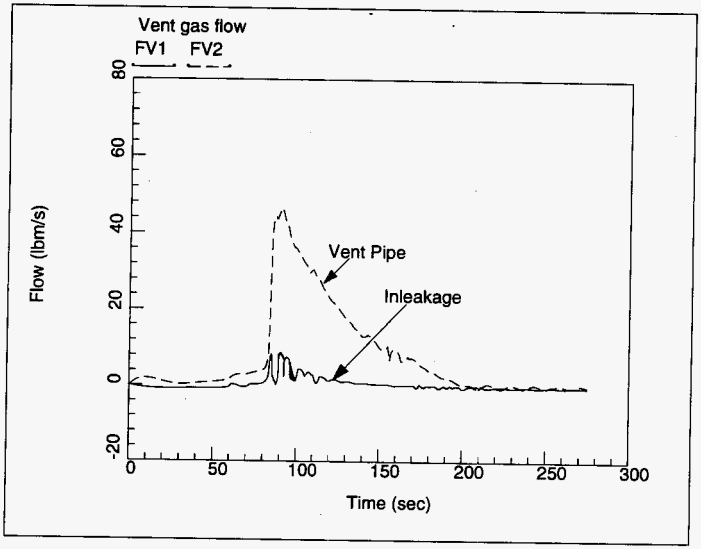

Figure 87. Steam Concentration Contours Showing the Rise of Plume to the Pool Surface in 11 ft of Sludge for Conservative Initial Temperature and Including Condensation.

b11conc-11 foot washed waste, conservative temperature at atmospheric pressure. condensat
Sun Jun 2 11:23:29 1996
GOTH Version 3.4 - April 1991

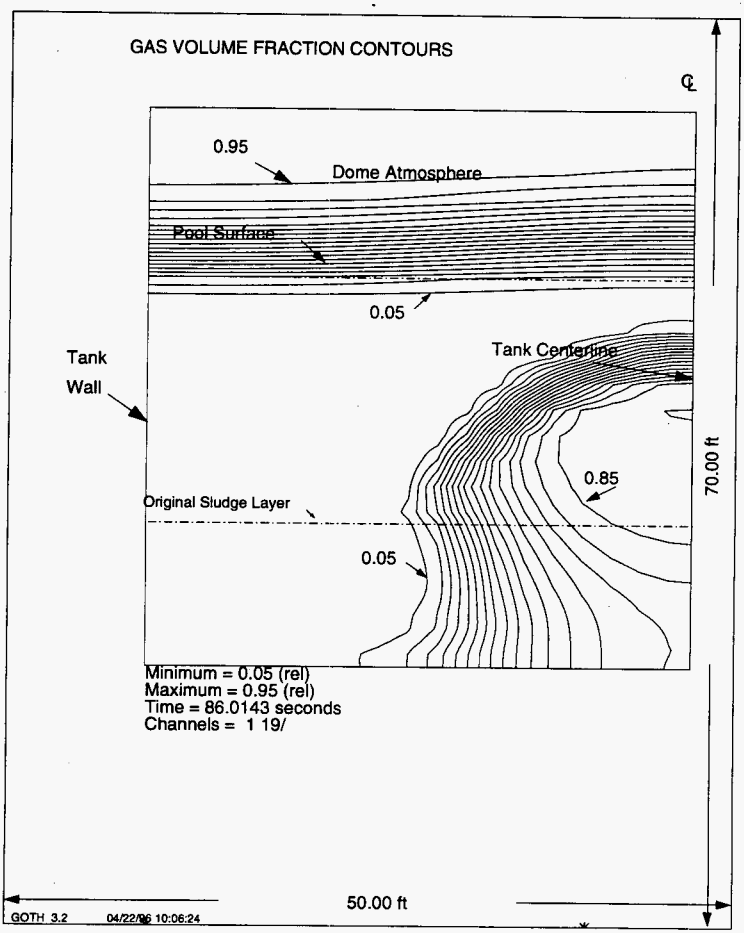

Figure 88. Steam Concentration Contours in 11 ft of Sludge Indicating Hot Sludge and Steam Bubble Break the Pool Surface With Open Risers as Inleakage Flow Paths.

b11conc-11 foot washed waste, conservative temperature at atmospheric pressure. condensat
Sun Jun 2 11:25:05 1996
GOTH Version 3.4 - April 1991

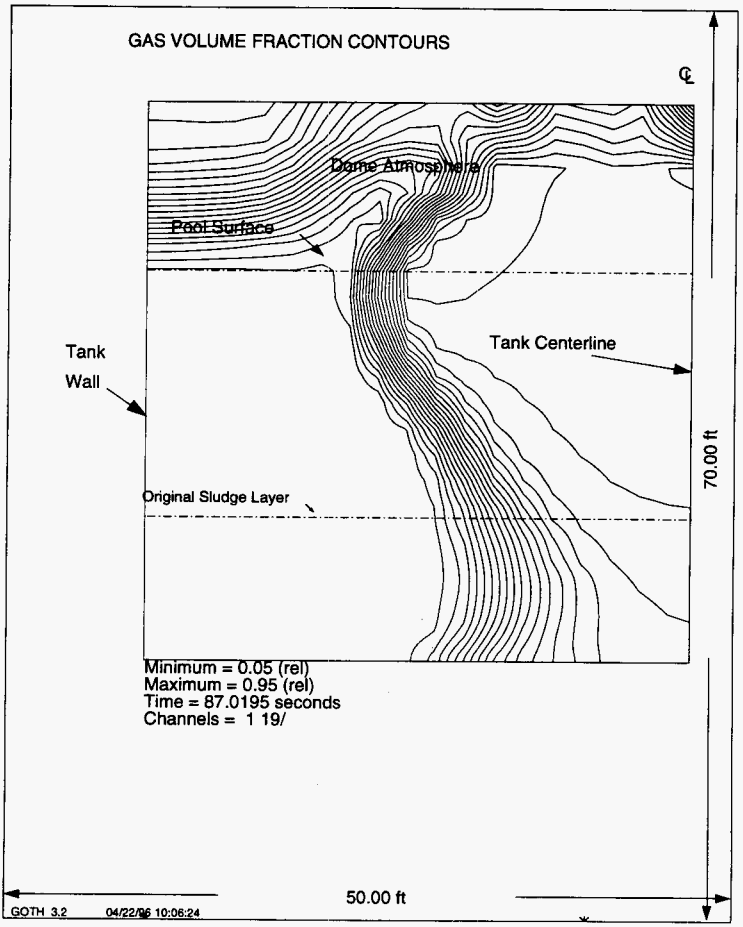

Figure 89. Steam Concentration Contours in 11 ft of Sludge Showing the Collapse of Steam Bubble Due to Condensation.

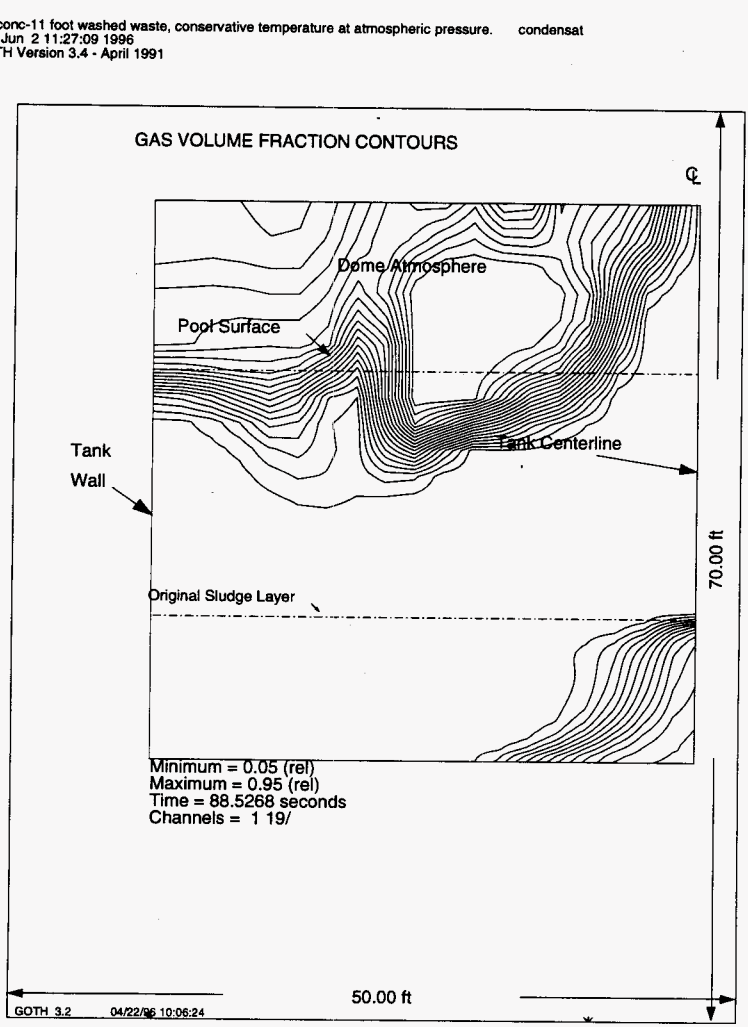

Figure 90. Liquid Droplet Flow Through Inleakage Flow Paths During the Steam Bump With Open Risers as Inleakage Flow Paths.

b11conc-11 foot washed waste, conservative temperature at atmospheric pressure. Condensat
Sun Jun 2 13:20:06 1996
GOTH Version 3.4 - April 1991

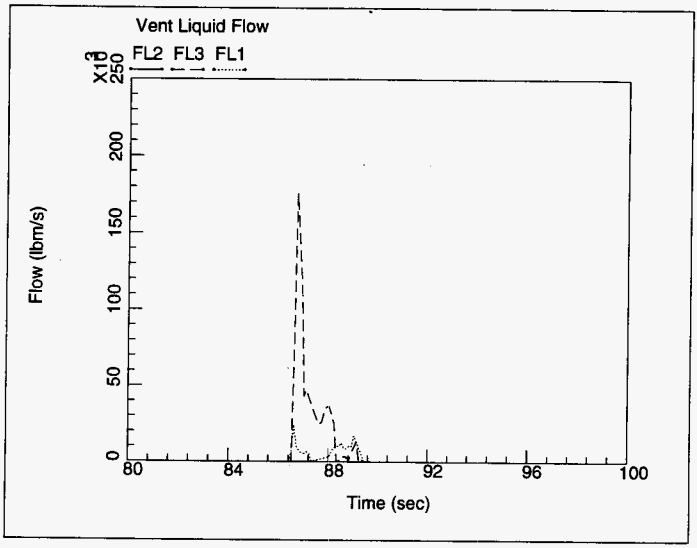

Figure 91. Solid Particle Flow Through Inleakage Flow Paths During the Steam Bump With Open Risers as Inleakage Flow Paths.

b11conc-11 foot washed waste, conservative temperature at atmospheric pressure. Condensat
Sun Jun 2 13:20:22 1996
GOTH Version 3.4 - April 1991

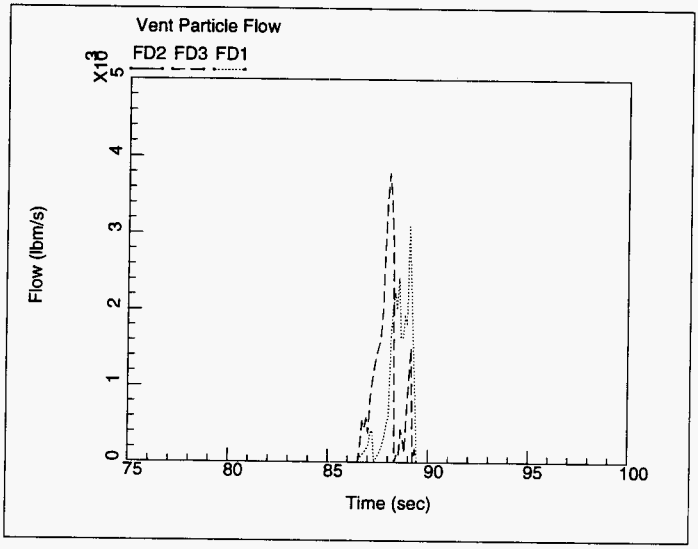

7.3.3 Best Estimate Initial Temperature and No Condensation

In this case the sludge temperature has been initialized with the realistic temperature distribution corresponding to the case with loss of both primary and secondary ventilation systems when the bottom sludge temperature reaches local saturation as shown in Figure 7. No condensation of steam in the waste is permitted in order to predict a bounding steam bump and its consequences. Using these conditions, steam bump simulations were performed for three different inleakage flow path areas. The results of simulations for waste release quantities are given in Table 7. Because of less energy content of the sludge due to its temperature distribution, the peak dome pressures are lower than those with the conservative temperature distribution in the sludge. As in other simulations, the liquid droplets and solid particles flow through the inleakage flow paths are higher for large openings and they decrease as the available area for leakage decreases. Initially, the hydrodynamic instability develops near the tank wall, as shown in Figure 92, and the plume rises towards the pool surface (see Figure 93). There is an increase in vapor flow but no liquid or particles are released due to this plume. However, later, another plume forms at the center of the tank as shown in Figures 94 and 95. This plume rises through the pool surface and carries with it liquid and particles through the pump pit leakage path as shown in Figures 96 and 97, respectively. For drain pipe leakage flow paths, the steam volume fraction contours illustrating the plume development near the outer wall and rise to the pool surface are shown in Figures 98 and 99. This plume rise is accompanied by another near the center of the tank (see Figure 100) and it rises to pool surface and carries with it liquid and solid particles as shown in Figure 101. The corresponding releases of liquid droplets and particle flows through the leakage flow paths are shown in Figures 102 and 103, respectively. For the smaller leakage flow path of 6 inch equivalent diameter, a similar behavior occurs though smaller in plume size (see Figures 104 and 105) and corresponding liquid and solids releases are shown in Figures 106 and 107.

7.3.4 Best Estimate Initial Temperature With Condensation

This simulation represents realistic initial bump conditions that lead to such an occurrence. However, continued loss of cooling can raise the waste temperatures such that the axial temperature distribution approaches the conservative temperature distribution. The bump simulation with these conditions has been performed for large leakage flow paths of open risers. The supernatant has been initialized at 112 °F, i.e., there is large subcooling available for any steam to condense. The steam plume develops as in other best estimate temperature cases, initially at the tank outer wall and the later at the tank center. The steam at the wall did not even leave the sludge before it collapsed as illustrated through the steam volume fraction contours in Figures 108 and 109. The plume at the center (see Figure 109) develops into a plume and rises above the sludge approaching the pool surface. The plume could not break the pool surface before it collapsed due to condensation (see Figure 109). The operating condition of limiting the peak sludge temperature below local saturation provides a large margin of time before an energetic bump can occur. The margin of time depends on a large number of factors that contribute to increasing the waste temperature.

Table 7. Vent Flows for a Best Estimate Tank Bump in 11 Feet of Combined Tank AY-102 and C-106 Sludge.

Parameters	Vent Flow Paths	Vent Flow Path	Vent Flow Path
	1. 42" dia-Pump Pit Path 2. 20" dia-Vent Path 3. Four 42" dia-Sluice Pits Path	1. Five 4" dia-Inleakage Paths 2. 24" dia-Vent Path	1. 6" dia-Inleakage Path 2. 24" dia-Vent Path
1. Tank Dome Peak Pressure, psia	18.8	19.2	19.7
2. Vapor Flow Flow path 1, lbm Flow path 2, lbm Flow path 3, lbm	 200 -- 1300	 400 1700 NA	 100 1500 NA
3. Liquid Flow Flow path 1, lbm Flow path 2, lbm Flwo path 3, lbm	 900 -- --	 620 -- NA	 235 -- NA
4. Particle Flow Flow path 1, lbm Flow path 2, lbm Flow path 3, lbm	 90 -- --	 78 -- NA	 32 -- NA

Figure 92. Steam Concentration Contours in 11 ft of Sludge for Best Estimate Initial Temperature Indicating the Rise of Initial Plume From Sludge.

b11be-11 foot washed waste, conservative temperature at atmospheric pressure. No condensat
Sat Jun 1 14:46:41 1996
GOTH Version 3.4 - April 1991

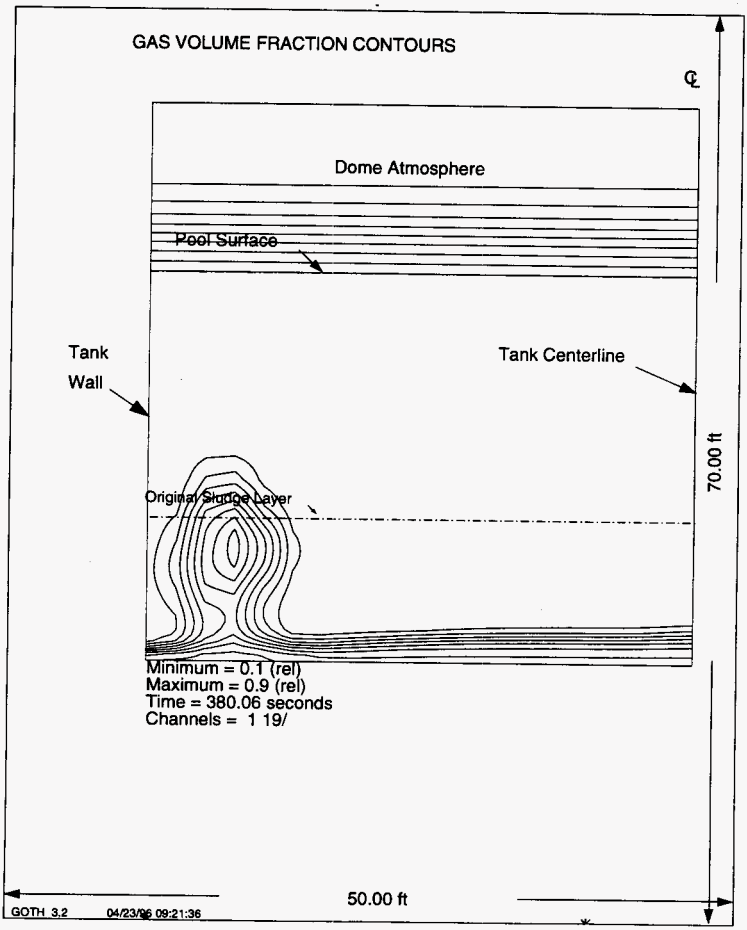

Figure 93. Steam Concentration Contours in 11 ft of Sludge for Best Estimate Initial Temperature Indicating the Rise of Initial Plume from Sludge to Pool Surface.

b11be-11 foot washed waste, conservative temperature at atmospheric pressure. No condensat
Sat Jun 1 14:47:31 1996
GOTH Version 3.4 - April 1991

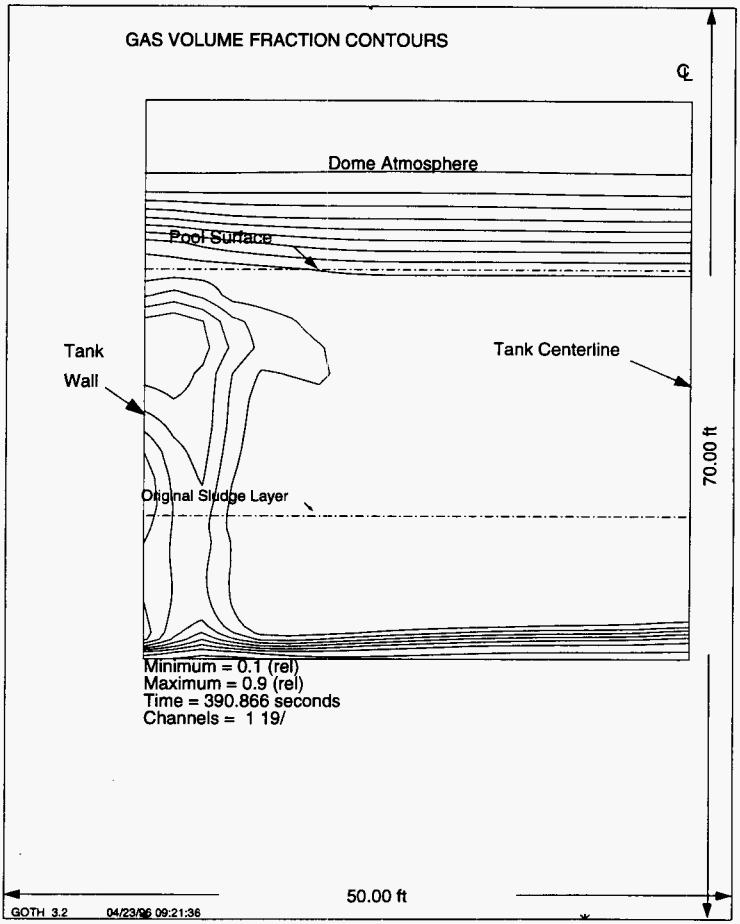

Figure 94. Steam Concentration Contours in 11 ft of Sludge For Best Estimate Initial Temperature Indicating the Rise of Second Plume From Sludge.

b11be-11 foot washed waste, conservative temperature at atmospheric pressure. No condensat
Sat Jun 1 14:51:03 1996
GOTH Version 3.4 - April 1991

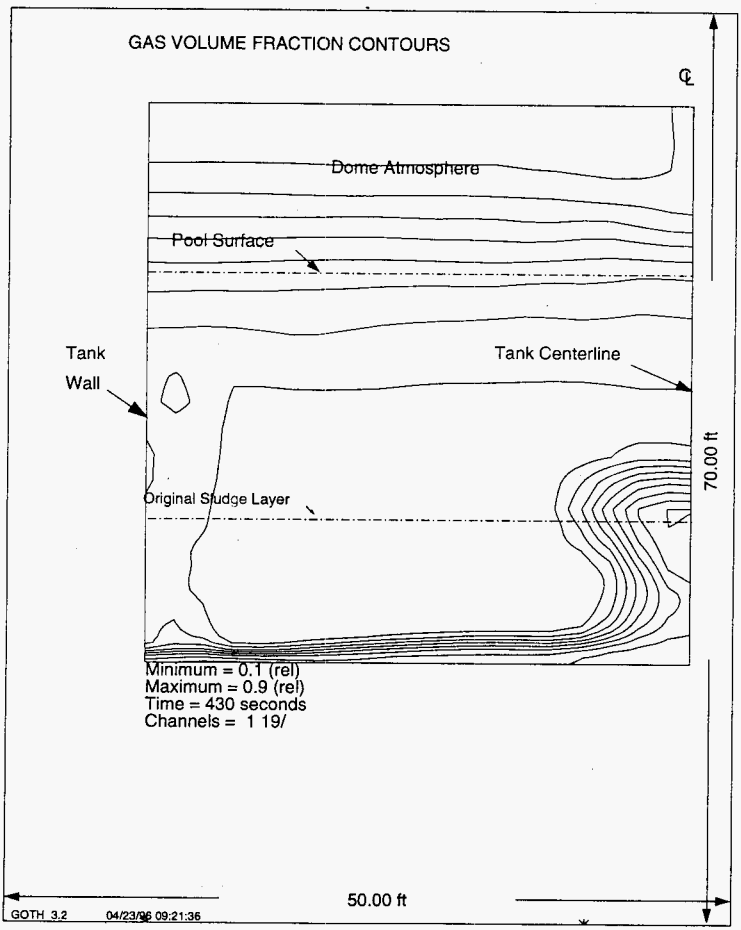

Figure 95. Steam Concentration Contours in 11 ft of Sludge Indicating Hot Sludge and Steam Bubble Break the Pool Surface With Open Risers as Inleakage Flow Paths.

b11be-11 foot washed waste, conservative temperature at atmospheric pressure. No condensat
Sat Jun 1 14:54:40 1996
GOTH Version 3.4 - April 1991

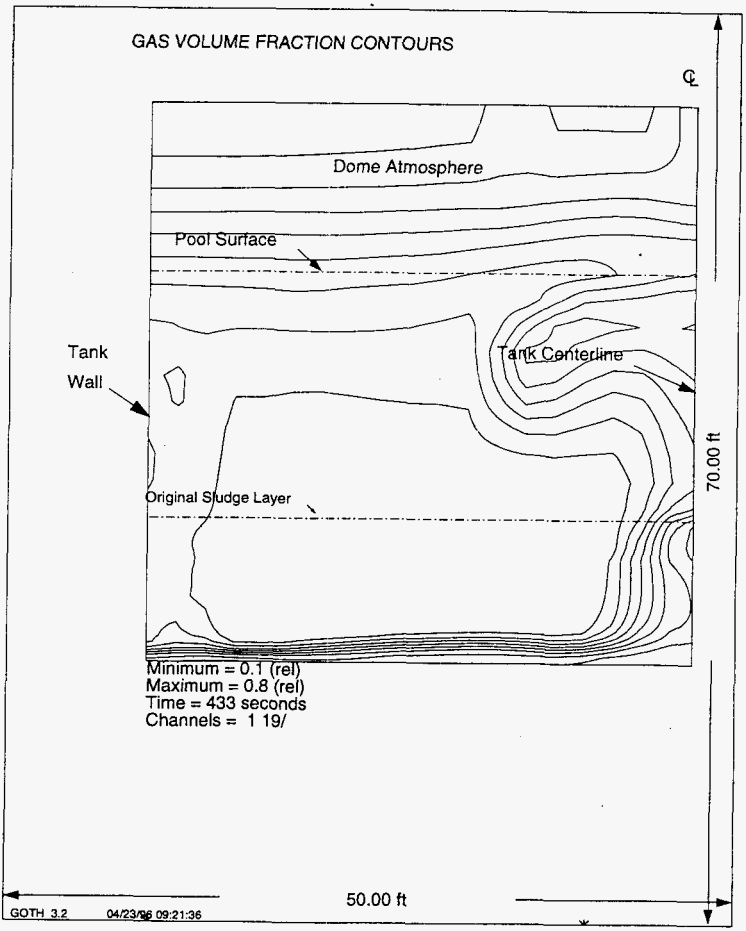

Figure 96. Liquid Droplet Flow Through Inleakage Flow Path During the Steam Bump.

b11be-11 foot washed waste, conservative temperature at atmospheric pressure. No condensat
Sat Jun 1 14:40:34 1996
GOTH Version 3.4 - April 1991

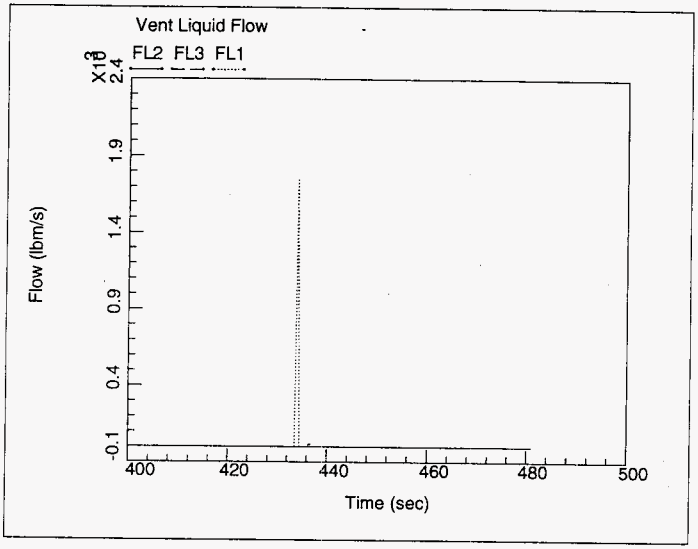

Figure 97. Solid Particle Flow Through Inleakage Flow Path During the Steam Bump.

b11be-11 foot washed waste, conservative temperature at atmospheric pressure. No condensat
Sat Jun 1 14:41:02 1996
GOTH Version 3.4 - April 1991

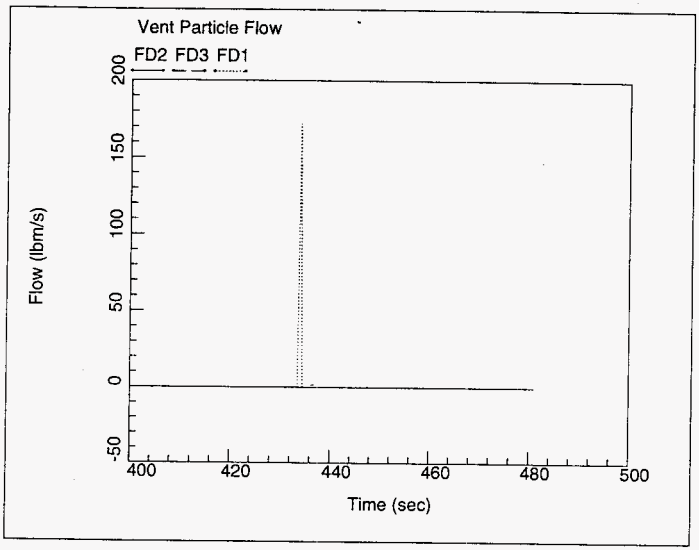

Figure 98. Steam Concentration Contours in 11 ft of Sludge for Best Estimate Initial Temperature Indicating the Rise of Initial Plume from Sludge With Drain Pipes as Leakage Flow Paths.

b11b9sv-11 foot washed waste, conservative temperature, simple vent. No condensat
Sat Jun 1 16:38:37 1996
GOTH Version 3.4 - April 1991

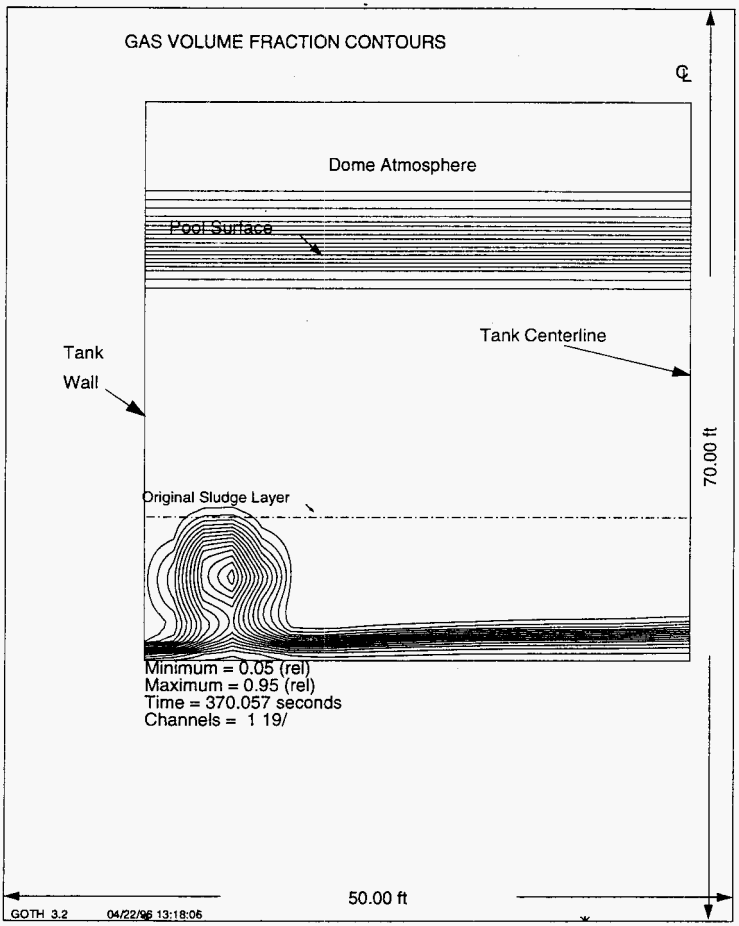

Figure 99. Steam Concentration Contours in 11 ft of Sludge for Best Estimate Initial Temperature Indicating the Rise of Initial Plume from Sludge to Pool Surface.

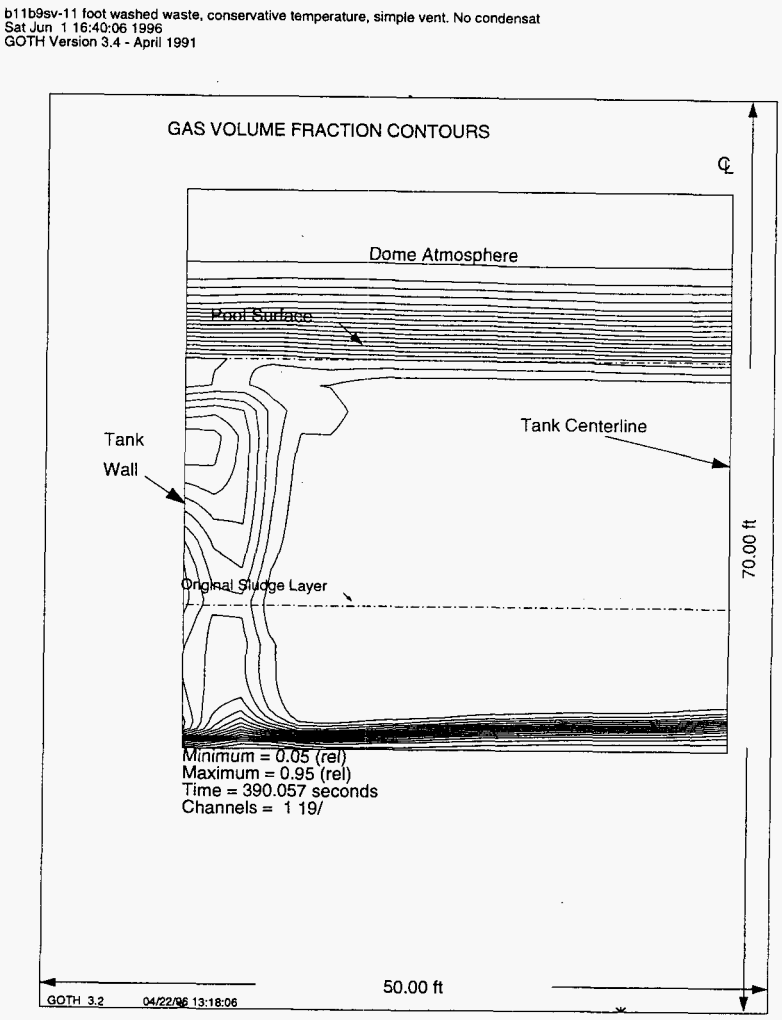

Figure 100. Steam Concentration Contours in 11 ft of Sludge for Best Estimate Initial Temperature Indicating the Rise of Second Plume From Sludge.

b11b9sv-11 foot washed waste, conservative temperature, simple vent. No condensat
Sat Jun 1 16:41:36 1996
GOTH Version 3.4 - April 1991

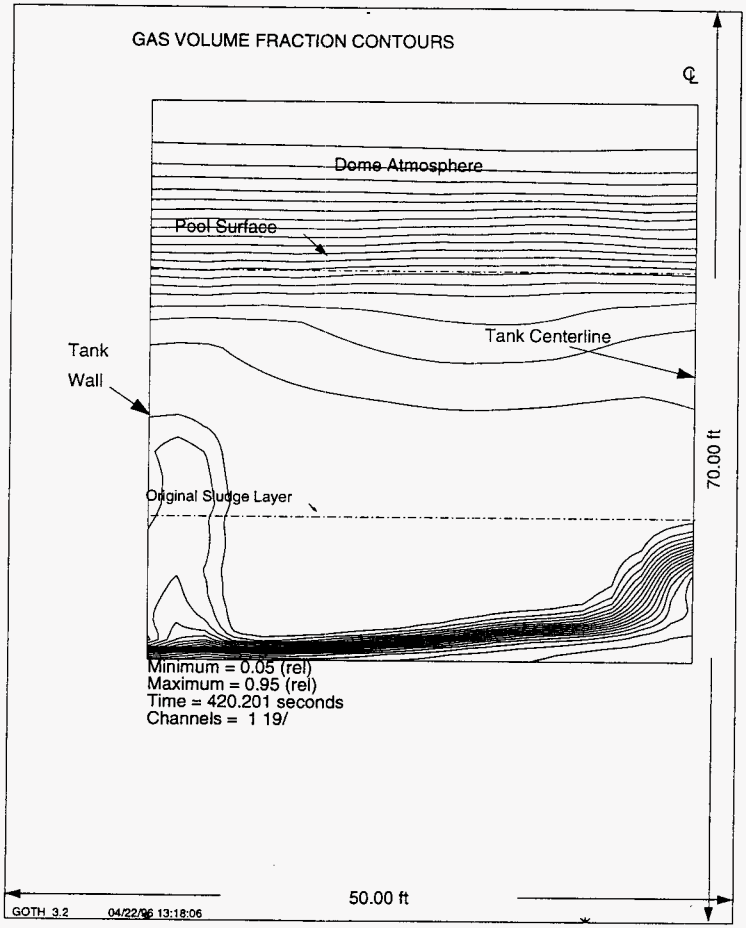

Figure 101. Steam Concentration Contours in 11 ft of Sludge Indicating Hot Sludge and Steam Bubble Break the Pool Surface With Open Risers as Inleakage Flow Paths.

b11b9sv-11 foot washed waste, conservative temperature, simple vent. No condensat
Sat Jun 1 16:44:51 1996
GOTH Version 3.4 - April 1991

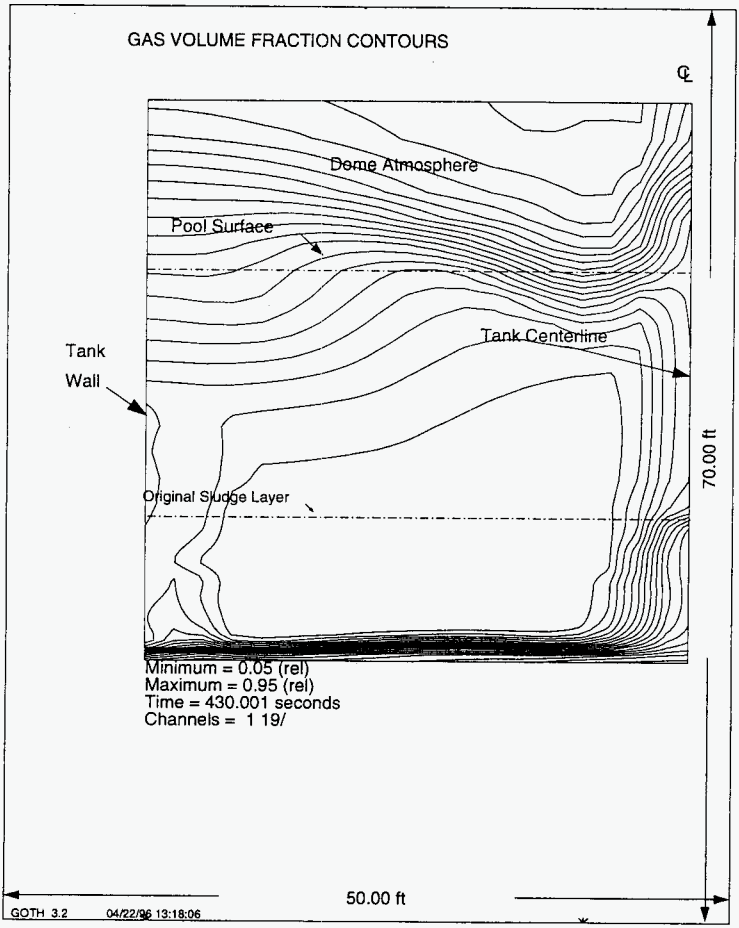

Figure 102. Liquid Droplet Flow Through Inleakage Flow Path During the Steam Bump.

b11b9sv-11 foot washed waste, conservative temperature, simple vent. No condensat
Sat Jun 1 16:47:24 1996
GOTH Version 3.4 - April 1991

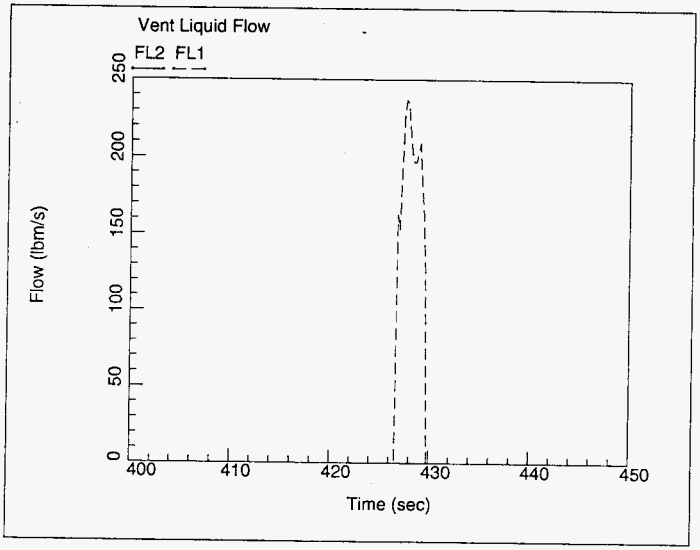

Figure 103. Solid Particle Flow Through Inleakage Flow Path During the Steam Bump.

b11b9sv-11 foot washed waste, conservative temperature, simple vent. No condensat
Sat Jun 1 16:47:49 1996
GOTH Version 3.4 - April 1991

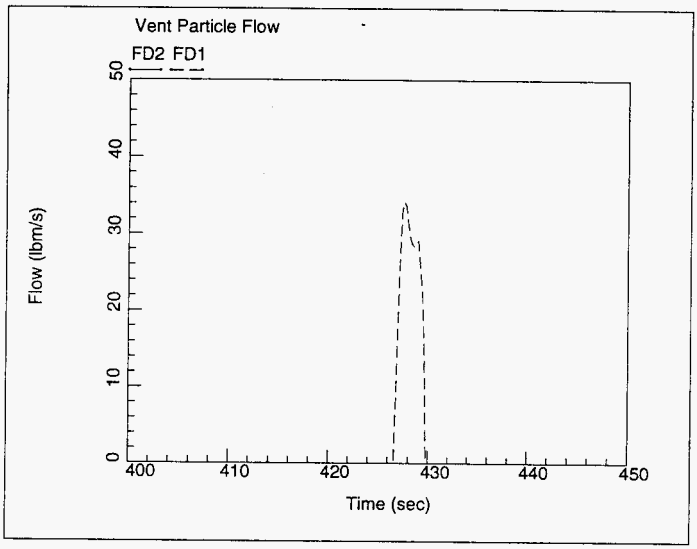

Figure 104. Steam Concentration Contours in 11 ft of Sludge for Best Estimate Initial Temperature Indicating the Rise of Initial Plume from Sludge to Pool Surface With 6 Inch Diameter Leakage Flow Path.

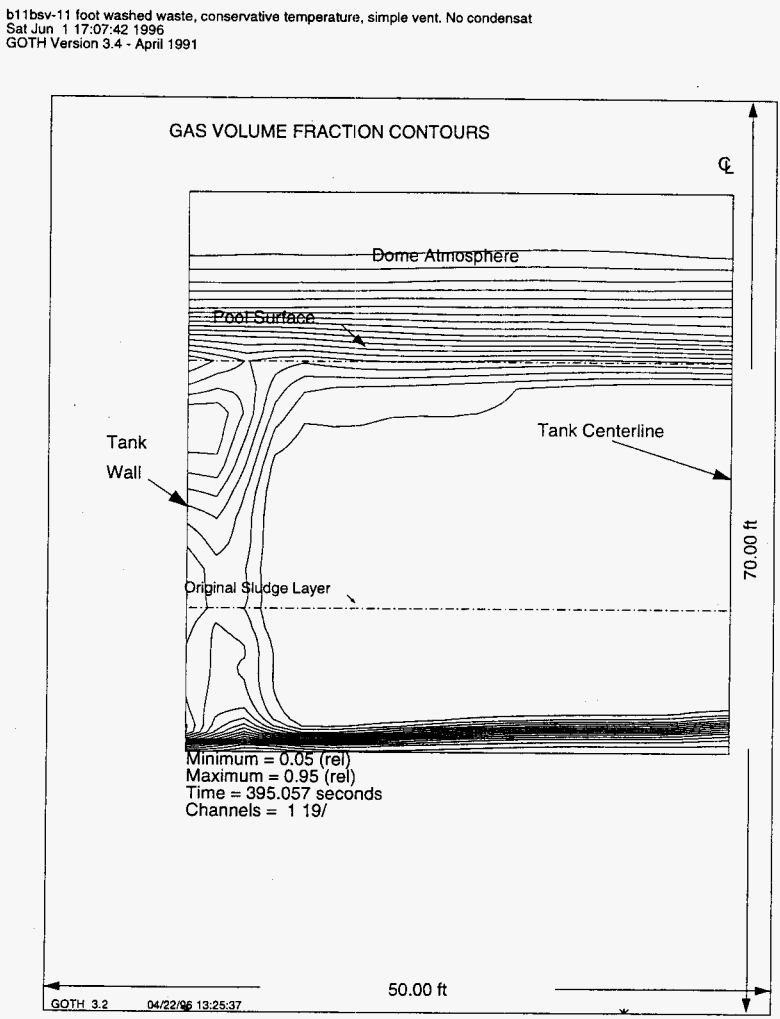

Figure 105. Steam Concentration Contours in 11 ft of Sludge Indicating Hot Sludge and Steam Bubble Break the Pool Surface With 6 Inch Diameter Inleakage Flow Path.

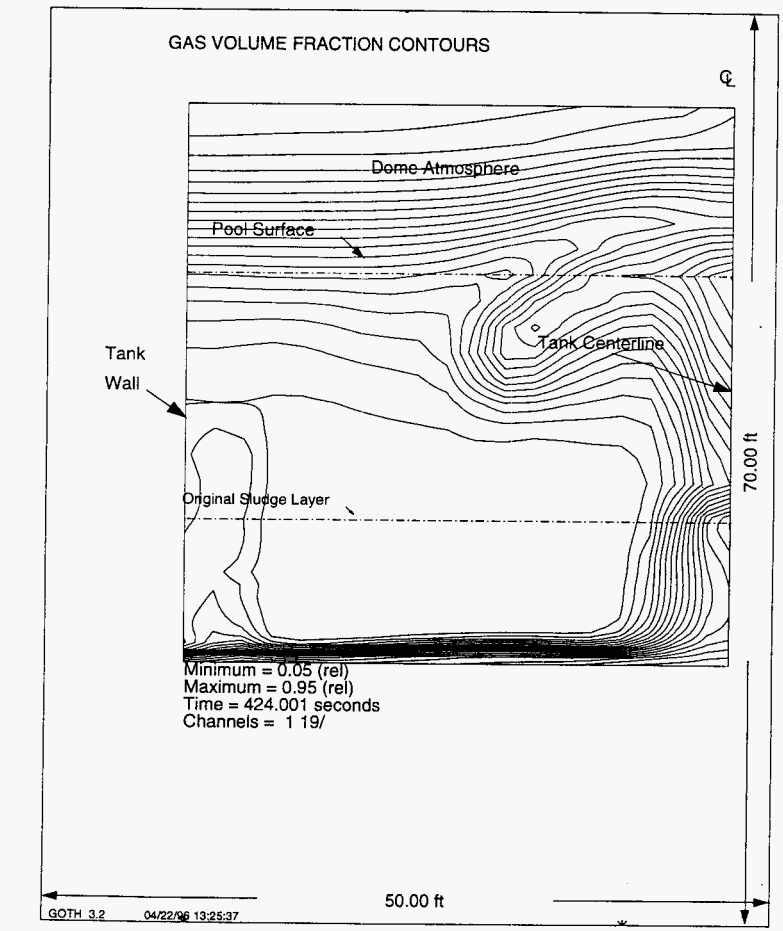

Figure 106. Liquid Droplet Flow Through Inleakage Flow Path During the Steam Bump.

b11bsv-11 foot washed waste, conservative temperature, simple vent. No condensat
Sat Jun 1 17:00:40 1996
GOTH Version 3.4 - April 1991

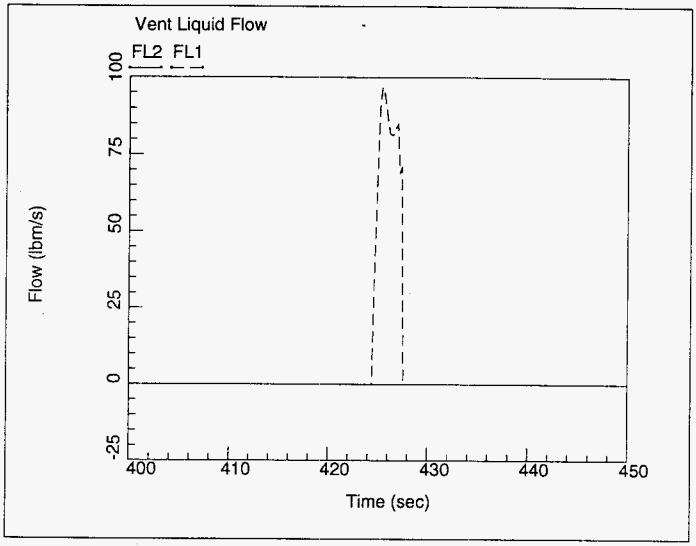

Figure 107. Solid Particle Flow Through Inleakage Flow Path During the Steam Bump.

b11bsv-11 foot washed waste, conservative temperature, simple vent. No condensat
Sat Jun 1 17:01:00 1996
GOTH Version 3.4 - April 1991

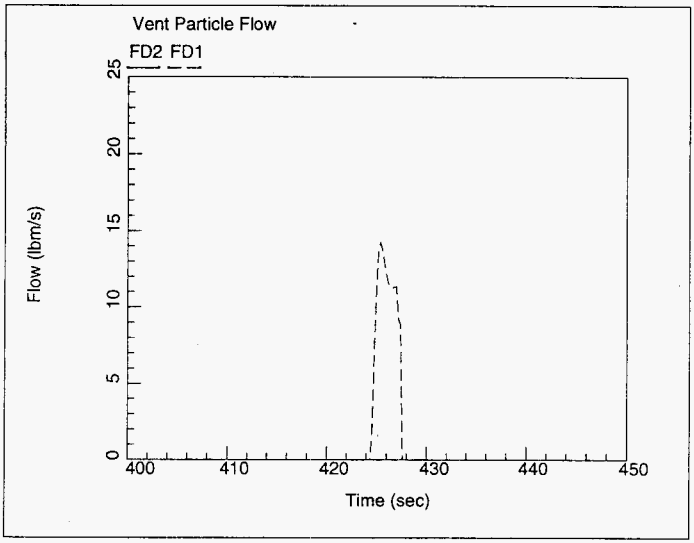

Figure 108. Steam Concentration Contours in 11 ft of Sludge Showing the Development of Plume in Sludge For Best Estimate Initial Temperature Including Condensation With Open Risers as Leakage Flow Paths.

b11bec-11 foot washed waste, Best Estimate temperature at atmospheric pressure. Condensat
Sun Jun 2 17:36:10 1996
GOTH Version 3.4 - April 1991

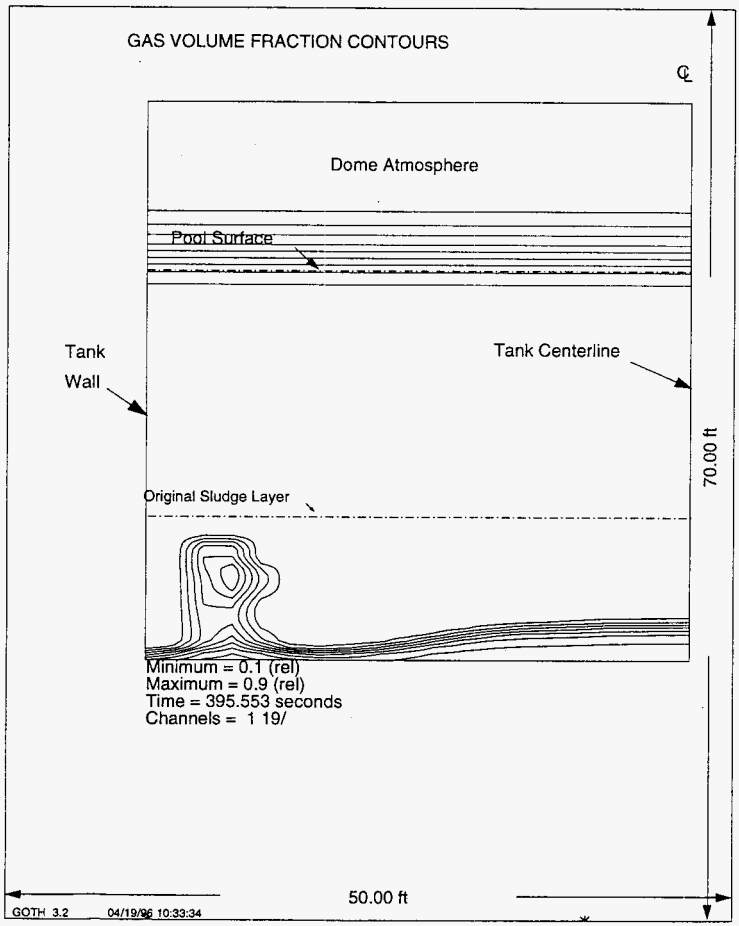

Figure 109. Steam Concentration Contours in 11 ft of Sludge Showing the Rise of Plume in Sludge For Best Estimate Initial Temperature Including Condensation With Open Risers as Leakage Flow Paths.

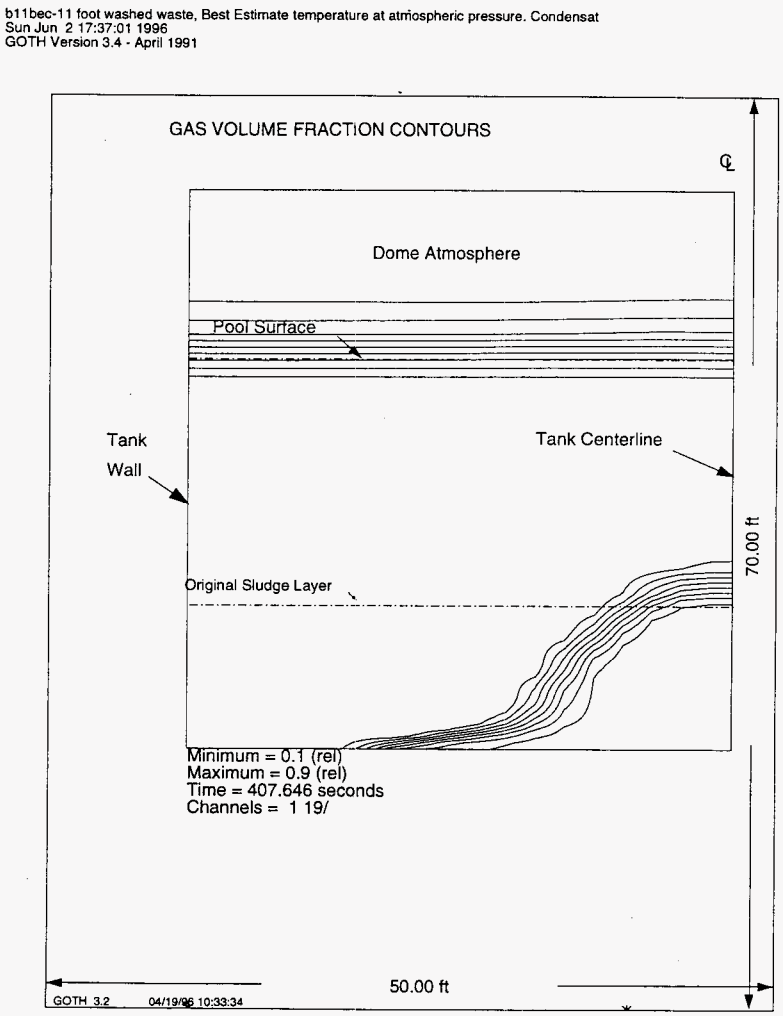

Figure 110. Steam Concentration Contours in 11 ft of Sludge Showing the Rise of Plume in Supernatant For Best Estimate Initial Temperature Including Condensation With Open Risers as Leakage Flow Paths.

b11bec-11 foot washed waste, Best Estimate temperature at atmospheric pressure. Condensat
Sun Jun 2 17:36:40 1996
GOTH Version 3.4 - April 1991

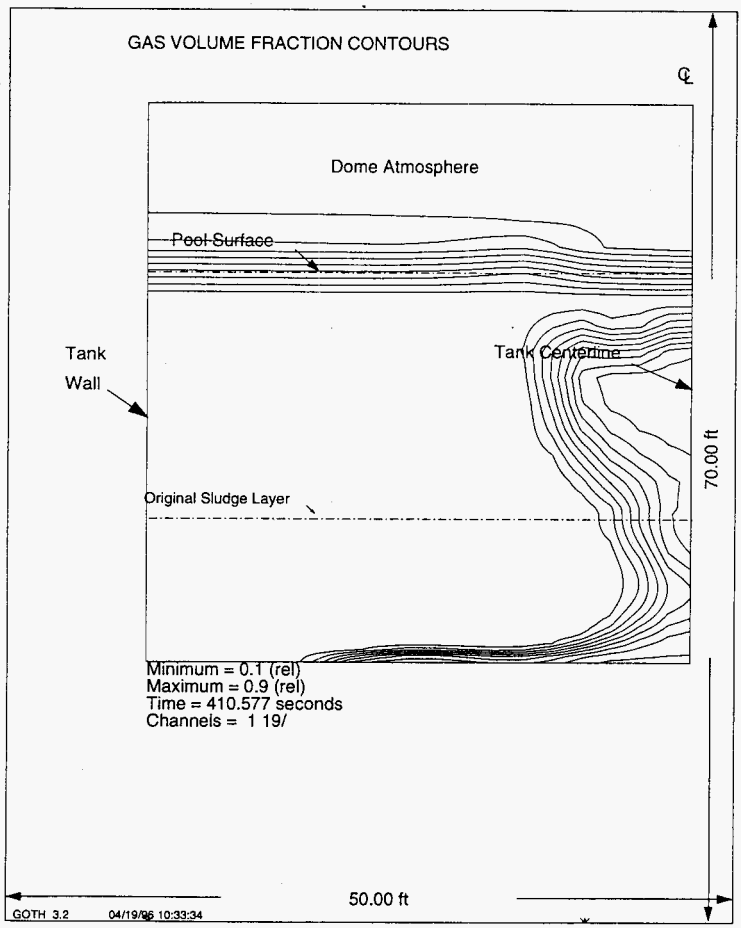

7.4 STEAM BUMP USING AZ/AY TANK FARM VENTILATION MODEL

The effect of the primary ventilation system, which includes the AZ-101, AZ-102, AY-101 and AY-102 tanks, ventilation equipment such as deentrainers, condenser, heaters, filters and fans that provide flow paths and flow resistances, which can affect the steam bump and associated radioactive material releases, was investigated using the model shown in Figure 111. In order to verify that the simple model of the vent path used in all of the above simulations is conservative, a steam bump simulation was performed for 11 ft of consolidated sludge of C-106 and AY-102 assuming that the sludge is in tank AZ-101. The individual component and piping loss coefficients were set to obtain normal flow rates into individual tanks for normal dome pressure conditions using the heat loads of individual tanks and set fan inlet pressure. A steady state flow calculation was performed to assure that correct dome pressures and flow rates are calculated.

It is assumed that the sludge is stored in tank AZ-101 and has a conservative initial temperature distribution as shown in Figure 8. It is also assumed that the steam will not condense in the waste. The tank dome inleakage flow paths correspond to five drain pipes. The results of simulation are compared in Table 8 with those obtained using the simplified vent model discussed in Section 7.3.1. The radioactive material releases using the complete ventilation system model are calculated to be less than those predicted with the simple model. The simple vent model used for the steam bump simulations provides conservative estimates of the size of the steam bump and its consequences, such as vent flows and dome pressure. However, the detailed ventilation system model will estimate more realistic conditions not only in the tank where the bump occurs but in all the other tanks connected to same ventilation system.

The steam concentration contours showing the formation of the plume in the sludge is shown in Figure 112. Figures 113 and 114 show the steam concentration contours for the plume rise and the plume breaking of the pool surface releasing liquid droplets and solid particles into the dome. The steam formed in the dome causes the dome pressure to increase as shown in Figure 115. It can be seen that the pressure rise in tank AZ-101 during the bump will also increase the tank dome pressure in the other three tanks. The radioactive material releases through the inleakage and vent flow paths from tank AZ-101 in the form of gas/steam, liquid droplets and solid particles are shown in Figures 116 through 118, respectively.

Table 8. Comparison of Potential Vent Flows for Steam Bump in 11 Feet of Combined Tank AY-102 and C-106 Sludge.

Parameters	Simple Vent Model	Complete Tank Farm Vent Model
	Dome Flow Paths 1. Five 4 " dia. -Inleakage Paths 2. 20 " dia.- Vent Path	Dome Flow Paths 1. Five 4" dia.-Inleakage Paths 2. 20" dia.-Vent Path
1. Tank Pressure, psia	25	22.2
2. Vapor Flow Path 1. Flow, lbm Path 2. Flow, lbm	 250 1900	 110 1850
3. Liquid Flow Path 1. Flow, lbm Path 2. Flow, lbm	 21,500 --	 4426 --
4. Particle Flow Path 1. Flow, lbm Path 2. Flow, lbm	 2100 --	 450 --

Figure 111. Schematic of AZ/AY Tank Farm Model Used For Simulation of Steam Bump in AZ-101 Including Other Tanks and Ventilation Equipment.

farm2d7-48 inch, conservative temperature, no condensation
Thu May 30 07:23:29 1996
GOTH Version 3.4 - April 1991

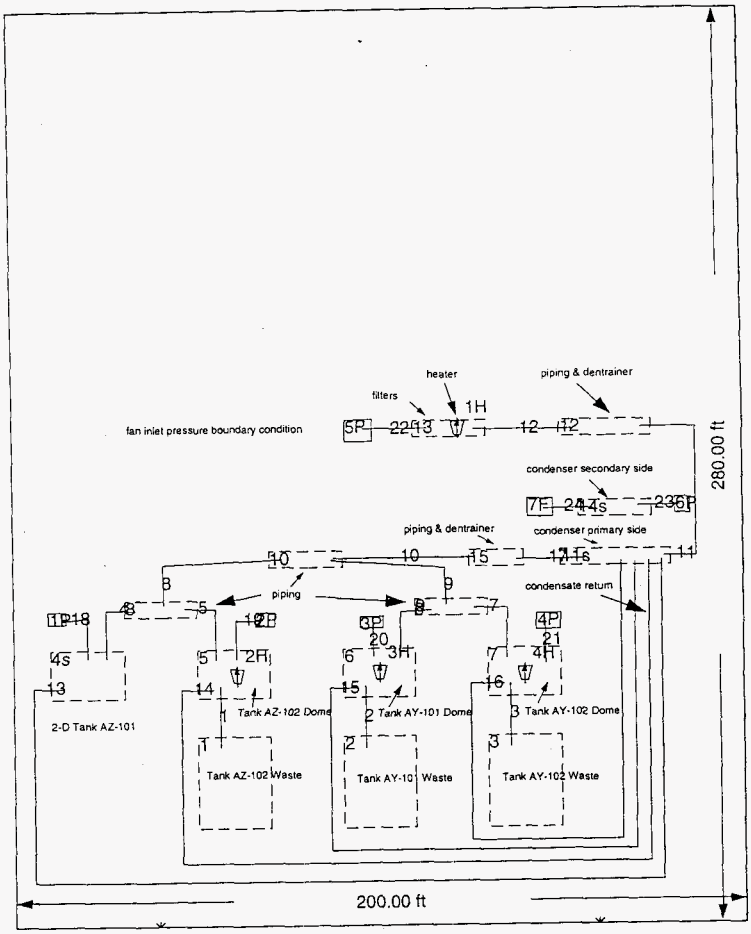

Figure 112. Steam Concentration Contours in 11 ft of Sludge showing the Development of Plume in Sludge For Conservative Initial Temperature and No Condensation With Drain Pipes as Leakage Flow Paths.

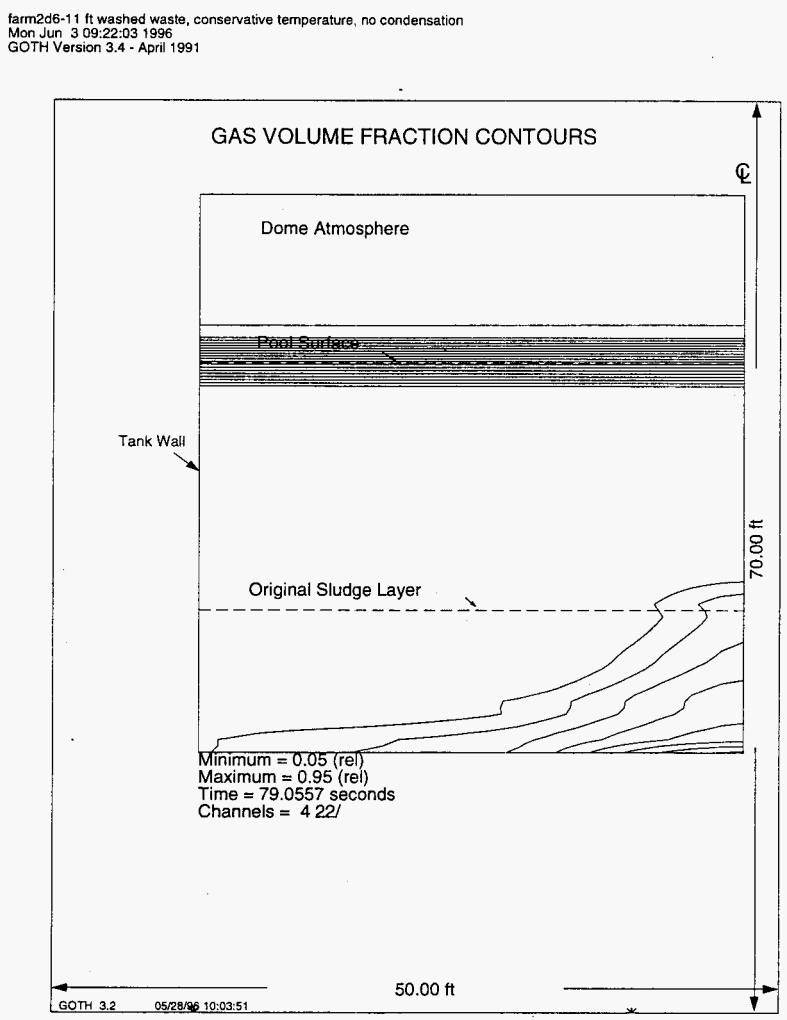

Figure 113. Steam Concentration Contours in 11 ft of Sludge Showing the Rise of Plume From Sludge For Conservative Initial Temperature With No Condensation and Drain Pipes as Leakage Flow Paths.

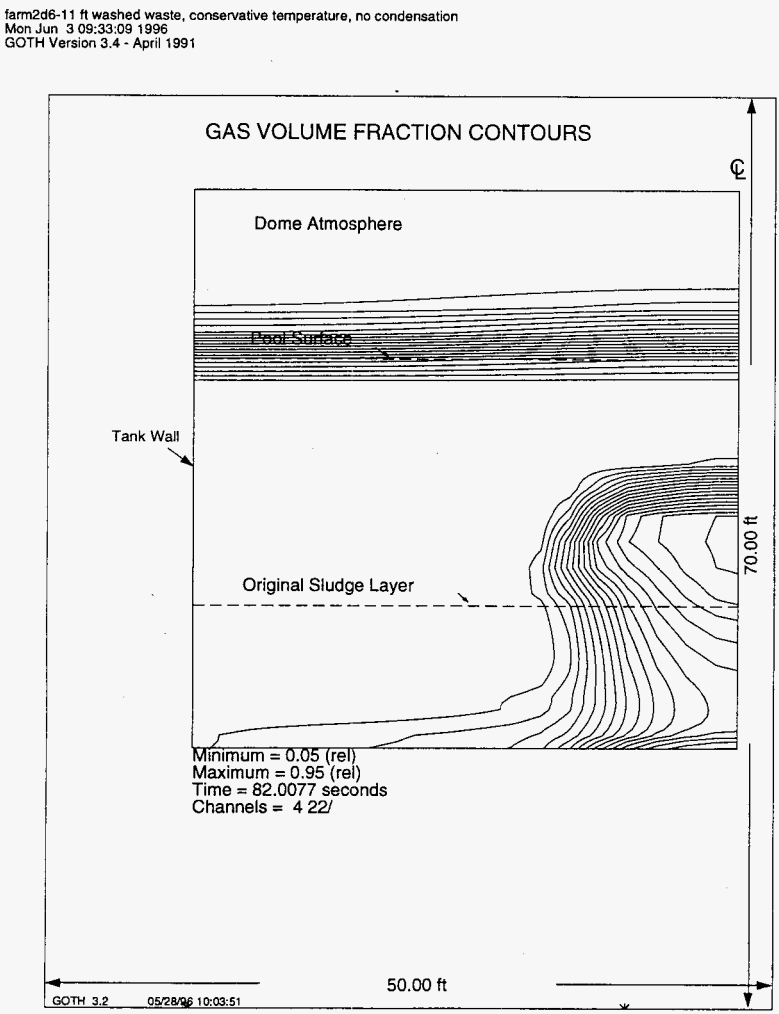

Figure 114. Steam Concentration Contours in 11 ft of Sludge Showing the Plume Breaking the Pool Surface For Conservative Initial Temperature and No Condensation With Drain Pipes as Leakage Flow Paths.

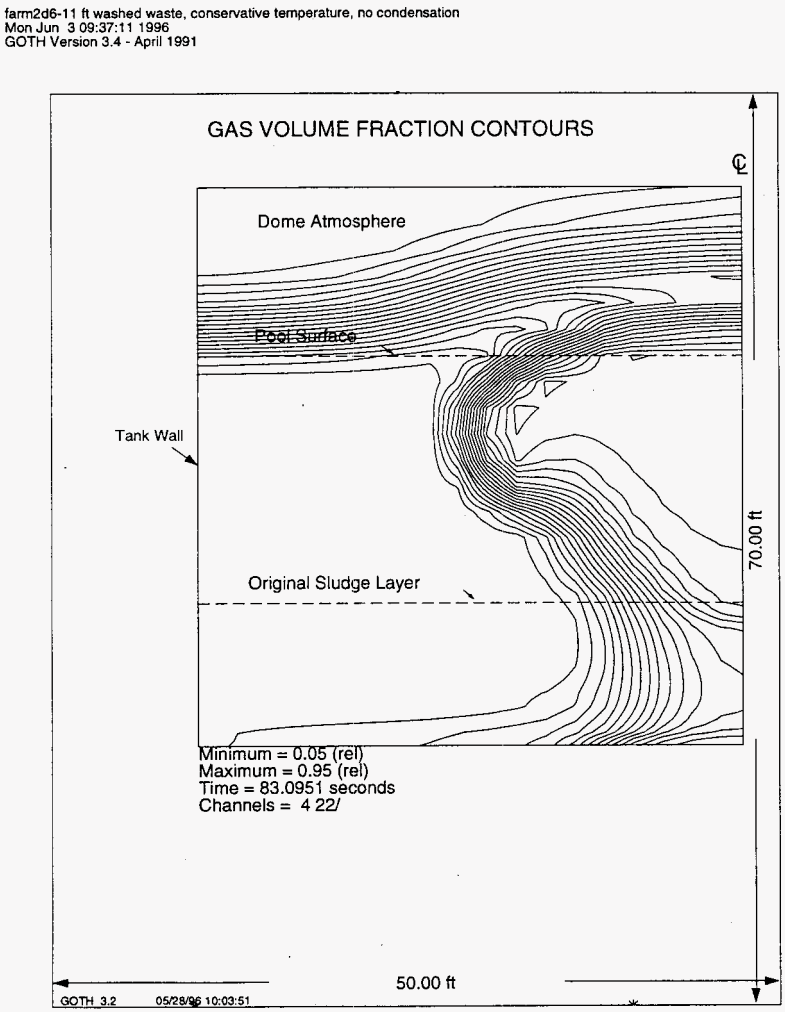

Figure 115. Pressure Variation in Aging Waste Tanks of AZ-101, AZ-102, AY-101 and AY-102 During the Steam Bump in AZ-101 With 11 ft of Sludge.

farm2d6-11 ft washed waste, conservative temperature, no condensation
Tue Jun 4 09:02:59 1996
GOTH Version 3.4 - April 1991

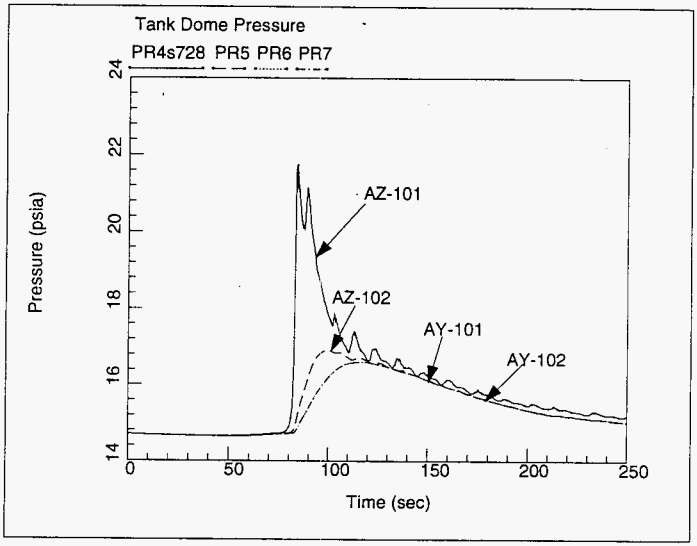

Figure 116. Gas/Steam Flow Through Inleakage and Vent Flow Paths During the Steam Bump in AZ-101 With Drain Pipes as Inleakage Flow Paths.

farm2d6-11 ft washed waste, conservative temperature, no condensation
Mon Jun 3 08:18:33 1996
GOTH Version 3.4 - April 1991

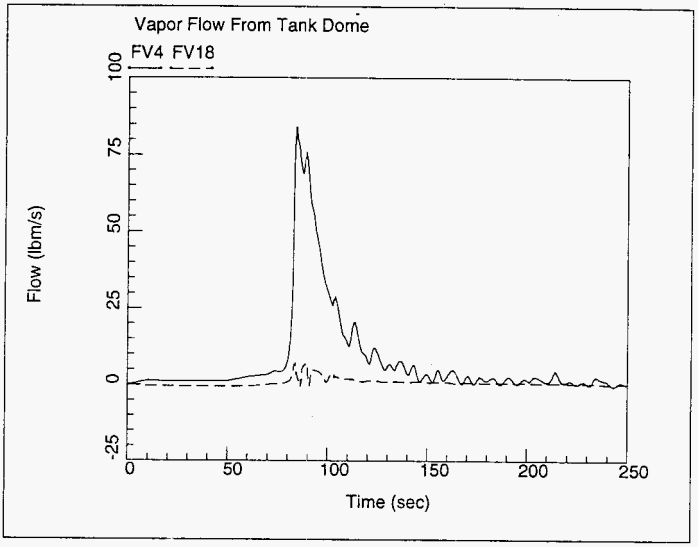

Figure 117. Liquid Droplet Flow From AZ-101 Through Drain Pipe Leakage Paths During Steam Bump in AZ-101.

farm2d6-11 ft washed waste, conservative temperature, no condensation
Mon Jun 3 08:19:05 1996
GOTH Version 3.4 - April 1991

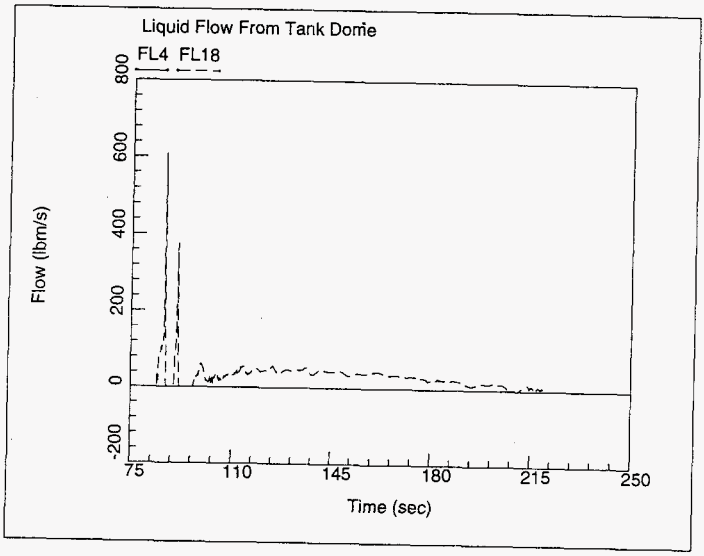

Figure 118. Solid Particle Flow From AZ-101 Through Drain Pipe Leakage Paths During Steam Bump in AZ-101.

farm2d6-11 ft washed waste, conservative temperature, no condensation
Mon Jun 3 08:19:23 1996
GOTH Version 3.4 - April 1991

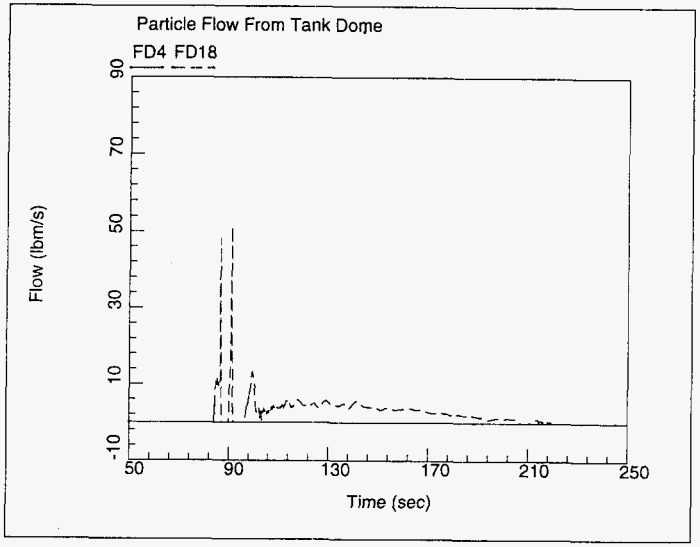

8.0 CONCLUSIONS

Steam bump simulations have been performed for the tank AZ-101 waste assuming two sludge thicknesses corresponding to the current 18 inches and with additional sludge up to 48 inches. In both cases, current waste properties are used. The steam bump simulations have been initiated from both a best estimate and a conservative axial temperature distribution for the sludge. The best estimate axial temperature distribution assumes the temperature profile that results from the transient event that causes the sludge to reach saturation. The conservative temperature profile assumes that the sludge is near its local saturation temperature at all levels. The transient event for the 18 inch sludge layer is the loss of primary ventilation system. The transient event for the 48 inch sludge layer is the addition of 30 inches of similar sludge on top of the current sludge. Further, these simulations have been performed both by suppressing steam condensation in the supernatant to simulate a bounding steam bump and by including the effects of steam condensation in the supernatant to estimate a realistic steam bump. In addition, these simulations have also been performed for three different inleakage flow areas. The first case assumes that the inleakage flow area corresponds to both the riser flanges and pit cover blocks are open and the second case corresponds to inleakage flow path areas due to drain pipes. The third case assumes that the equivalent inleakage flow area corresponds to the 6 inch diameter flow duct.

Results of simulations show that the conservative temperature profile for both 18 and 48 inch sludge thickness cases with the assumption of no condensation results in steam bumps and release of waste material to the environment. The size of the steam bump and release quantities drastically vary depending on the size and location of leakage flow paths. The extremely conservative bounding steam bump will occur for open risers and pits where significantly large quantities of liquid and solid particles will be released. For five, 4 inch drain pipe leakage paths, the size and location of steam bump is smaller and occurs away from the centerline of the tank where the leak path is located. Therefore, the release quantities are also smaller. However, for the 6-inch leak path, the steam bump is smaller but occurs near the center of the tank. In this case, the release quantities are higher than for the drain pipes leakage path. In general, the steam bumps generated by the 48 inch sludge layer are much more severe than those produced by the 18 inch sludge layer.

The results for a conservative initial temperature profile, but including condensation effects, show that all cases of AZ-101 waste, except for the 48 inches of sludge layer with open risers and pits condition, the steam formed will condense before it can reach the waste surface. The plume that tries to form induces enough mixing and cools the sludge below the saturation temperature causing the collapse of steam bubbles in the sludge. For the 48 inch sludge layer with open risers and pits case, the steam bubble leaves the pool surface and carries a large quantity of liquid and solid particles before the steam bubble collapses in the sludge.

The results show that the plume of sludge rises to the top of waste surface for the 48 inch sludge case but no release of aerosols are predicted for simulations using the best estimate initial temperature profile and with condensation suppressed. In the case of the 18 inch sludge layer, the plume

does not even rise much above the sludge layer itself. The simulations with the best estimate initial temperature, including condensation effects, represent close to realistic conditions if actions are taken to prevent any further heat up of the waste. If condensation effects are included for the 48 inch sludge layer case, the plume cannot rise much above the sludge layer. Since the best estimate temperature cases for both the 18 and 48 inch sludge layer show no steam bump possibility, one must expect that there is no potential for generating aerosols that could flow through the ventilation system if it is operating.

Steam bumps will not occur for the 11 ft of consolidated sludge of C-106 and AY-102 if the sludge and supernatant temperature correspond to best estimate values and condensation can occur. This condition is more realistic situation as far as initial bumps are concerned. However, continued loss of ventilation will, in time allow the sludge and supernatant temperature to approach the conservative temperature with no condensation case. If necessary, actions can be taken to reactivate the cooling system in a short time following system failure, and the bumps can be prevented. If the temperature distribution approaches the conservative values, then, for the 11 ft sludge case, even including condensation, the steam bumps will be large and the consequences are not acceptable.

The complete ventilation system model, including all four tanks and other ventilation equipment, show that the consequences of a steam bump in AZ-101 are less severe than those predicted using a simple vent path model. The simplified ventilation model provides a conservative estimate of the size and the consequences of the steam bump.

Steam bumps with increased sludge loading must be avoided as seen from the results of the bump simulations. The results also show that under realistic operating conditions, even if the sludge reaches the saturation condition, there is sufficient subcooling available in the supernatant that the steam can condense. However, to take advantage of the available margin due to the condensation process, sludge yield strength and supernatant layer thickness, further evaluations of model uncertainties with respect to these parameters on bump behavior should be conducted.

9.0 REFERENCES

Fauske, H. K., 1989, *Independent Review of Aging Waste Tank Bump Phenomena*, FAI/89-94, Fauske and Associates, Burr Ridge, Illinois.

Sathyanarayana, K. and Fryer, B. C., 1996, *Thermal Hydraulic Evaluation of Consolidating Tank C-106 Waste Into AY-102*, WHC-SD-WM-ER-534, Rev. 0, Westinghouse Hanford Company, Richland, Washington.

Sathyanarayana, K., et al., 1994, Summary Report - *Thermal Hydraulic Safety Analysis of Aging Waste Tank AZ-101*, WHC-SD-WM-335, Rev. 0, Westinghouse Hanford Company, Richland, Washington.

Sathyanarayana, K., 1994, *Thermal Bump Consequences using GOTH for AZ-101*, (internal letter 71120-94-KS-004 to K. O. Fein, October 19), Westinghouse Hanford Company, Richland, Washington.

Sathyanarayana, K., et al., 1993, *Development of a Dynamic Computer Simulator for Tank AZ-101*, WHC-SD-WM-198, Rev. 0, Westinghouse Hanford Company, Richland, Washington.

Sathyanarayana, K., 1994, *Temperature Distribution in the Waste of Tank 101-AZ*, (internal letter 7E880-94-KS-001 to B. E. Vonderfecht, May 3) Westinghouse Hanford Company, Richland, Washington.

Thurgood, M.J., 1992, *Simulation of Gas Release Event in Tank 101-SY Using the GOTH Computer Program*, WHC-SD-WM-ER-150, Rev. 0, Prepared by Numerical Applications Inc. for Westinghouse Hanford Company.

Waters, E. D., G. K. Allen, and D. E. Place, 1991, *Analysis of Tank Bump Potential During In-Tank Washington Operations Proposed for the 241-AZ Tanks*, WHC-SD-WM-ER-114, Rev. 0, Westinghouse Hanford Company, Richland, Washington.

Appendix - A

Assessment and Validation of GOTH

For Application to Steam Bump Analysis

TABLE OF CONTENTS

LIST OF TABLES

LIST OF FIGURES

1. INTRODUCTION.

The GOTH thermal hydraulic computer program has been used to perform a variety of simulations for waste tank fluid flow and heat transfer phenomena. These include simulations of tank sludge instabilities resulting from the accumulation of trapped gases, the release and distribution of flammable gases in tank dome spaces and ventilation systems, the transient heat up of tank sludge and supernatant due to loss of ventilation and or evaporative cooling, the formation of steam in tank sludge resulting from sludge heatup, evaporation from tank pool surfaces, steam bumps and aerosol generation resulting from steam bumps, tank farm ventilation system operation, tank waste retieval operations such as sluicing and pump mixing, in-tank waste washing operations including particulate separation, decanting and transient sludge heat up due to particulate settling, decanting, and mixing and accident conditions due to loss of pump operation and/or loss of ventilation.

Simulation of such a wide range of problems involves a wide range of thermal and fluid flow parameters requiring the full multi-phase, multi-component, three-fluid, three-dimensional modeling capabilities of GOTH, including its ability to model engineering systems such as pumps, fans, valves, heat exchangers, heaters and so forth.

GOTH is a state-of-the-art finite volume program that solves the transient conservation equations for mass, momentum and energy for multi-component, multi-phase flow. The multiphases may consist of liquids, gases and solids. The gas phase may consist of a number of non-condensible gases and water vapor. The conservation equations are coupled by mechanistic models for interfacial mass, energy and momentum transfer that cover the entire flow regime map

from single phase gas or liquid flow to through multiphase gas, liquid and solid particle flow. The entire two-phase flow regime from bubbly gas or particle flow in liquids through film/droplet or particulate flow in gas are covered. It includes a full treatment of the three-dimensional transport terms, including a one-parameter turbulence model for turbulent momentum, mass and energy transfer. The program calculates the relative velocities between the phases, including the effects of slip between the phases on pressure drop and heat transfer between phases and between solid surfaces and the fluid. It includes the calculation of laminar and turbulent shear stresses and fluid conduction and turbulent heat transport. The three-fields may be in thermal non- equilibrium since separate energy equations are solved for each field.

The program solves for the velocities of the solid particle, liquid and gas fields using interfacial shear and momentum transfer between each of the phases and the momentum balance equation for each phase. It also solves for the volume fractions and temperature of each phase as well as the density of each phase by solving the mass and energy conservation equations for each phase and the equation of state for each phase. Mass and heat transfer between the phases is calculated using appropriate interfacial exchange models. The model also treats the non-Newtonian behavior of liquid-particle mixtures and liquids including the effects of mixture yield strength.

Having these modeling capabilities, the model can calculate phase change as the liquid saturation temperature is exceeded, the migration of gas/vapor bubbles through liquid/particle mixtures, the settling of solid particles through liquid, temperature gradients in settled liquid-particle layers, hydrodynamic instabilities resulting from trapped gas in sludge, evaporative cooling of liquid surfaces, convection currents driven by density gradients in the mixture, fluid jets, condensation of vapors in subcooled liquid, concentration of flammable gases through

out the computational domain and so forth.

The purpose of this report is to document the applicability of GOTH specifically to steam bump phenomena and to waste tank analysis in general. A complete description of the code and the verification and assessment efforts that have been conducted throughout its development is beyond the scope of this report. Rather, reference is made to other documents, which when taken together, form a more complete compilation of the code capabilities, verification and assessment. Assessment calculations that are not adequately documented elsewhere and which are applicable to the application of GOTH to waste tank analysis are included in this report.

2. GOTH PEDIGREE.

GOTH is a derivative of COBRA family of codes which have their assessment and code development efforts that have been conducted for over 25 years. The earliest ancestor of GOTH is the COBRA-TF [Kelly, 1990] code that has been developed at Battelle Northwest Laboratories for the United States Nuclear Regulatory Commission (USNRC). COBRA-TF has been incorporated into the TRAC-P1A [Liles, 1977] as the vessel module, forming a transient code for nuclear reactor primary system transient two-phase flow and heat transfer analysis called COBRA/TRAC [Thurgood, 1983]. This code, with some modification, is currently used by the Westinghouse Nuclear Power Division as its best estimate small and large break analysis code for nuclear power plant licensing calculations and is called WCOBRA/TRAC [Hochrieter, 1986] . Subsequent to the development of COBRA/TRAC, COBRA-TF has been extracted from COBRA/TRAC and

non-condensible gas modeling capabilities added to provide the capability to model steam/water blowdowns into containment buildings and to model hydrogen releases into containment buildings. This version of the code is called COBRA-NC [Thurgood, 1986] which also has been funded by the USNRC and developed at the Battelle Northwest Laboratories.

System component models such as fans, pumps, valves and heat exchangers along with flow junctions have been added to the code through the private funding of Numerical Applications, Inc. A graphical pre- and post-processor has also been added to form FATHOMS [Thurgood, 1986]. FATHOMS has been sold to the Electric Power Research Institute, which funded further assessment of the code and some minor development to form the GOTHIC computer program [George, 1993]. GOTHIC is currently used by more than 35 US and foreign nuclear utilities and vendors to perform safety and licensing related analyses.

GOTHIC has been modified, under funding from Westinghouse Hanford Company (WHC), to incorporate the solid particle field, treat non-newtonian fluid behavior, add an improved interfacial mass transfer model in the presence of non-condensable gases, include a more implicit treatment of the shear stress terms and add improved differencing schemes to maintain shaper interfaces between gas and liquid surfaces and between sludge and supernatant. These enhanced capabilities are incorporated into the code, GOTH, which is the current version of the code being used to perform simulations of waste tank thermal hydraulic behavior [Thurgood, 1992]. GOTH has been further assessed against experimental data relating to waste tank analysis.

The accumulative assessment of COBRA-TF, COBRA/TRAC, COBRA-NC, FATHOMS, GOTHIC and GOTH provide the overall validation of all of the models currently existing in GOTH. The reader should refer to the COBRA-TF, COBRA/TRAC and COBRA-NC documentation for assessment of the fundamental two-phase flow relationships and equations currently used

in GOTH. The GOTHIC documentation, together with the GOTHIC standard problems, should be referred to for assessment of newer models added to form GOTHIC.

Models incorporated in GOTH are documented in [Thurgood, 1992], which should be considered the base code documentation for GOTH. This document provides complete description of the basic code assessment simulations as well as its application to Tank SY-101 episodic Gas Release Events (GRE). The hydrodynamics of these simulations are similar to those of steam bumps. In addition steam bumps involve more complex heat transfer and phase change phenomenon.

Additional assessments are contained in various other documents that have been produced over the duration of the development and application of GOTH at WHC. These documents, and in some cases, excerpts from this documents will be referred to in the following sections.

The following section is broken into phenomenological areas that effect GOTH's ability to simulate steam bumps in Hanford waste tanks. Each subsection contains descriptions of code assessment calculations that have been conducted in support of the important phenomena.

3. IMPORTANT PHENOMENA RELATED TO STEAM BUMPS.

Several different phenomena come together to determine if a bump will occur and if one does, what the nature of the bump will be. The current justification for applying GOTH to steam bump analysis must be based on an assessment of the code's ability to address each of the separate phenomena since no effort has yet been made to directly

assess GOTH against actual tank steam bump data. The important phenomena affecting steam bump development and behavior are as follows:

1. Evaporative and convective cooling from waste surface.
2. Conduction heat transfer in sludge.
3. Natural convection in supernatant.
4. Particle and liquid heat generation.
5. Effect of particle concentration on viscosity.
6. Ability of sludge to trap gas bubbles.
7. Sludge plume formation and viscous flow.
8. Waste thermodynamic and transport properties.
9. Hot water flashing and steam formation.
10. Bubble migration through sludge.
11. Steam bubble condensation.
12. Particle and droplet entrainment.
13. Yield Strength.
14. Structural heat transfer.
15. Particle settling velocities.
16. Frictional loss through ventilation system components.

Each of these parameters is discussed in the following sections.

3.1. Evaporative and Convective Cooling From Waste Surface.

The evaporative and convective cooling of the waste supernatant by the tank ventilation flow determines, for a given tank heat load, the supernatant temperature in ventilated tanks. The supernatant temperature, in turn, is the boundary condition for performing the conduction solution on the sludge which, ultimately, determines if the sludge temperature will exceed the local saturation temperature so that steam will form in the sludge.

The most direct assessment of the evaporative and convective cooling model in GOTH is the assessment of the model against the Battelle Grout Mold Evaporation Test. The model has also been assessed against actual tank data for tank C-106.

3.1.1. Assessment Against Battelle Grout Mold Evaporation Test.

Simulations against the liquid surface heat and mass transfer data from the Battelle grout vault evaporative cooling tests [Ref. 4] has been conducted and the results of that assessment is briefly discussed in this section. The results of that comparison for two tests which are somewhat typical, and somewhat bounding, of tank operating conditions are presented below. The test facility is illustrated in Figure 3.1. Each test was initiated by heating a few inches of water (or sodium nitrate solution to simulate waste) to about 113 °F in this insulated vault. The heater was turned off and forced ventilation inlet air was turned on and the tank liquid was allowed to cool to about 85 °F over a period of 7-18 hours, depending on the

air flow rate. The inlet and outlet air temperatures and relative humidities, and also the temperature of the liquid pool were measured. Ventilation air inlet conditions were apparently at Hanford ambient conditions, and with the temperature and relative humidity ranging from 65-80 °F and 20-30% respectively over the time period of the tests. Air flow rates were held constant for each test and were varied over the series of tests from 6 to 36 SCFM. Scaling these air flow rates to that of Tank C-106 on the basis of tank waste surface area/vault liquid surface area would correspond to tank flow rates of 1194 to 7164 SCFM. Tank C-106 air flow rates during 1994 varied from 1484 to 2300 CFM.

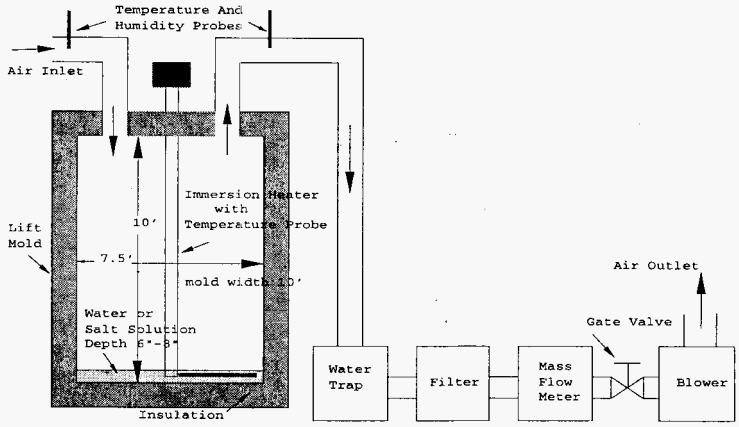

Figure 3.1 Battelle Grout Heat Removal Test Facility

At low air flow rates the exit air data was observed to be at saturation during the initial portion of the test when liquid temperatures were high, dropping to about 95% relative humidity as the liquid cooled to about 85 °F. Heat removal rates dropped off dramatically as liquid

and consequently air outlet temperatures decreased. At the high ventilation flow rates, the heat and mass transfer rates from the pool surface, for a given liquid temperature increase significantly, thus speeding the cool down of the vault liquid compared to low air flow rates. The heat and mass transfer rates, however, do not increase in proportion to the increase in ventilation flow rate. The net result is that the air exits at a lower temperature, and the relative humidity of the exiting air does not approach saturation.

A single lumped parameter model was utilized to simulate the grout vault evaporative cooling tests. In the model the liquid temperature was controlled to match the liquid temperature data, and the outlet air temperature and relative humidity or steam partial pressure were calculated for a given air flow and ambient air conditions.

GOTH comparisons to data for both low and high ventilation air flow rate cases with water in the vault are shown in Figures 3.2 through 3.5. At a low air flow rate of 6 SCFM, GOTH slightly overpredicts the exit air temperature, however, the steam outlet volume fraction, (i.e. steam partial pressure/total gas pressure) compare well with the data as illustrated in Figures 3.2 and 3.3. This appears to be due to minor heat losses from the vault dome which would result in lower air temperature in the data. These losses were not included in the model.

gmold6
Fri Jan 13 11:54:51 1995
GOTH Version 3.4 - April 1991

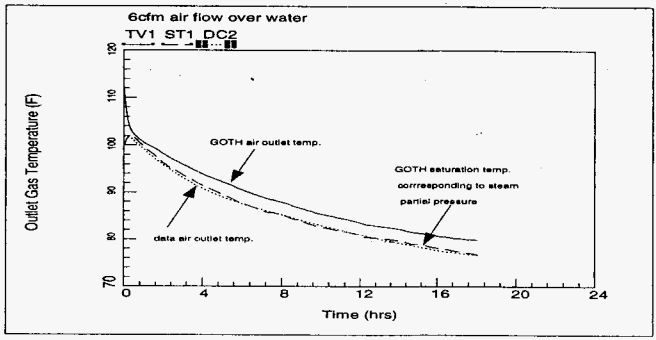

Figure 3.2 Calculated and Measured Outlet Gas Temperature Comparison at 6 SCFM

gmold6
Fri Jan 13 12:01:16 1995
GOTH Version 3.4 - April 1991

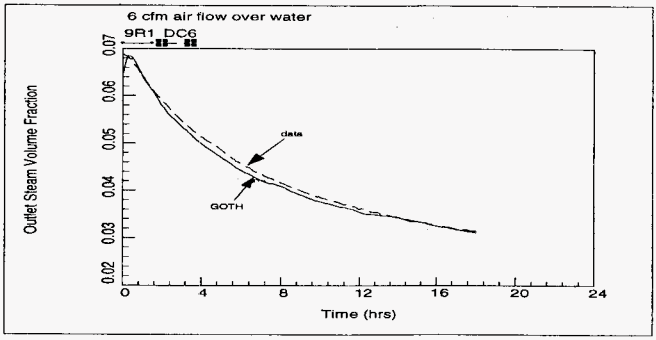

Figure 3.3 Calculated and Measured Steam Volume Fraction Comparison at 6 SCFM

At a high flow rate of 36 SCFM GOTH initially slightly underpredicts the air temperature and overpredicts the outlet steam volume fraction as shown in Figures 3.4 and 3.5. Later in time the steam volume fraction matches with the data and there is only a minor difference between calculated and measured temperatures. At the initial high liquid temperatures it appears the mass transport is slightly over predicted and the convective heat transfer is slightly underpredicted.

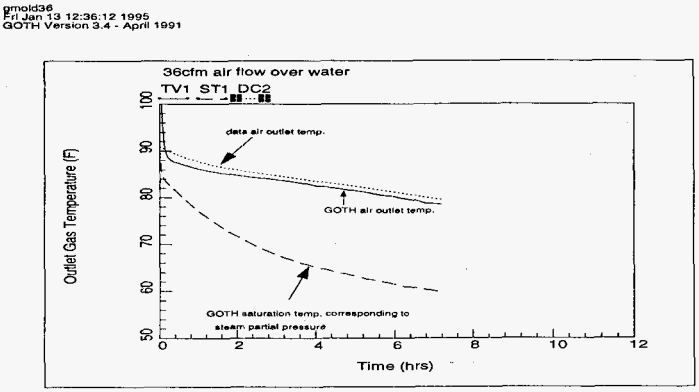

Figure 3.4 Calculated and Measured Outlet Gas Temperature Comparison at 36 SCFM

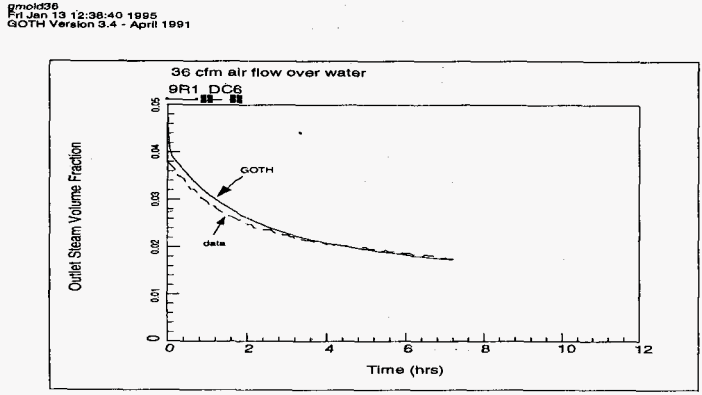

Figure 3.5 Calculated and Measured Steam Volume Fraction Comparison at 36 SCFM

In summary GOTH internal heat and mass transport models perform an excellent job of predicting the heat and mass transfer from liquid surfaces over a wide range of air inlet flow rates and over transient liquid temperature ranges quite typical of seasonal variations.

3.1.2. Assessment Against Tank C-106 Data.

Further assessment of the model can be made from the comparisons of calculated liquid level versus time for Tank C-106 [Thurgood, 1994], [Fryer, 1995]. The rate of liquid level drop during the process test of 1994 is a good demonstration of the codes ability to correctly calculate the evaporation as are the rate of level drop between water additions, Figure 3.6. The reasonable agreement with the measured dome air temperature and the pool temperature also provide further validation of the model, Figures 3.7 and 3.8.

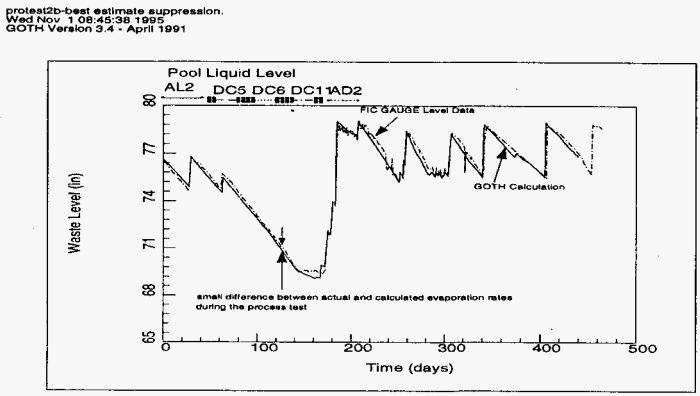

Figure 3.6 Comparison of calculated waste level and FIC level gauge measurements.

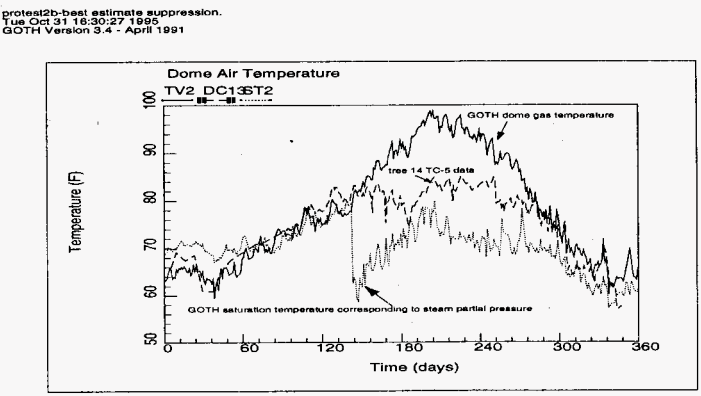

Figure 3.7 Comparison of calculated dome gas temperature and thermocouple tree 14 TC-5 dome gas measurements.

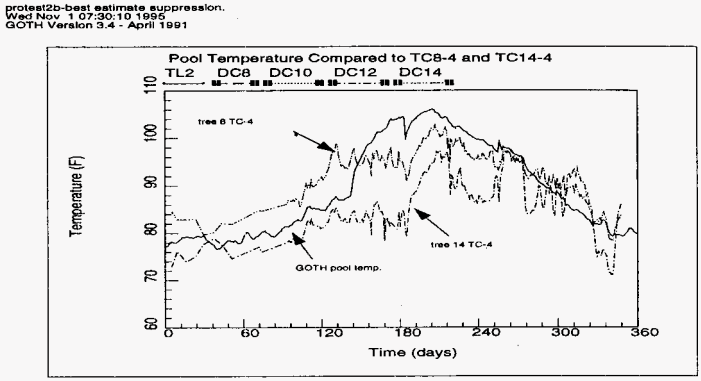

Figure 3.8 Comparison of calculated liquid pool temperature and thermocouple trees 8 & 14 TC-4 liquid pool measurements.

3.2. Conduction Heat Transfer In Sludge.

Conduction heat transfer through the sludge layer on the bottom of a tank is a key parameter, along with the sludge heat load, in determining if the sludge temperature will reach the local saturation temperature. The conduction solution in the sludge has been tested against analytical solutions for conduction in the sludge. These tests demonstrate that the fluid conduction equations are being solved correctly. However, for application to tank waste, the value for the sludge conductivity is often the greatest uncertainty. GOTH has been useful, in this respect, in determining the value of the sludge conductivity and heat load given the measured temperature profile in the sludge and measured dome and pool temperatures. A good example of the ability of GOTH to correctly calculate the temperature

gradient in the sludge is given in [Ogden, 1996]. The calculated waste temperatures for Tank A-101 for several axial elevations in the waste are compared with the measured data in Figure 3.9.

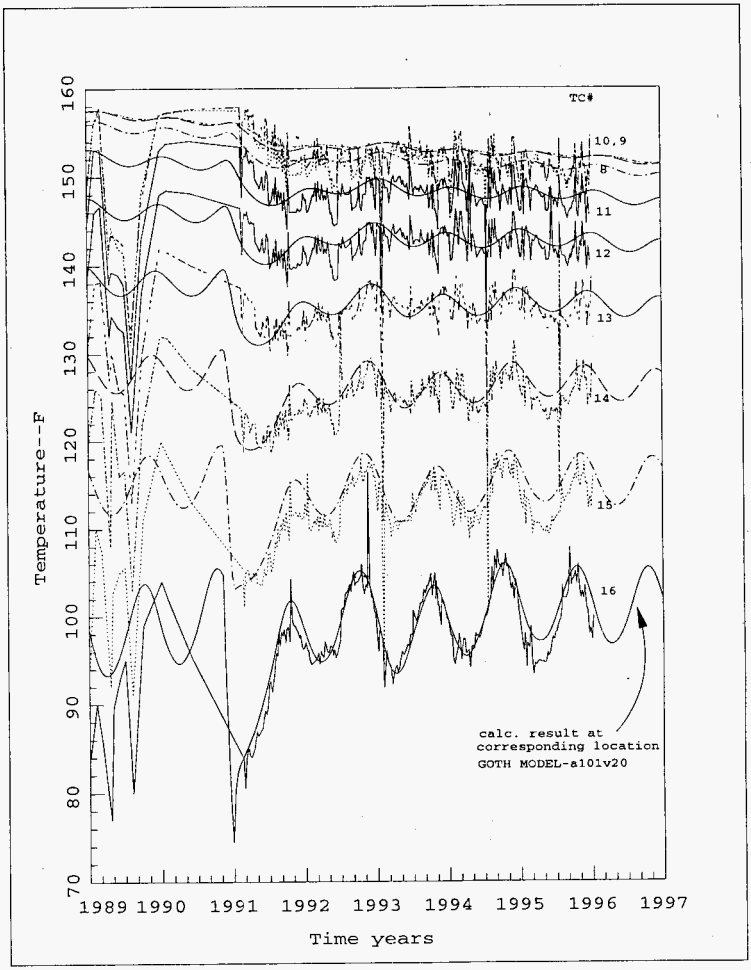

Figure 3.9 Data versus GOTH Model--1989 to present, upper axial waste region.

3.3. Natural Convection In Supernatant.

Fluid temperature measurements in Tank SY-101, Tank AZ-101 and other tanks show that there is no significant vertical temperature gradient in the supernatant. This is because small temperature gradients in the liquid generate a sufficiently large density gradient to promote convection of the liquid which keeps the supernatant at a nearly uniform temperature. While a direct comparison between GOTH simulations and tank data have not been made, two dimensional GOTH simulations of the dome gas, supernatant and sludge in Tank AZ-101 agree with the observation that temperature gradients in the liquid are small [Sathyanarayana, 1993]. This observation is important because it suggests that all tanks that have a significant amount of supernatant on top of the waste will have subcooled liquid above the waste. This will have been true even for tanks that have bumped in the past. Even if the tanks are boiling at the surface, the increase in hydrostatic pressure at the level of the sludge will cause the local supernatant temperature to be significantly below the local saturation temperature since no significant temperature gradient can develop in the liquid. The local pressure at the sludge surface will be about 21.2 psia if there is 15 feet of water above the sludge. The saturation temperature for water at this pressure is about 20°F higher than the saturation temperature of water at atmospheric pressure so the water is 20°F subcooled at the interface of the sludge when the supernatant surface is boiling. This means that tanks that have bumped in the past have done so in the presence of substantial subcooling in the bulk of the supernatant.

The supernatant convection flow patterns and supernatant temperature distribution for Tank 101-AZ that have been calculated by GOTH are shown in Figures 3.10 and 3.11 respectively.

agerev4
Wed Apr 14 11:27:05 1993
GOTH Version 3.4 - April 1991

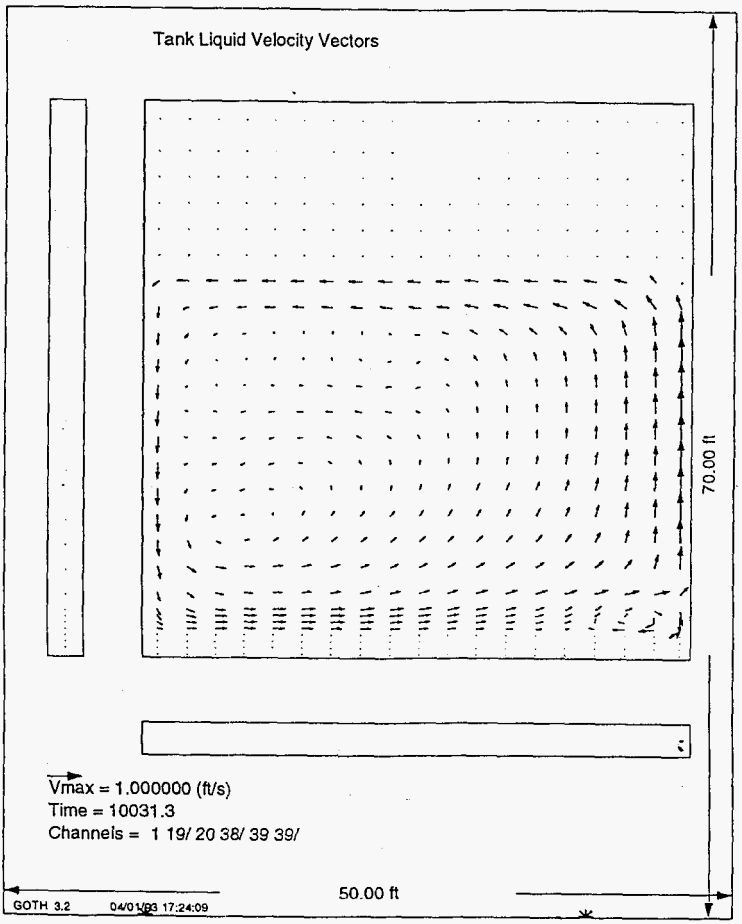

Figure 3.10 Liquid Velocity Vectors in Ageing Waste Tank Convective Layer at Steady State.

agerev4
Wed Apr 14 11:27:17 1993
GOTH Version 3.4 - April 1991

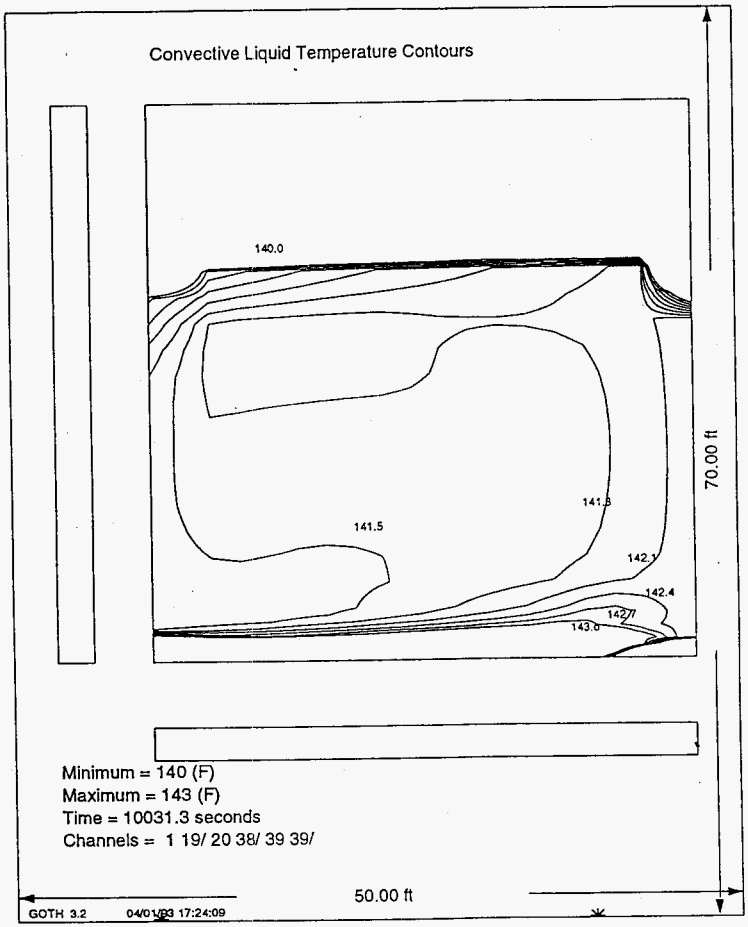

Figure 3.11 Convective Liquid Temperature Contours in Ageing Waste Tank at Steady State.

3.4. Particle and Liquid Heat Generation.

Studies done on Tank A-101 [Ogden, 1996], C-106 [Fryer, 1995] and comparison with analytical solutions [Thurgood, 1992] provide the assessment basis for the particle and liquid heat generation rate and interfacial heat transfer between particles and liquid.

3.5. Effect of Particle Concentration on Viscosity.

The effect of particle concentration on viscosity is given in [Thurgood, 1992] along with the data base for the correlations used in GOTH. The model has been assessed indirectly against tank data by comparing the measured waste roll over rate with the calculated roll-over rate for Tank SY-101 [Thurgood, 1992] as indicated by the waste temperature history for the upper and lower thermocouples in the tank as shown in Figure 3.12. The lower thermocouple cools as the waste rolls over and the upper thermocouple heats as hot waste from the bottom of the tank arrives at the top of the tank. The rate that these temperatures change is an indication of the roll-over rate of the sludge. The roll-over rate is governed by the balance between the shear stresses in the sludge (which are a function of the sludge viscosity) and the buoyancy provided by the gas in the sludge, which increases as the sludge rises to higher elevations having lower hydrostatic pressure. The fact that GOTH predicts the rate of temperature change for these two thermocouples suggests that the shear rates in the sludge are correctly calculated by GOTH. The sludge viscosities predicted by GOTH in these simulations has since been verified by direct viscosity measurements of the actual sludge from SY-101.

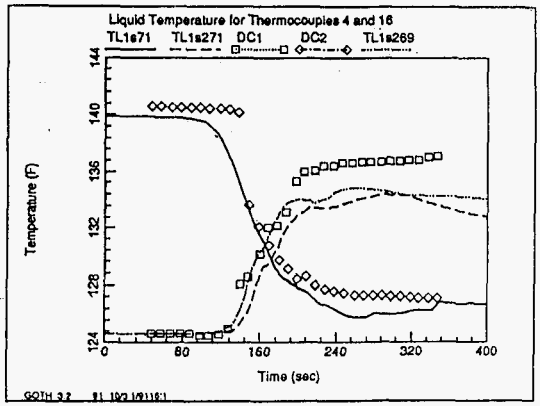

Figure 3.12 Liquid Temperature as a Function of Time for Thermocouple Locations 4 and 16 During A Rollover in Tank SY-101.

Figure 3.12 also shows that the sludge in Tank 101-SY rolls over without significant mixing between the supernatant and the sludge. This is indicated by the nearly perfect inversion of the temperature profile following the roll-over. This is an important observation when considering the amount of mixing that will occur between the rising sludge and supernatant during a steam bump. The rising steam laden sludge may remain insulated from the subcooled supernatant.

3.6. Ability of Sludge to Trap Gas Bubbles.

The ability of the sludge to trap gas is a function of the actual sludge properties. Gas may be trapped in sludge because the sludge has a yield strength and gas cannot deform the sludge to flow through it, or the sludge may have a high viscosity and the rate that bubbles can move

through the sludge is low compared to the rate that gas is being generated in the waste or surface tension may hold the gas bubbles to the solid particles in the sludge preventing the gas from moving through the sludge. The trapping mechanism assumed in GOTH is either yield strength or high viscosity. No direct assessment of the ability of the code to predict gas trapping is possible although the models in GOTH have been used to predict the viscosity of the waste in tank SY-101 [Thurgood, 1992] and the yield strength of the waste in C-106 [Thurgood, 1992]. With these predictions, GOTH has been able to predict the amount of gas released during GRE's in tank SY-101 and the amount of steam trapped in the waste of C-106 during the process test of 1994 required to produce the observed waste level change during the process test.

3.7. Sludge Plume Formation and Viscous Flow.

The nature of the hydrodynamic instability of the steam laden sludge is determined, in part, by the viscous flow generated within the sludge as perturbations in the system cause oscillations to develop between the steam laden sludge and the steam free sludge or supernatant. As these oscillations grow, changes in hydrostatic pressure due to elevation change cause the steam to expand and contract, water to flash to steam and steam to condense. Eventually, sufficient steam is formed to cause a plume to develop. The lower density of this plume, caused by increased steam formation and expansion as the waste rises causes an upwards displacement of the plume. Sludge moves in viscous flow to replace the volume displaced by the rising plume. The flow pattern in the sludge and the plume is then governed, in part, by the viscous shear forces in the sludge and, in part, by the net buoyancy force created by the increasingly steam laden sludge. The ability of the code to calculate viscous shear stresses in the waste has been demonstrated in a number of calculations.

3.7.1. Laminar Flow in a Square Duct.

GOTH predictions of laminar flow in a pipe are given in [Thurgood, 1992]. Predictions of both radial and centerline velocity profiles are given. These results demonstrate that the viscous shear stress terms are formulated correctly in GOTH.

3.7.1.1. Purpose for the Test Problem.

The purpose of this test problem is to test the formulation of the laminar shear stress terms in the liquid momentum equation and also to test the formulation of the mixture viscosity as a function of particle concentration.

3.7.1.2. Problem Description.

The reference for this test problem is the COBRA-SFS Modifications and Cask Model Optimization Report [Rector, 1989]. In this report, the flow channel is described as a ten inch square duct. The length of the duct is not given, however, data for a dimensionless length (x/d) of 15 is provided, indicating that the duct is at least 150 inches long. The COBRA-SFS report references a paper by Goldstein and Kried [Goldstein, 1967] and compares COBRA-SFS calculated centerline velocities with those reported in that paper. The paper describes experiments conducted in a 1 cm square duct that is 30 centimeters long. The reference for the 10 inch square duct is not known. The cross-sectional dimension of the duct used in the calculation should not be important as long as the data comparison is made using the dimensionless length, x/d, since the laminar solution for the centerline velocity of any square duct will be the same. Since the purpose of this problem was to compare against the COBRA-SFS result as well as the experimental data, the same duct size has been used in these calculations so that direct comparison of

calculated cross-sectional velocity profiles as well as the axial center line velocity profile can be made.

The test section includes both an inlet and outlet plenum box. Flow is injected into the inlet plenum at a constant rate. The centerline velocity is then measured at regular intervals starting at the connection of the rectangular test section to the inlet plenum. These velocities are non-dimensionalized by dividing the local velocity by the channel bulk or mean velocity. Tests were run for a variety of channel Reynolds numbers. The case for a Reynolds number of 200 is used for comparison in these calculations.

3.7.1.3. Description of input model.

The computational models for both COBRA-SFS and GOTH include the rectangular test section only, and do not include the inlet and outlet plenums in the model. In the computational model, flow is injected into the inlet of the test section assuming that the velocity distribution is uniform. The cross-section is simulated using a Cartesian mesh that assumes 1/4 section symmetry. The mesh cells are 1 inch square in the plane normal to the flow and, in the GOTH simulation, a cell length of 1.0 ft is used in the direction of flow. A sketch of the mesh normal to the flow direction is shown in Figure 3.13.

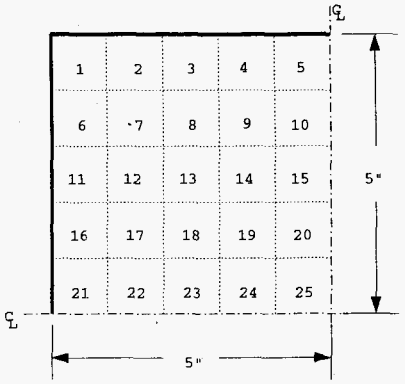

Figure 3.13 Cross section of Square Duct Mesh.

A uniform flow boundary condition is specified at the inlet to the channel and a constant, uniform pressure boundary condition is specified at the outlet to the test section. The calculation is run until the flow within the channel reaches steady state and the velocity distribution within the channel becomes constant. The calculated velocity distributions are then compared with the COBRA-SFS calculation and the calculated centerline velocities are compared with COBRA-SFS and with the measured data. Two GOTH calculations were performed, one with water for comparison with COBRA-SFS and the data and one using water with enough suspended particles to produce a mixture viscosity of 1000 lbm/ft-s.

3.7.1.4. Comparison With Data.

The first calculation performed with GOTH is for water flowing at a Reynolds Number of 200 in the test section geometry described above. This is the same test that has been simulated with the COBRA-SFS code. GOTH predictions

for the radial velocity profiles at three axial locations along the length of the test section are compared with the COBRA-SFS results in Figures 3.14 through 3.16. It is clear from these results that the uniform velocity profile specified at the inlet to the test section, still evident at the x/d=1.0 location, is developing into a parabolic velocity distribution further along the test section with the center line velocity approaching a value of 2.0 near the outlet of the test section. It is also apparent in these figures that both codes predict nearly identical velocity distributions at each location. Minor deviations between the two codes can be attributed to differences in the axial node length used by the two codes.

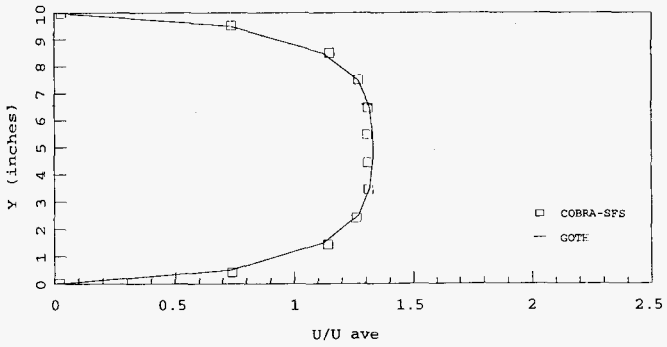

Figure 3.14 Velocity Profile, x/d = 1.0

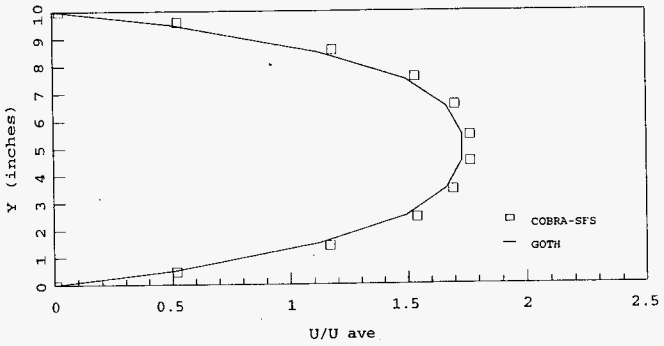

Figure 3.15 Velocity Profile, x/d = 5.0

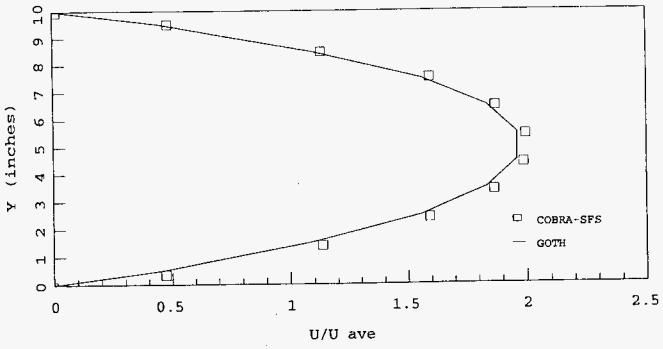

Figure 3.16 Velocity Profile, x/d = 15.0

The non-dimensional centerline velocities from the measured data, the COBRA-SFS calculation and the two GOTH calculations are compared in Figures 3.17 and 3.18. In Figure 3.17, the axial length is nondimensionalized using the duct diameter and Reynolds number. The GOTH and COBRA-SFS calculations are nearly identical, with the GOTH calculated centerline velocity falling slightly under the COBRA-SFS prediction. This difference is attributed to the longer node lengths used in the GOTH calculations. Both codes underpredict the center line velocity slightly. A similar behavior has been observed for TEMPEST simulations of the same test section. The authors of the TEMPEST code have argued that this difference is due to inlet effects caused by the contraction of the flow path from the inlet plenum into the test section. A vena-contracta is formed at the test section inlet that will generate higher centerline velocities in the test than are predicted in the computational models that assume a uniform velocity at the inlet. The TEMPEST code developers went on to demonstrate this effect by modeling the inlet plenum. This argument is further substantiated by the GOTH run which used a water particle mixture having a high mixture viscosity. The predictions for this case fall nearly on top of the measured data for water. This is because the effects of the vena contracta would be negligible at such high viscosities. The centerline velocity for water flow in the duct is compared in Figure 3.18 with the measured data. The axial length of the duct in this case is nondimensionalized by dividing by the duct length.

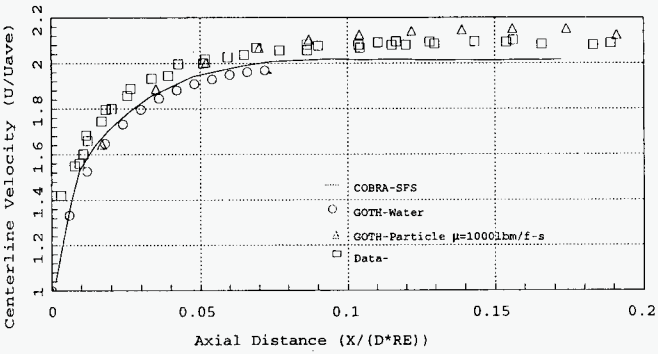

Figure 3.17 Centerline Velocity Profile.

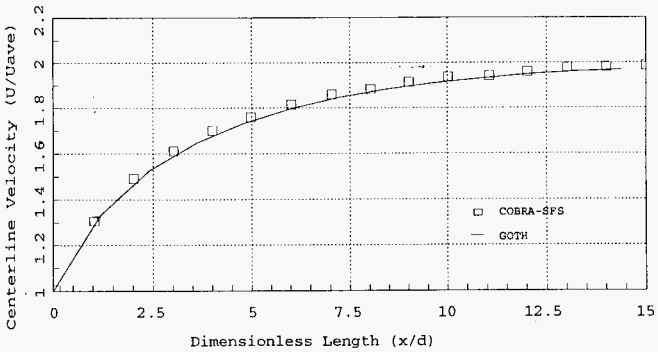

Figure 3.18 Centerline Velocity Profile.

3.7.1.5. Conclusions.

The results of this test problem indicate that the viscous shear stress terms have been correctly implemented into GOTH and that the more implicit formulation of these terms have been incorporated correctly. Prior to making this term more implicit in the cell velocity, the case having a viscosity of 1000 lbm/ft-s section required extremely small time steps to run. The problem ran at the courant time step limitation without difficulty with the more implicit formulation.

In addition, this test problem has shown that GOTH provides predictions for laminar flow that are comparable to those provided by single phase fluid dynamic codes commonly used to perform for pipe flow calculations. In addition, it has shown that models for the particle mixture viscosity are properly coded and that the numerical scheme is capable of performing simulations with large viscosities.

3.7.2. Turbulent Flow of a Round Jet.

GOTH has also been applied to predict Jet flow which is similar to plume flow. The comparison of predicted axial velocity profile for a round jet versus empirical data is shown in Figure 3.19. The radial velocity profile comparisons at 24, 48, 72, 96 and 144 inches from the fluid nozzle are shown in Figures 3.20 through 3.22. Similar comparisons have been made for planar jets.

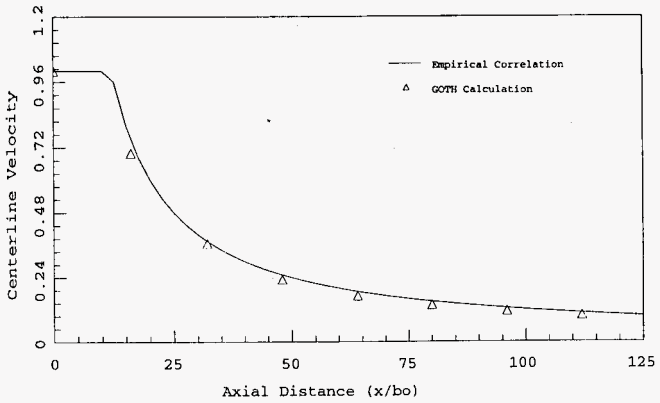

Figure 3.19 Centerline Velocity for a Round Jet Turbulent Jet as a Function of Axial Distance.

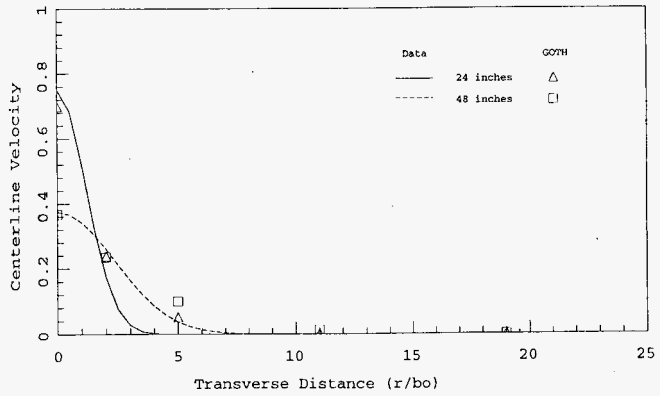

Figure 3.20 Radial Velocity Profile for a Turbulent Round Jet.

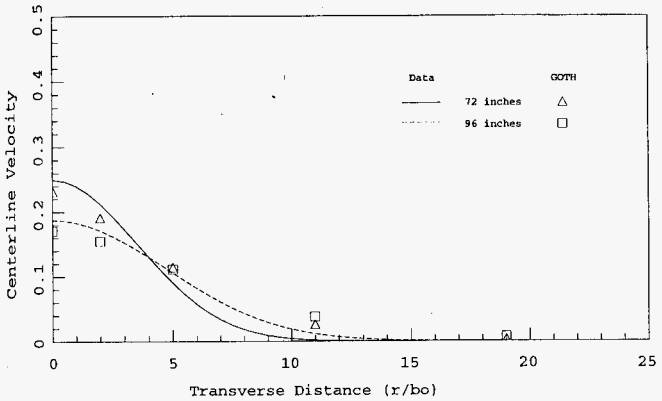

Figure 3.21 Radial Velocity Profile for a Turbulent Round Jet.

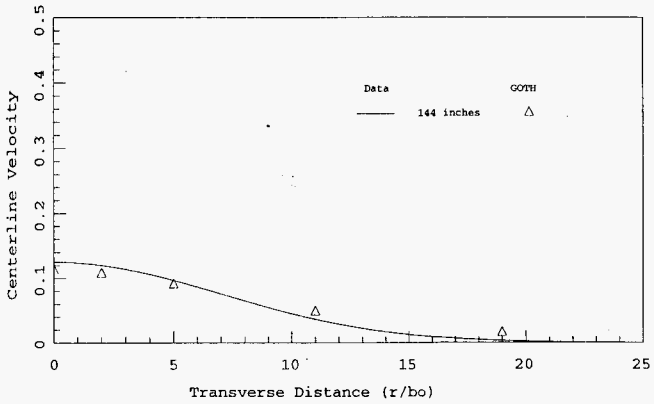

Figure 3.22 Radial Velocity Profile for a Turbulent Plane Jet.

GOTH predictions of roll over rates during gas release events in Tank SY-101 also provide evidence that GOTH does a reasonable job of predicting the rise velocity of gas laden sludge plumes [Thurgood, 1992].

3.8. Waste Thermodynamic Properties.

The formation of steam in the settled sludge depends on the axial temperature profile in the sludge and the corresponding local saturation temperature of the sludge. Steam will form if the local saturation temperature is less than or equal to the local sludge temperature. The saturation temperature for the waste supernatant is generally higher than that for water because of the presence of dissolved salts in the supernatant. The implementation and assessment of aqueous solution

thermodynamic properties into GOTH is documented in [Sathyanarayana, 1993] . GOTH predictions of the saturation conditions in tank C-106 also indicate that this model is appropriate [Thurgood, 1994].

3.8.1. GOTH Validation of Waste Vapor Pressure Capability

To validate implementation of the waste vapor pressure capability into GOTH a 4 volume blowdown simulation was conducted to see if the saturation pressure versus saturation temperature relationship for waste would be followed. The model used and the resultant pressure temperature relationships for both water and waste are illustrated in Figures 3.23 and 3.24 respectively.

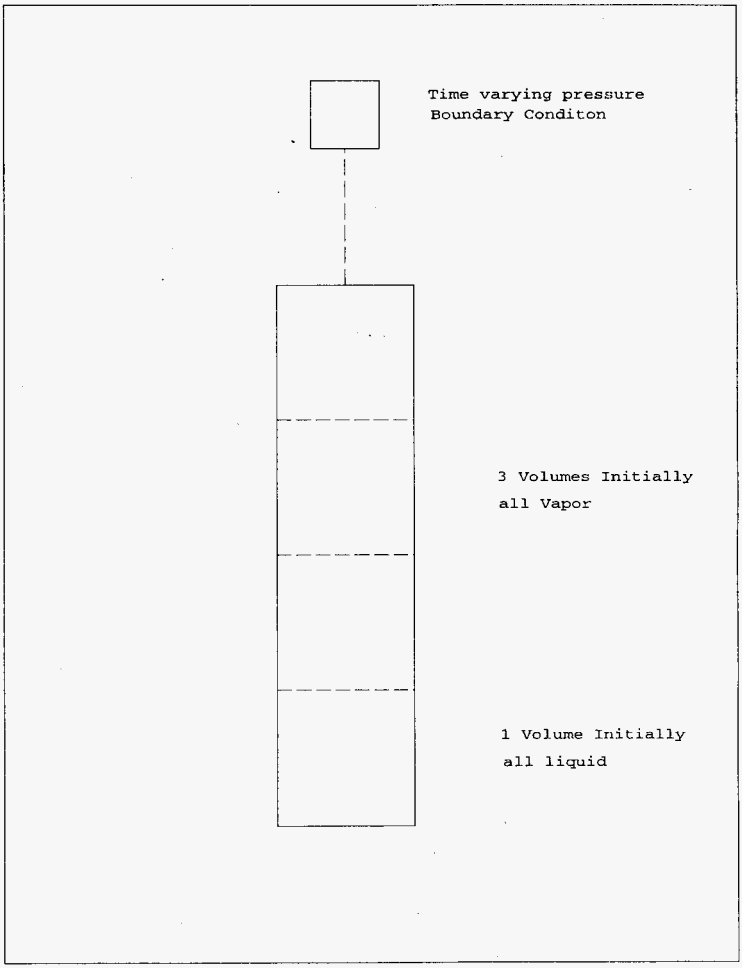

Figure 3.23 Goth Waste Thermodynamic Properties Verification Model

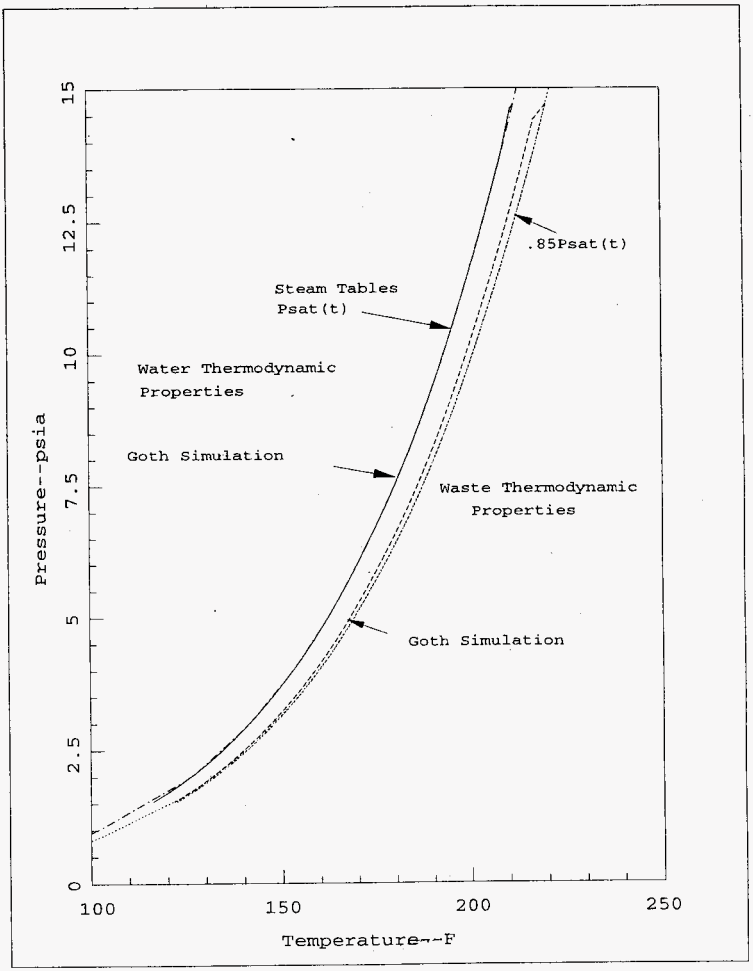

Figure 3.24 Pressure versus Temperature--GOTH Blowdown Simulation--Water versus Waste Properties

3.9. Hot Water Flashing and Steam Formation.

Fundamental models for the formation of steam when water reaches the saturation temperature have been assessed in the documentation of several of the predecessors of GOTH such as COBRA/TRAC [Thurgood, 1983],and COBRA-NC [Thurgood, 1986]. The plume rise velocities are slow compared with typical flashing rates so no significant superheating of the liquid is expected. This is particularly true since there are many nucleation sites provided by small solid particles in the waste. Results of tank bump simulations indicate no significant superheating of the liquid occurs. The rate of steam formation is, therefore, governed by the local saturation properties, the rate of sludge plume rise and the quantity of hot sludge entrained in the rising plume. The size of the sludge plume depends on the depth of the sludge and the radial location where the plume forms.

3.10. Bubble Migration Through Sludge.

The rate of bubble migration through the sludge is determined by the size of the bubble, the viscosity of the sludge mixture containing the bubble and the density of the surrounding sludge. The interfacial drag laws governing the slip between the bubble and the liquid phase are documented and assessed in COBRA/TRAC [Thurgood, 1983], COBRA-NC[Thurgood, 1986], and GOTHIC [George, 1993]. The application of the mixture viscosity to bubble interfacial drag is discussed in [Thurgood, 1992].

3.11. Steam Bubble Condensation.

Interfacial heat and mass transfer models between subcooled liquid and steam bubbles and assessment of these models are described in COBRA/TRAC·[Thurgood, 1983],COBRA-NC [Thurgood, 1986] and GOTHIC [George, 1993]. These relationships produce heat and mass transfer rates that will rapidly condense steam that comes into direct contact with subcooled water or sludge. The ability of steam to rise through a subcooled pool of water is mainly governed by the amount of hot sludge that surrounds the steam, insulating it from the subcooled water. The rate at which steam condenses in a sludge plume is controlled by the rate that heat can be transferred through the sludge by conduction or by mixing of the hot sludge with cooler supernatant, both of which are controlled by the viscous and turbulent shear stresses, conduction and turbulent heat transfer. The ability of expanding steam to break up the sludge and escape into the supernatant are also governed by these properties.

3.12. Particle and Droplet Entrainment.

The entrainment of liquid droplets and solid particles from the waste by the steam flow exiting the waste surface and exiting the tank through the tank leakage paths is a key parameter that is obtained from bump simulations. The amount of solids and liquids that will be entrained from the waste depend on several important parameters, discussed in other sections of this report, that effect the quantity of material involved in the bump, the strength of the bump and dome pressurization and flow through the ventilation system and leakage paths. The most important parameter affecting droplet and particle entrainment is the magnitude of the steam flow through the ventilation system and leakage paths which depends on the volume of waste

water flashing into steam and the flow resistance of the vents.

Once the magnitude and duration of the steam flow is known, then the slip between the particles/droplets and the vapor has a secondary effect on determining the waste particle entrainment rate. Since the vapor velocities leaving the waste surface and in the ventilation system and leakage paths are generally quite large (60-120 ft/s) and since the particle and droplet sizes are small (10 μm), the slip between the phases is likely to be small. The interfacial model used for the calculations assumes that the two-phase entity on which interfacial drag is calculated is on the order of the particle size. Descriptions and assessment for the interfacial drag between gas and liquid and between particles and liquid are given in COBRA/TRAC [Thurgood, 1983], COBRA-NC [Thurgood, 1986], GOTHIC [George, 1993]and[Thurgood, 1992].

Another parameter affecting the entrainment of waste material is the density of the materials involved. Since separate momentum equations are solved for the particle, liquid and gas phases, the effect of the density and concentration of each phase affects the overall mixture flow field. The importance of this parameter has been demonstrated in air lift circulator simulation performed with GOTH [Fryer, 1993].

3.13. Yield Strength.

Yield strength may play an important role in determining the time, location and the magnitude of the bump if it will occur. While GOTH has the ability to model materials with a yield strength, the yield strength of the sludge within a given tank is often not known. In general, a significant sludge yield strength will reduce the magnitude of, or

possibly even eliminate, the bump. A steam bump did not occur in tank C-106 when steam formed during the process test because the yield strength of the material in that tank is probably on the order of 1 psi or higher, [Thurgood, 1994]. This permitted a significant amount of steam to form in the waste without producing a steam bump. The void profile in the tank during this period is shown in Figure 3.25.

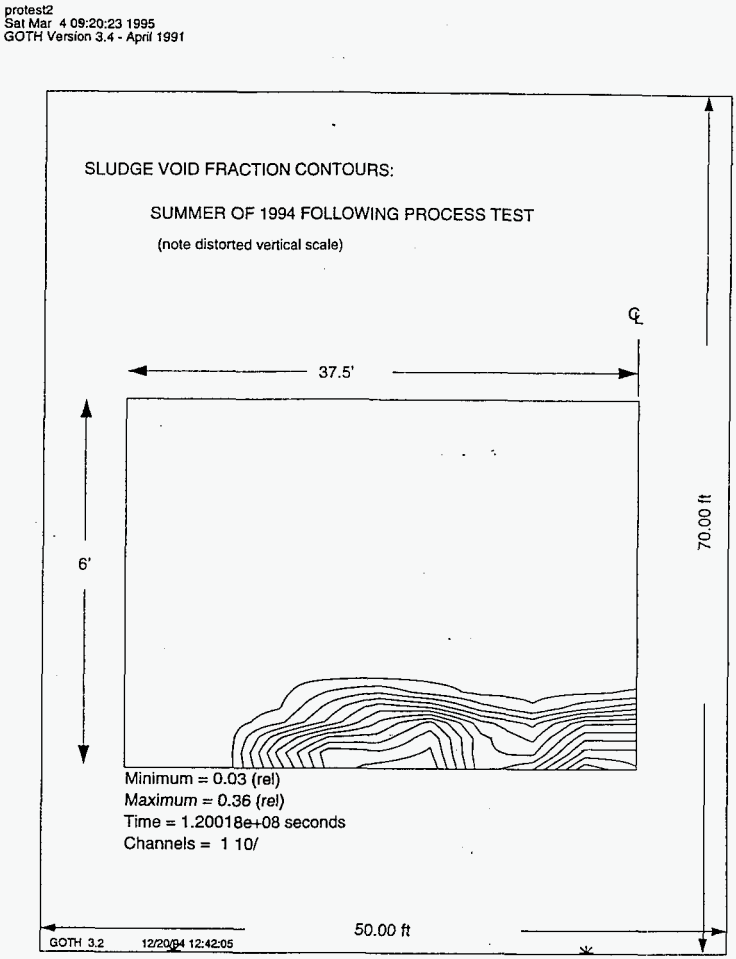

Figure 3.25 Calculated Void Distribution in Sludge at 231.5 days from January 1, 1994.

However, since the yield strength of the waste is not known for all tanks in general, it has been assumed for the present bump studies that the waste has no yield strength. This is expected to produce larger material involvement in the bump.

3.14. Structural Heat Transfer.

Heat transfer to tank walls, ventilation system walls and heat exchanger surfaces may play a role in increasing the steam flow out of the tank. Heat transfer to these surfaces have been included in the bump model when the entire ventilation system is modeled. The heat transfer to solids has been assessed and is documented in COBRA/TRAC [Thurgood, 1983], COBRA-NC [Thurgood, 1986] and GOTHIC [George, 1993].

3.15. Particle Settling Velocities.

The models for interfacial drag between solid particles and the liquid phase are discussed in [Thurgood, 1992]. GOTH calculated particle settling rates for simulated waste have been assessed against Battelle settling data. A description of this assessment is presented in this section. Additional discussion of particle settling can be found in [Fryer, 1994].

The purpose of these simulations is to validate the GOTH settling model against available experimental data. In these simulations, a mixture viscosity model having a maximum packing of 0.0417 and an exponent of -5.0 has been

used. The experimental tests and data are provided in [Norton, 1993].

3.15.1. Cold Settling Test With Downwind Differencing.

Results of GOTH simulations of the unwashed waste simulant in the Battelle Tests are shown in Figures 3.26 and 3.27. The results are similar to those obtained for the tank settling simulations using downwind differencing.

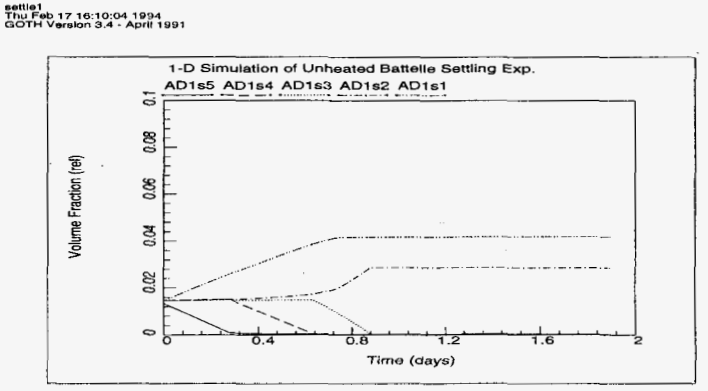

Figure 3.26 Particle fractions in the tank.

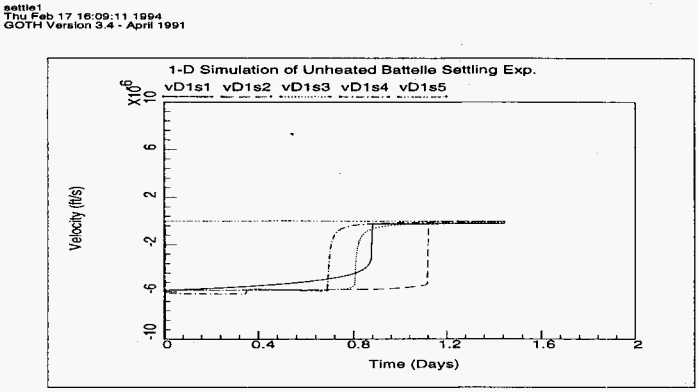

Figure 3.27 Particle velocities the tank.

The experimental data is presented as a plot of normalized solids/liquid level as a function of time. The calculated data from the above curves is recast in these terms and plotted against the measured data in Figure 3.28.

The liquid level in the numerical model is:

$$H_1 := 4 \cdot 2.676\ \text{in} + 2.444\ \text{in} = \boxed{13.15\ \text{in}} \tag{3.1}$$

The Normalized S/L Height for each of the four cells as each cell empties of particles is:

$$sl1 := 1 - \frac{2.444\ \text{in}}{H_1} = \boxed{0.8141} \tag{3.2}$$

$$sl2 := 1 - \frac{2.444\ \text{in} + 2.676\ \text{in}}{H_1} = \boxed{0.6106} \tag{3.3}$$

$$sl3 := 1 - \frac{2.444\ \text{in} + 2 \cdot 2.676\ \text{in}}{H_1} = \boxed{0.4071} \tag{3.4}$$

The last cell will have 0.669 in of particle free liquid

after all of the particles have settled so:

$$sl4 := 1 - \frac{2.444\ in + 2 \cdot 2.676\ in + 0.669\ in}{H_1} = \boxed{0.3562} \qquad (3.5)$$

Table 3.1 Cold Settling Calculation.

0.0000	1.0000
6.7200	0.8141
15.3600	0.6106
21.1200	0.4071
24.0000	0.3562
180.0000	0.3562
Array: coldc	

Table 3.2 Cold Settling Data.

0.740685	0.994987	4.382712	0.854656
4.351031	0.829537	5.410144	0.800588
5.835155	0.779315	6.119878	0.755086
10.537195	0.603534	20.358473	0.539504
22.399548	0.530659	24.019039	0.518559
26.939512	0.508541	29.999979	0.503547
44.529621	0.470888	49.138893	0.456158
54.274704	0.448821	67.817253	0.432997
71.721558	0.429489	78.686188	0.422170
102.675697	0.395219	121.844551	0.385360
150.193771	0.367908	172.000854	0.354529
Array: cold			

Acold := string_to_num (redim (cold, 22, 2)) (3.6)

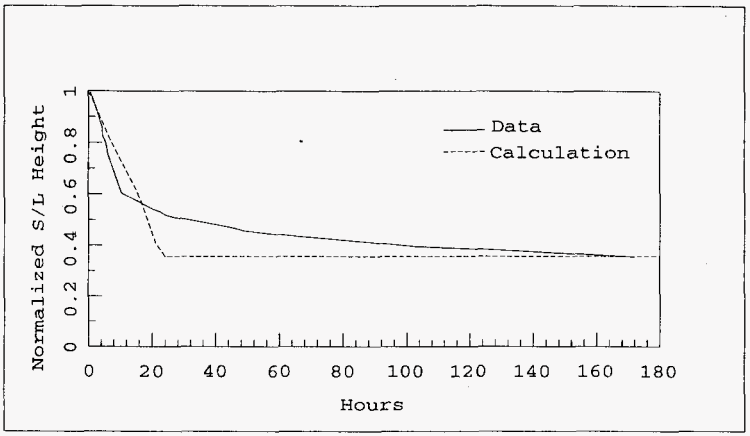

Figure 3.28 Settling Curves for Run 1, Unwashed NCAW Simulant at Ambient Temperature.

The calculation shows a linear decrease in solids level with time, as is expected for a single particle size system. The data also decreases linearly initially and then tapers off asymptotically to a final level that is presumably determined by either some maximum packing particle concentration or a particle concentration that causes the solution to behave as a gel. The calculation does not exhibit the asymptotic behavior since only a single particle size is used in the calculation. Therefore, the accumulation of particles in the lower regions of the tank which have not completely settled that would cause the mixture viscosity to increase is not calculated.

3.15.2. Cold Settling Test With Donner Cell Differencing.

Results of the cold settling test simulation with donner cell differencing is shown in Figures 3.29 and 3.30. Numerical diffusion causes the particles fractions in each

level of the mesh to trail off more gradually, as has been shown earlier. This calculation exhibits the asymptotic behavior shown in the data.

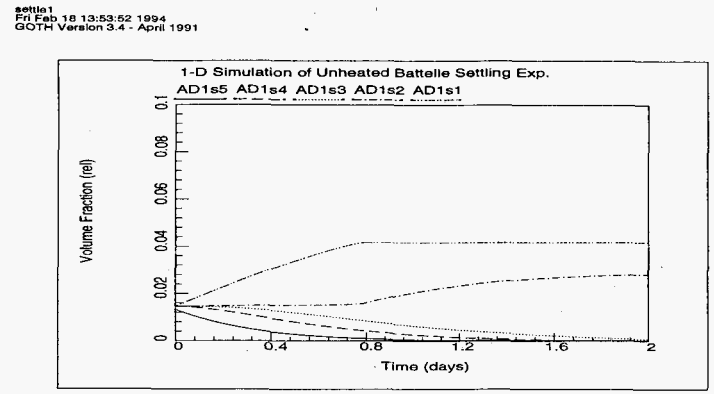

Figure 3.29 Particle fractions in the tank.

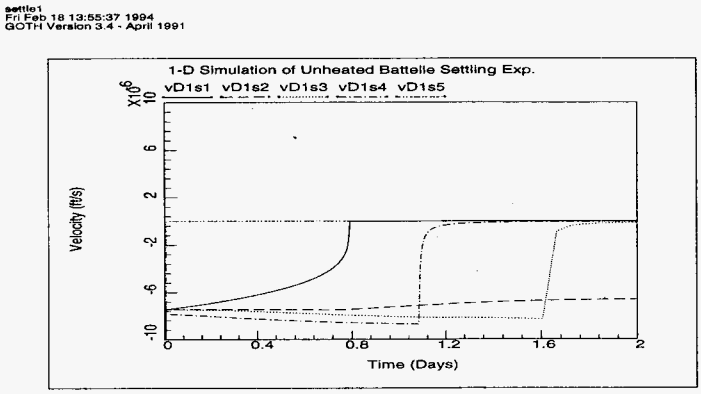

Figure 3.30 Particle velocities the tank.

3.15.3. Hot Settling Test with Downwind Differencing.

The same calculation has been repeated with the vessel contents heated to 47°C to represent the heated vessel in the experiments. The higher vessel temperature causes the supernatant viscosity to decrease resulting in more rapid settling rates. These more rapid settling rates are reflected in the calculation where the viscosity of the supernatant is assumed to decrease in the same fashion as the viscosity of water decreases with increasing temperature.

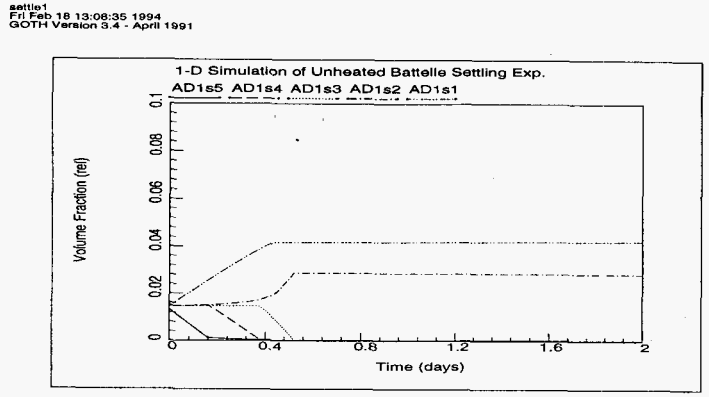

Figure 3.31 Particle fractions in the tank.

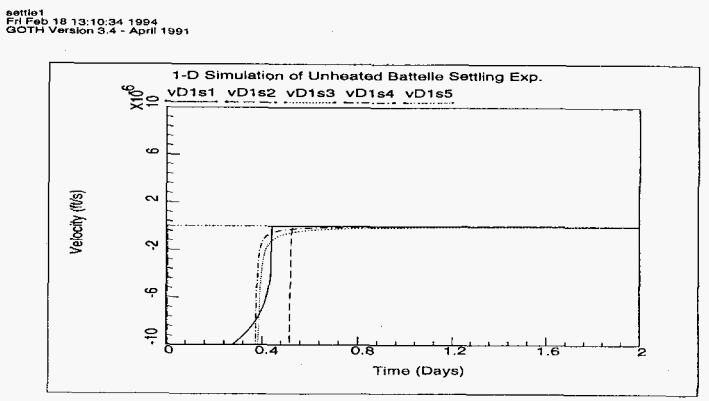

Figure 3.32 Particle velocities the tank.

Table 3.3 Hot Settling Calculation.

0.0000	1.0000
3.8400	0.8141
9.1200	0.6106
12.4800	0.4071
13.0000	0.3562
180.0000	0.3562
Array: hotc	

Table 3.4 Hot Settling Data.

-0.517465	1.009549	1.033736	0.954479
4.030741	0.712018	4.368531	0.686730
5.093741	0.663509	5.824469	0.650694
5.675463	0.634642	6.653153	0.623900
10.342426	0.560720	20.026875	0.477686
21.599241	0.462461	24.192459	0.451657
26.782223	0.434312	29.866180	0.421706
43.676140	0.369440	47.954983	0.358274
53.600533	0.341408	67.886154	0.325104
70.483810	0.322626	78.941826	0.311004
102.180946	0.290197	121.705681	0.285290
149.868896	0.277974	172.062180	0.271776
Array: hot			

```
Ahot := string_to_num (redim (hot,24,2))                    (3.7)
```

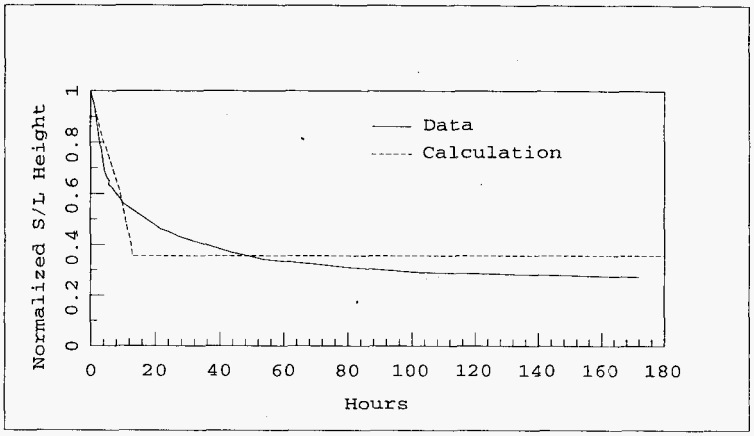

Figure 3.33 Settling Curves for Run 1, Unwashed NCAW Simulation Heated Vessel.

Table 3.5 Hot Settling Data.

0	0	0	0
-0.517465	1.009549	1.033736	0.954479
4.030741	0.712018	4.368531	0.686730
5.093741	0.663509	5.824469	0.650694
5.675463	0.634642	6.653153	0.623900
10.342426	0.560720	20.026875	0.477686
21.599241	0.462461	24.192459	0.451657
26.782223	0.434312	29.866180	0.421706
43.676140	0.369440	47.954983	0.358274
53.600533	0.341408	67.886154	0.325104
70.483810	0.322626	78.941826	0.311004
102.180946	0.290197	121.705681	0.285290
149.868896	0.277974	172.062180	0.271776

3.15.4. Comparison of Hot and Cold Settling Calculations.

The normalized solids/liquid height curves for the heated and ambient GOTH simulations are shown in Figure 3.34 to illustrate the effect of supernatant temperature on settling rates. The difference in the calculated settling rates are comparable to the difference in the measured settling rates. The final level of solids in the heated vessel is the same as that for the ambient vessel in the calculation since it has been assumed that the maximum particle fraction is not effected by temperature. The data appears to indicated that increasing temperature either increases the effective maximum packing of particles or some of the particles dissolve at higher temperatures or the mass fractions in the two vessels were not the same.

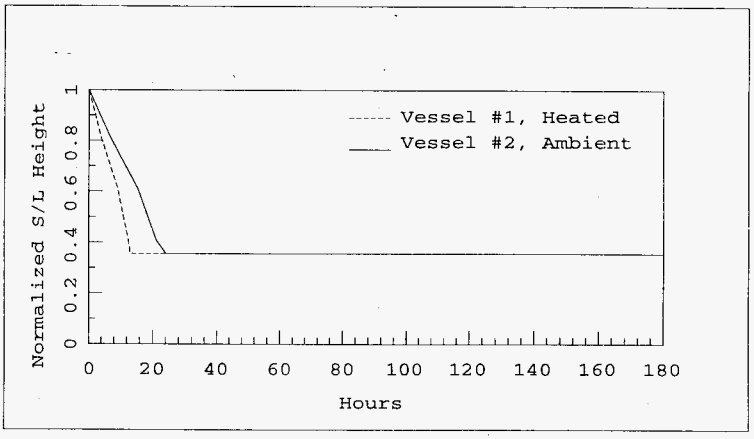

Figure 3.34 Settling Curves for Run 1, Unwashed NCAW Simulant, Heated and Ambient Vessel.

3.16. Frictional Loss Through Ventilation System Components.

The frictional loss in ventilation system components is calculated using the user specified component lengths and equivalent hydraulic diameters and form loss coefficients. The total frictional pressure loss is given by:

$$\Delta P = \frac{f\frac{L}{D} + K}{2} \rho V^2 \qquad (3.8)$$

The friction factor is calculated using either the laminar friction factor or the turbulent friction factor for smooth tubes. The model for frictional losses, including the effects of two-phase flow has been assessed in COBRA/TRAC [Thurgood, 1983], COBRA-NC [Thurgood, 1986] and GOTHIC [George, 1993].

4. REFERENCES

Thurgood, M.J. et. al., *COBRA-TF Development,* paper presented at the Eigth Water Reactor Safety Information Meeting, Gaithersburg, Maryland, October 1980.

Liles, D.R., et. al., *TRAC-PD2, An Advanced Best-Estimate Computer Program for Pressurized Water Reactor Loss-of-Coolant Accident Analysis,* LANL, USNRC Report NUREG/CR-2054, 1981.

Thurgood, M.J. et. al., *COBRA/TRAC - A Thermal-Hydraulics Code for Transient Analysis of Nuclear Reactor Vessels and Primary Coolant Systems,* Battelle Northwest Laboratories, USNRC Report NUREG/CR-3046, March 1983.

Hochrieter, Larry et. al, *WCOBRA/TRAC - A Best Estimate Computer Program for Pressurized Water Reactor Transient Analysis,* Westinghouse Nuclear Power Division, Monroeville, Pennsylvania, 1995.

Thurgood, M.J. et. al., *COBRA-NC: A Thermal-Hydraulic Code* For Transient Analysis of Nuclear Reactor Components, USNRC Report NUREG/CR-3262, May, 1986.

Thurgood, M.J. and T.L. George, *CAP Containment Analysis Package User's Manual,* Numerical Applications, Inc., Richland, WA, September, 1987.

George, T.L. et. al., *GOTHIC Containment Analysis Package, Version 3.4e,* EPRI TR-103053, Electric Power Research Institute, October, 1993.

Thurgood, M.J., *Simulation of Gas Release Event In Tank 101-SY Using the GOTH Computer Program,* NAI-9101-1, February, 1992.

Fryer, B.C. and M.J. Thurgood, *Revised Tank Heat Load Estimate for Tank C-106 Based on GOTH Analysis fo the Process Test,* JMI-WT002, John Marvin, Inc., November, 1995.

Thurgood, M.J. et. al., *GOTH Tank C-106 Thermal Hydraulics Analysis Related to the 1994 Process Test,* NAI-940708-3, February, 1994.

Ogden, D.M., *Thermal-Hydraulic Behavior Evaluation of Tank A-101,* WHC-SD-WM-ER-555, WHC, JMI-WT002, John Marvin, Inc.,March, 1996.

Sathyanarayana, K. et. al., *Development of A Dynamic Computer Simulator For Aging Waste Tank Operations and Safety Assessment,* WHC-SD-WM-ER-198, Westinghouse Hanford Company, November, 1993.

Sathyanarayana, K. et. al., *Summary Report - Thermal Hydraulic Safety Analysis of Aging Waste Tank AZ-101,* WHC-SD-WM-ER-335, Westinghouse Hanford Company, May, 1994.

Bagaasen, L.M., 106-AN Grout Pilot-Scale Test HGTP-93-0501-02, Report No. PNL-8618, Pacific Northwest Laboratory, Richland, WA., May 1993.

Thurgood, M.J. and B.C. Fryer, *GOTH Simulation of Ageing Waste Tank 101-AZ with Air Lift Circulator Operation Terminated and Primary And Secondary Ventilation Systems Operational And Addition of Aqueous Solution Thermodynamic Property Capability to GOTH,* NAI-9101-5, Numerical Applications, Inc., Richland, WA, March 1993.

Norton, M.V. and F. Torres-Ayala, "Summary Letter, Laboratory Testing In-Tank Sludge Washing", September, 1993, Pacific Northwest Laboratory, TWRSPP-93-060.

Fryer, B.C. and M.J. Thurgood, *GOTH and HUB Ageing Waste Tank Thermal Hydraulics Analysis For In-Tank Washing, High Power Pump Mixing and Settling Operations For Current Unwashed Tank Particle Loading Conditions and Washed High Particle Loading Conditions,* NAI-9101-6, Numerical Applications, Inc., Richland, WA, April 15, 1994.

Rector, D.R. and T.E. Michener, "COBRA-SFS Modifications and Cask Model Optimization", PNL-6706, Pacific Northwest Laboratory, January 1989.

Goldstein, R. J. and D. K. Kried, "Measurements of Laminar Flow Developed in a Square Duct Using a Laser-Doppler Flow Meter." Journal of Applied Mechanics, Trans. ASME. 34(89): 813-818.

Fryer, B.C. and M.J. Thurgood, *GOTH Simulation of Ageing Waste Tank 101-AZ With Air Lift Circulators and Primary and*

Secondary Ventilation Systems Operational And Comparison of the GOTH Air Lift Circulator Model to Full Scale Air Lift Circulator Tests., NAI-9101-7, Numerical Applications, Inc., Richland, WA, June 1993.

DISTRIBUTION SHEET

To	From	Page 1 of 1
Distribution	Process Engineering Analysis	Date June 5, 1996
Project Title/Work Order		EDT No. 614678
Evaluation of Potential and Consequences of Steam Bump in High Heat Waste Tanks and Assessment and Validation of GOTH Computer Code/N1FC3		ECN No. N/A

Name	MSIN	Text With All Attach.	Text Only	Attach./ Appendix Only	EDT/ECN Only
B. D. Board	A3-37	X			
C. A. Carro	A2-34	X			
G. L. Dunford	A2-34	X			
G. R. Franz	R3-09	X			
B. C. Fryer	H0-34	X			
G. T. MacLean	H5-61	X			
R. M. Marusich	A3-34	X			
D. M. Ogden	H0-34	X			
K. Sathyanarayana (2)	H0-34	X			
J. P. Sloughter	R2-54	X			
M. J. Thurgood	H0-34	X			
A. H. Umek	H6-35	X			
Central Files (Original + 2)	A3-88	X			
PEA File (Burstad 2)	H0-34	X			
J. C. Conner	A2-25	X			